PRODUCTION AND CHARACTERIZATION OF ACTIVATED CARBON FROM HORSE CHESTNUT KERNEL

A THESIS SUBMITTED TO
THE GRADUATE SCHOOL OF NATURAL AND APPLIED SCIENCES
OF
THE MIDDLE EAST TECHNICAL UNIVERSITY

BY

TUĞBA DEMİROK

IN PARTIAL FULFILLMENT OF THE REQUIREMENTS
FOR
THE DEGREE OF MASTER OF SCIENCE
IN
CHEMICAL ENGINEERING

MAY 2015

Approval of the thesis:

PRODUCTION AND CHARACTERIZATION OF ACTIVATED CARBON FROM HORSE CHESTNUT KERNEL

submitted by **TUĞBA DEMİROK** in partial fulfillment of the requirements for the degree of **Master of Science in Chemical Engineering Department, Middle East Technical University** by,

Prof. Dr. Gülbin Dural Ünver _____
Dean, **Graduate School of Natural and Applied Sciences**

Prof. Dr. Halil Kalıpçılar _____
Head of Department, **Chemical Engineering**

Prof. Dr. Hayrettin Yücel _____
Supervisor, **Chemical Engineering Dept., METU**

Examining Committee Members:

Prof. Dr. Naime Aslı Sezgi _____
Chemical Engineering Dept., METU

Prof. Dr. Hayrettin Yücel _____
Chemical Engineering Dept., METU

Assoc. Prof. Dr. Burcu Akata Kurç _____
Central Lab., METU

Dr. Cevdet Öztin _____
Chemical Engineering Dept., METU

Dr. Ahmet Kemal Behlülgil _____
Central Lab., METU

Date: 04.05.2015

I hereby declare that all information in this document has been obtained and presented in accordance with academic rules and ethical conduct. I also declare that, as required by these rules and conduct, I have fully cited and referenced all material and results that are not original to this work.

Name, Last name: TUĞBA DEMİROK

Signature:

ABSTRACT

PRODUCTION AND CHARACTERIZATION OF ACTIVATED CARBON FROM HORSE CHESTNUT KERNEL

Demirok, Tuğba
M.S., Department of Chemical Engineering
Supervisor: Prof. Dr. Hayrettin Yücel
May 2015, 124 pages

The production of activated carbon from horse chestnut kernel by chemical activation using phosphoric acid and characterization of produced activated carbons are presented in this work. To investigate effect of process parameters on porous structure of activated carbons, chemical activation was performed at the temperature of 300, 400, 500, 600, 700 and 800 ºC for impregnation ratios (weight of activation agent / weight g of sample) of 1:1 and 2:1.

Chemical activation experiments were carried out in a quartz tube with diameter of 30 mm and length of 90 cm under a nitrogen flow of 100 cm^3/min. To produce activated carbon, all the impregnated samples were heated to the desired activation temperature at heating rate of 10 ºC/min and were held at that temperature for activation time of 1 hour.

Structural characterization of the obtained activated carbons was investigated by nitrogen gas adsorption analysis at 77 K. BET surface areas of activated carbons by horse chestnut kernel ranged between 9.7 and 862.4 m^2/g. The highest BET surface area of 872.4 m^2/g was attained for activated carbon which was produced

with an impregnation ratio of 2:1 (weight of H_3PO_4 / weight of raw material), at activation temperature of 800 ºC at a yield of 21.7 %. The BET surface area of the activated carbon produced at 500 ºC for 2:1 impregnation ratio at a yield of 44.9 % was found as 713.4 m^2/g. It was seen from the t plot analysis that activated carbon products have a microporous structure with a significant contribution of mesoporosity.

It was seen that produced activated carbons have methylene blue numbers (MBN's) varying between 2.7 and 49.9 mg/g. It was observed that the ratios of surface area covered by methylene blue to total surface area were small for activated carbon products except sample produced at 300°C and impregnation ratio of 1:1(weight of H_3PO_4 / weight of horse chestnut kernel).

Nitrogen adsorption measurements and methylene blue experiments showed that produced activated carbons in present study are more suitable for gas phase applications due to the microporous structure of products.

The results confirm that the properties of activated carbons depend on the impregnation ratio and chemical activation temperature. The results of the study show that the horse chestnut kernel can be used as raw material for preparation of activated carbon.

Keywords: Activated Carbon, Horse Chestnut Kernel, Chemical Activation, Phosphoric Acid, Characterization

ÖZ

AT KESTANESİ ÇEKİRDEĞİNDEN AKTİF KARBON ÜRETİMİ VE KARAKTERİZASYONU

Demirok, Tuğba
Yüksek Lisans, Kimya Mühendisliği Bölümü
Tez Yöneticisi: Prof. Dr. Hayrettin Yücel
Mayıs 2015, 124 sayfa

Bu çalışmada, at kestanesi çekirdeğinden fosforik asitli kimyasal aktivasyon yöntemi ile aktif karbon üretimi ve üretilen aktif karbonların karakterizasyonu sunulmuştur. Proses parametrelerinin üretilen aktif karbonun gözenek yapısı üzerindeki etkisinin tespiti için, kimyasal aktivasyon işlemi, 300, 400, 500, 600, 700 ve 800 ºC aktivasyon sıcaklığında, 1:1 ve 2:1 (g aktivasyon ajanı / g örnek) emdirme oranlarında gerçekleştirilmiştir.

Kimyasal aktivasyon deneyleri 30 mm çapında ve 90 cm boyunda kuvars tüp içerisinde, 100 cm^3/dk nitrojen akışı altında gerçekleştirilmiştir. Aktif karbon üretmek için, fosforik asit emdirilmiş örnekler 10 ºC/dk ısıtma hızı ile oda sıcaklığından istenilen aktivasyon sıcaklığına kadar ısıtılıp, bu sıcaklıkta 1 saat tutularak aktivasyon yapılmıştır.

Elde edilen aktif karbonların yapısal analizleri 77 K de nitrojen gazı adsorpsiyon analizi ile belirlenmiştir. At kestanesi çekirdeği kullanılarak üretilen aktif karbonların yüzey alanları 9.7 ile 862.4 m^2/g arasındadır. En yüksek yüzey alanı, 862.4 m^2/g, 2:1 (g fosforik asit / g örnek) emdirme oranında, 800 ºC aktivasyon

sıcaklığında % 21.7 verim ile üretilen aktif karbon için elde edilmiştir. 2:1 (g fosforik asit / g örnek) emdirme oranında, 500 ºC aktivasyon sıcaklığında % 44.9 verim ile üretilen aktif karbonun yüzey alanı 713.4 m^2/g olarak bulunmuştur. T plot analizi ile üretilen aktif karbonların, önemli payda mezo gözenekliliğe sahip mikro gözenekli bir yapıda olduğu görülmüştür.

Üretilen aktif karbonlar 3.2 ile 49.9 mg/g arasında değişen metilen mavisi sayılarına sahip olduğu görülmüştür. 300°C sıcaklıkta ve 1:1 emdirme oranında üretilen örnek dışındaki aktif karbon ürünleri için, metilen mavisi tarafından kaplanan yüzey alanının toplam yüzey alanına oranının düşük olduğu gözlenmiştir.

Nitrojen adsorpsiyonu ölçümleri ve metilen mavisi deneyleri, üretilen aktif karbonların mikro gözenekli yapıları nedeniyle gaz fazlı uygulamalara daha uygun olduğunu göstermiştir.

Deneysel sonuçlar, aktif karbonun özelliklerinin emdirme oranına ve kimyasal aktivasyon sıcaklığına bağlı olduğunu doğrulamıştır. Yapılan çalışmanın sonuçları at kestanesi çekirdeğinin aktif karbon üretiminde hammadde olarak kullanılabileceğini göstermiştir.

Anahtar kelimeler: Aktif Karbon, At Kestanesi Çekirdeği, Kimyasal Aktivasyon, Fosforik Asit, Karakterizasyon

To My Family…

ACKNOWLEDGEMENTS

Firstly, I would like to thank to my supervisor Prof. Dr. Hayrettin YÜCEL for his support, supervision and recommendations during my study.

I should mention Dr. Kemal BEHLÜLGİL for his support, sharing his recommendations and comments with me.

I also want to express thanks Turgut AKSAKAL, Mihrican AÇIKGÖZ, Gülten ORAKÇI and Yavuz GÜNGÖR for their support and help in laboratory work.

I want to express my gratitude to all of my classmates at METU for their friendship. I also would like to thank to my colleagues at Ministry of Labor and Social Security.

I am very grateful to my parents Nuran ÖZMEN, Veysel ÖZMEN and to my siblings for their love, reliance and support. I also appreciate to my husband Murat DEMİROK for his love, support and encouragement during my research and whole life.

TABLE OF CONTENTS

LIST OF TABLES

TABLES

LIST OF FIGURES

FIGURES

LIST OF SYMBOLS

A_m : Cross-sectional area of the adsorbate, m^2

C : A constant BET equation

C_{final} : Final concentration of solution, mg/L

C_{blank} : Concentration of solution in blank experiment, mg/L

CSA_{N2} : Cross sectional area of nitrogen molecule, m^2

D_p : Pore diameter, μm

I : Intercept of the BET plot

K : A constant in DR equation

MBN : Methylene Blue Number, mg/g

N_A : Avagadro's constant, 6.023×10^{23} mol^{-1}

P : Pressure, mmHg

P_o : Saturation pressure, mmHg

q_1 : Heat of adsorption of the second and subsequent layers

q_2 : The gas constant, 8.314×10^{-3} kJ/mole-K

r_p : Actual pore radius, mean radius of the liquid meniscus, nm or μm

r_K : Kelvin radius

RDS : Relative Standard Deviation

s : Standard Deviation

S : Slope of the BET plot

S_{BET} : BET surface area, m^2 /g

SMB : Surface area covered by Methylene Blue, m2/g

T : Thickness of the adsorbate layer

tm : Thickness of the monolayer

T : Temperature, °C

$\bar{x}$: Mean value of sample data set

V : Volume adsorbed, cm^3/g

Vo : Micropore Volume, cm^3/g

Vm : Monolayer volume, cm^3/g

Vmol : Molar volume of gas adsorbed at standard temperature and pressure (STP)

w : Pore width, Å

W : Limiting adsorption space volume value

Wo : Limiting adsorption space volume value

Greek Letters

μm : Micrometer (10^{-6} meter)

Å : Angstrom (10^{-10} meter)

ρ : Liquid density, g/cm^3

β : Affinity coefficient in DR method

θ :Contact angle of mercury, 130º and Fraction of surface occupied by adsorbate

σ : Surface tension

CHAPTER 1

INTRODUCTION

The use of carbon extends far back in time, so that the origin of carbon is impossible to determine exactly. Prior to the use of what we call today activated carbon (which has a highly developed porous structure), either wood char, or coal char or simply a partially devolatilized carbonaceous material was employed as an adsorbent. (Bandozs, 2006)

Activated carbon which has an extremely large surface area and pore volume is mainly an amorphous solid. Due to this characteristic, activated carbon is used as an adsorbent in various gas phase and liquid phase applications. The activated carbon is a multipurpose adsorbent since the distributions and size of the pores in the carbon structure could be controlled to satisfy the needs of industries. The adsorptive properties of products can be made suitable for various applications such as potable water purification and the gasoline emissions control with the raw material selection, activation method, and control of process conditions. (Kirk-Othmer, 2003)

Activated carbon could be obtained from several materials like resins, biomass, coals (Özsin, 2005). Any low-cost material with low inorganic materials and high carbon content can be a starting material for activated carbon production. Agricultural by products are also considered as important precursor for production of activated carbon since they are low-cost and renewable resources (Ioannidou and Zabaniotou, 2007). Agricultural by products are rich source of cellulosic material which has an average composition of 20-25% lignin, 40-50% cellulose,

20-30% hemicellulose and 1-5% ash. This composition makes them desirable precursor for production of activated carbon (Rafatullah et al. 2013).

Basically, activated carbon production involves two main steps. First step is the carbonization of the starting materials under 800 ºC in the absence of oxygen; second step is the activation of the resulting carbonized product. (Ioannidou and Zabaniotou, 2007)

The carbonization process is the pyrolysis of the starting material. During the process, the carbonaceous material degrades thermally under an inert atmosphere and the raw material devolatilizes. This step is usually critical in the production of activated carbons, because the micropore structure starts to form during this step (Bandozs, 2006). But this porosity is not enough because it has low adsorption capacity. Thus the carbonization process is followed by activation process for improve porosity (Balcı, 1992).

The objective of activation is to remove organic content from biomass that leads to increase pore volume and enlarge micropores in its structure. Generally two main techniques exist for activation that resulting chars from the pyrolysis step: physically and chemically activation. The physical activation has two main process steps. First step is carbonization of a starting material and second step is the activation of the char product at higher temperatures in the existence of suitable oxidizing gases such as steam, carbon dioxide, oxygen or their mixtures. Chemical activation is carried out by chemical treatment of the raw material with a chemical agent (such as phosphoric acid, zinc chloride, potassium hydroxide and sulfuric acid) then heat treatment of the impregnated sample under an inert atmosphere to form the final porous structure. Chemical activation is generally performed for the degradation of the lignocellulosic materials and removal of the organic residues. “Single step activation”, “low activation temperatures”, “higher yields”, “low activation times” and “better porous structure” are some advantages of the chemical activation method. (Rafatullah et al. 2013)

Recent studies have revealed that, activated carbons prepared from agricultural side products are comparable to commercial activated carbons used in market with regard to their adsorption capacities (Balcı, 1992).

The purpose of the present work is to produce activated carbons from an agricultural waste horse chestnut kernel by phosphoric acid activation method, to characterize these produced activated carbons with respect to surface area and pore size distribution and to examine the effect of preparation conditions on the porous structure of the prepared activated carbon. To determine the effect of temperature and impregnation ratio on prepared activated carbons, samples were produced at a temperature range of 300-800 ºC; and an impregnation ratio of 1:1 and 2:1 (weight of H_3PO_4 / weight of Horse Chestnut Kernel). The products were characterized by N_2 adsorption measurements at 77 K in terms of BET surface area, adsorption desorption isotherm and pore size.

CHAPTER 2

LITERATURE SURVEY

Activated carbon is used widely as an adsorbent. As a result, adsorption systems including active carbon have become crucial in separation and purification processes. Since pollution problem is critically growing, the need of activated carbons keeps expanding. The characteristic of activated carbon depends on both the chemical and physical properties of the precursor and activation method. In this work, activated carbons produced from horse chestnut kernel and the characteristics of the produced activated carbons have been investigated.

2.1. ACTIVATED CARBON

2.1.1. Definition and Properties of Activated Carbon

Activated carbon is a term that includes amorphous carbon-based materials that have “a high degree of porosity” and “an extended internal surface area” (Bansal and Goyal, 2005; Marsh and Rodriguez-Reinoso, 2006). “The structure of activated carbon is best described as a twisted network of defective carbon layer planes, cross-linked by aliphatic bridging groups.” (Kirk Othmer, 2003)

Activated carbon composes of elementary graphite crystallites that stacked in random orientation. The gap between these graphitic microcrystallites creates the porosity of activated carbon (Marsh and Rodriguez-Reinoso, 2006). Orientation of microcrystalline layers is less ordered in active carbon than graphite (Smisek and Cerny, 1970). X-ray diffraction analyses of activated carbon show that activated

carbon is non-graphitic and the structure remains amorphous since "the randomly cross-linked network inhibits reordering of the structure even when heated to 3000 ºC". (Kirk Othmer, 2003) "Activated carbons have highly developed porosity, large surface area, high degree of surface reactivity and variable characteristics of surface chemistry." (Kwiatkowski, 2011) "Typical commercial products have specific surface areas in the range 500–2000 m^2/g, but values as high as 3500–5000 m^2/g have been reported for some activated carbons" (Kirk Othmer, 2003). These unique characteristics enable its use as adsorbent and as well as catalysts and catalyst support used for different purposes; for example pollutant removal and solvent recovery (Kwiatkowski, 2011).

> "The availability of favorable pore size makes the internal surface accessible and enhances the adsorption rate. The most widely used activated carbons have a specific surface area of 800 to 1500 m^2/g. This surface area is contained predominantly within micropores that have effective diameters smaller than 2 nm. In fact, a particle of active carbon consists of a network of pores that have been classified into micropores (diameters < 2 nm), mesoporous (diameter between 2 and 50 nm) and macropores (diameter > 50 nm)." (Bansal and Goyal, 2005)

2.1.2. History of Activated Carbon

The first known use of carbon dates back to the ancient times. According to the Egyptian papyrus from 1550 B.C., Hippocrates used activated carbon in treatment of various diseases. Also the use of char for removal of odors from ulcers was discussed by Kehl in 1793. The ancient Hindus in India used charcoal for purifying their drinking water. (Hassler, 1974; Bansal and Goyal, 2005)

The adsorptive powers were discovered in 1773 by Scheele who defined experiments with gases. In 1785, decolorizing effect was observed by Lowitz. Then wood char was used to purify cane sugar and in 1808 the usage was extended to beet sugar industry. Figuer discovered that bone char had grater decolorizing power than vegetable charcoal that led to adoption by beet and cane sugar industries in 1811 (Deitz, 1944).

During the nineteenth century, extensive research was made to improve decolorizing carbons from other materials. Bussy heated blood with potash and developed a carbon with 20 to 50 times the decolorizing power of bone char in 1822. The gas adsorbing ability of coconut char was reported by Hunter in 1965. It was understood that coconut char is superior to all others for some purposes. Stenhouse, in 1856, produced a decolorizing char by heating a mixture of tar, magnesium carbonate and flour. Winser and Swindells heated paper mill waste with phosphates. In 1954 Stenhouse described the patent of the modern gas mask and 1862 Lipscombe prepared a carbon for purification of potable water. Many of approaches are related to processes now in industrial use.

In 1900 and 1901, Ostrejko patented his works and this led to the development of modern commercial activated carbons. Eponite is the first powdered activated carbon that was produced using wood and worked under Ostrejko patents in Europe in 1909. Norit first appeared in 1911 in Holland and soon became widely known in the sugar industry (Hassler, 1974).

In 1915, during the World War I, gas mask containing activated carbon was developed. This activated carbon gas mask provided to protect soldiers from poisonous gas during the warfare. (Hassler, 1974)

“More recent innovations in the manufacture and use of activated carbon products have been driven by the need to recycle resources and to prevent environmental pollution”. (Kirk Othmer, 2003)

2.1.3.Classification of Activated Carbon

Classification of activated carbons relying on their adsorption behavior, preparation methods and surface characteristics is difficult because of its complexity. But, a general classification is made based on their physical characteristics to meet the engineering needs of specific applications. (Kwiatkowski, 2011; Kirk Othmer, 2003)

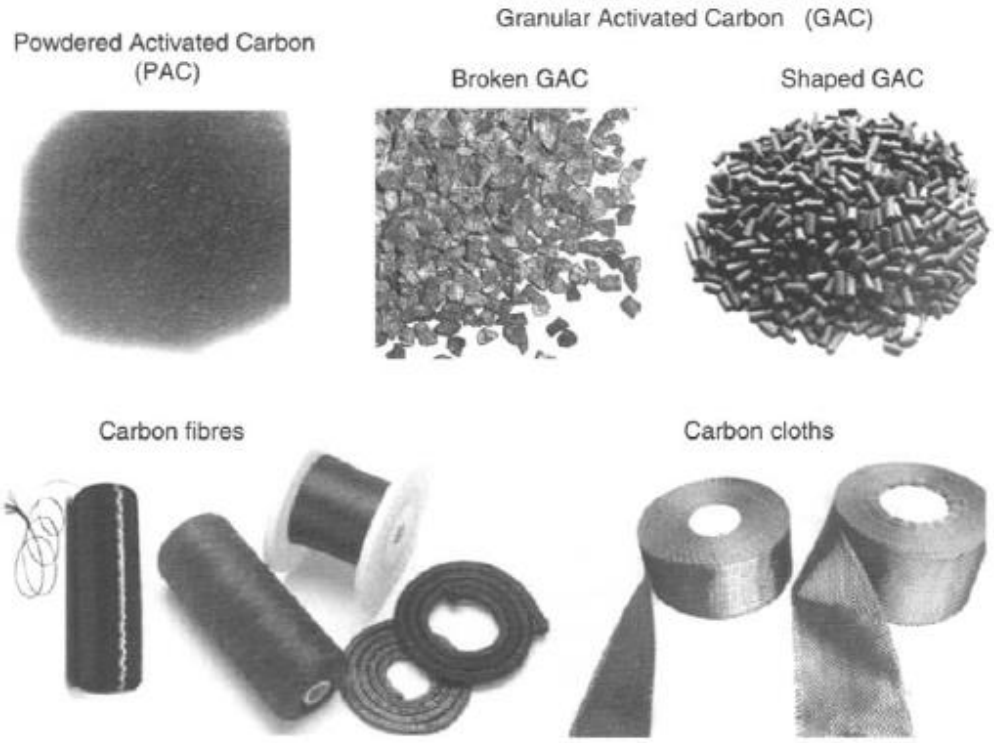

Figure 2.1. Different forms of activated carbon (Bandozs, 2006)

Activated carbons have two major forms, “powdered activated carbon” and “granulated activated carbon”. (Kwiatkowski, 2011) Powdered activated carbons are fine particles “less than 1 mm in size with an average diameter between 0.15 and 1.25 mm”. (Kwiatkowski, 2011) They show large external surface area. Powdered activated carbons are applied in batch contact treatment. On the other hand, granular activated carbons are relatively large particles up to 5 mm in diameter and present a smaller external area compared to powdered activated carbons. Granular activated carbons were used primarily in vapor-phase applications formerly. But in recent years usage of granular carbons have been extended to liquid-phase applications. Granular activated carbon commonly used as column filler and can be regenerated after use. In addition to these two main forms of activated carbon, there is extruded (shaped) activated carbon which is

commonly formed as cylindrical pellets by extrusion of the powdered activated carbon. They are chiefly used in gas phase processes due to their “low dust content”, “low pressure drop” and “high mechanical strength”. Activated carbon is also presented in specials forms such as cloths and fibers (Kwiatkowski, 2011).

2.1.4.Applications of Activated Carbon

“Activated carbons are excellent and versatile adsorbents.” (Bansal and Goyal, 2005) Their important applications relate to their adsorptive properties. The activated carbons have applications in liquid and gas phase. Activated carbons are used for liquid phase applications for example “removal of color, odor, taste, and other undesirable organic and inorganic impurities from drinking waters”; the purification of many chemical, medical and food products; the removal of color from sugar, fats and oils; “the urban ground and industrial waste water treatment”. (Bansal and Goyal, 2005) Gas phase applications of activated carbon consist of air purification for food processing, restaurants and chemical industries; solvent recovery; “in respirators for work under hostile environments”; catalysts and catalysts support and gas storage. (Bansal and Goyal, 2005)

Activated carbons are more and more being used as catalyst and catalyst supports and in metallurgy for the recovery of silver and gold. The usage of activated carbons in medicine and health is to fight significant types of bacterial diseases and for the removal of significant toxins. Applications of activated carbon are interested by various fields such as food, chemical, pharmaceutical, vacuum industries, automobile, mining and nuclear.

> “Nearly 80% of the total activated carbon is consumed for liquid-phase applications, where both the granulated and powdered forms of active carbon are used. However, with the commercial production of fibrous activated carbons in the form of fibers and fabric, these materials may be in preference, especially for water treatment processes, because they produce low hydrodynamic resistance to flow and can easily be molded into any shape in the adsorption equipment” (Bansal and Goyal, 2005).

The summary of industrial and municipal applications of activated carbon is presented in Table 2.1 (Bandosz, 2006).

Table 2.1. Industrial applications of activated carbons as filtering material

Industrial applications of activated carbons as filtering material	
Application field	**Adsorption from liquid phase**
Potable water treatment	Removal of dissolved organics, control of taste and odor, lead, chlorine, colour
Food industry	Decolourization of liquid sugars (glucose, maltose)
Soft drinks and brewing	Removal of chlorine and dissolved organic contaminants from potable water, after disinfection with chlorine
Pharmaceutical	Purification and separation of antibiotics, vitamins, hormones, etc.
Semi-conductors	Production of ultra high purity water
Petrochemical	Removal of oil and hydrocarbon contaminations from recycled steam condensate for boiler feed water
Groundwater	Reduction of total organic halogens and adsorbable organic halogens in industrial reserves of contaminated groundwater
Industrial waste water	Process effluent treatment to meet the environmental legislation
Swimming pools	Removal of residual ozone and control of chloramine levels
	Adsorption from gas phase
Solvent recovery	Control of vapour emissions and recovery of organic solvents
Carbon dioxide	Purification of carbon dioxide from fermentation processes
Industrial respirators	Adsorption of organic vapours and inorganic gases
Waste disposal	Removal of heavy metals and dioxins from flue gas formed during incineration of various wastes
Cigarettes	Removal of some harmful substances (nicotine and tar)
Air conditioning	Removal of contaminants from air subjected to heating, ventilation, and air conditioning in airports, offices, hospitals
Semi-conductors	Production of ultra high purity air
Toxic gas removal	Purification of industrial off-gases
Fridge deodorizers	Removal of general food odours

2.1.5. Physical Structure of Activated Carbon

Activated carbon has “a microcrystalline structure” that begins to form during the carbonization. “The microcrystalline structure” of activated carbon is different from graphite structure in terms of interlayer spacing. Interlayer spacing is 0.335 nm in graphite structure whereas it is in the range of 0.34 to 0.35 nm in activated carbons. (Smisek and Cerny, 1970)

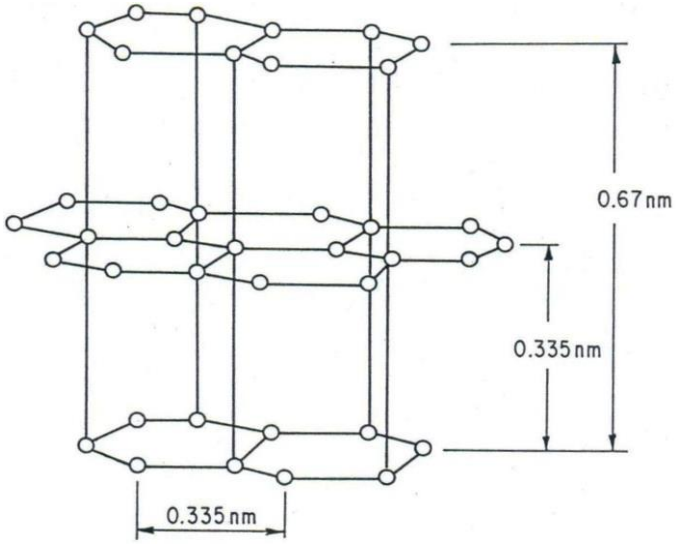

Figure 2.2. Structure of graphite (Smisek and Cerny, 1970)

The alignment of the microcrystalline layers is also not the same; these layers are less ordered in activated carbons. The term “turbostratic” for activated carbon structure is suggested by Biscoe and Warren (1942). Figure 2.3 illustrate graphite structure and the turbostratic structure of activated carbon (Bansal and Goyal, 2005).

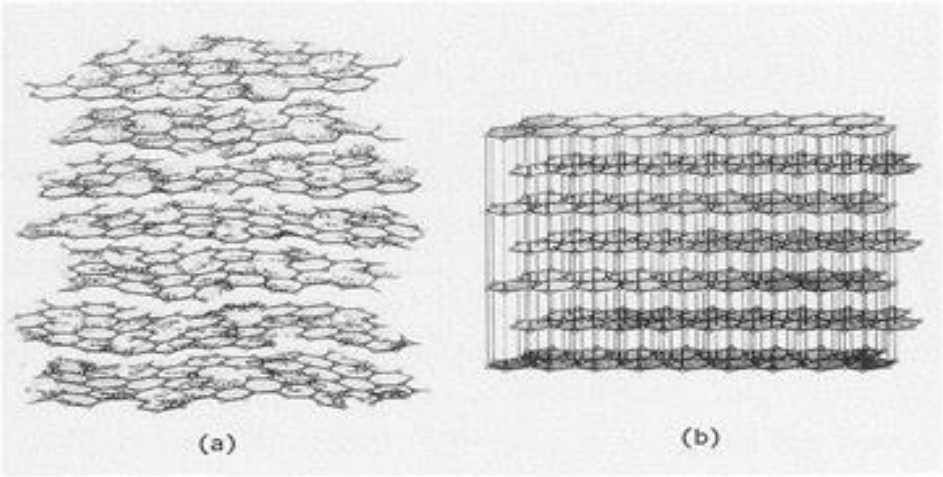

Figure 2.3. Comparison of schematic diagrams of (a) a three-dimensional graphite lattice with (b) a turbostratic structure (Bokros, 1969)

Activated carbon has disordered microcrystalline structure, the schematic representation of this structure presented in Figure 2.4.

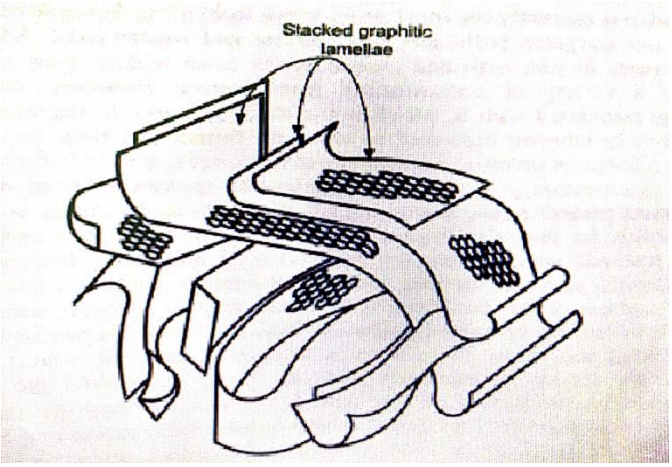

Figure 2.4. Microcrystalline structure of activated carbon (Kwiatkowski, 2011)

Franklin (1951) classified activated carbons into two types, “graphitizing” and “non-graphitizing carbons” based on X-ray analyses. The difference in the alignment of the crystallites due to the difference graphitizing abilities resulted in the two types of carbons.

During carbonization, the elementary crystallites which are randomly oriented in the structure during carbonization cross-linked between strongly in the non-graphitizing carbons. As a result, a rigid immobile mass is formed. The existence of associated oxygen or the inability of hydrogen in the starting material promotes the formation of the non-graphitizing structure with strong cross-links. Franklin saw that “the elementary crystallites were mobile and had weak cross-linking from the beginning of the carbonization process”. (Franklin, 1951) The graphitizing carbons are obtained from materials containing more hydrogen. Thus, softer and less porous carbon is prepared. The schematic representations of “graphitizing” and “non-graphitizing” active carbon structure are shown in Figure 2.5.

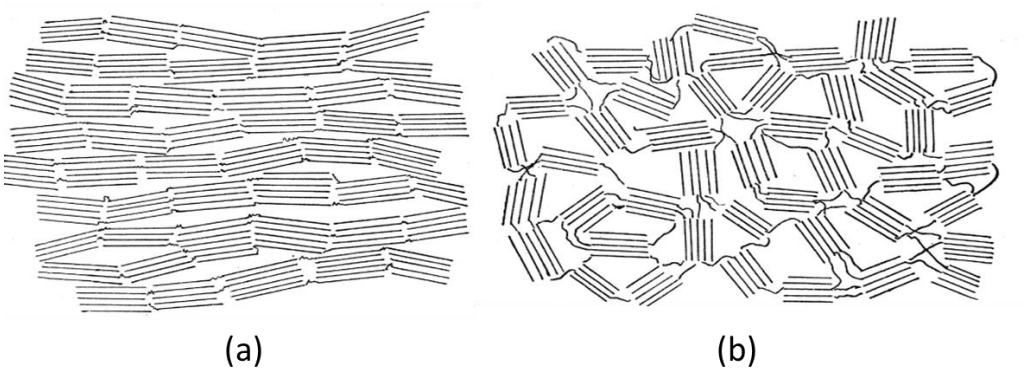

Figure 2.5. Schematic illustration of the activated carbon structure: "(a) graphitizing and (b) non-graphitizing" (Franklin, 1951)

2.1.6. Porous Structure of the Activated Carbon Surface

Activated carbons have a highly developed pore structure due to random orientation of microcrystallites and strong cross-linking between them. "They have relatively low density (less than 2 g/cm^3) and a low degree of graphitization." (Bansal and Goyal, 2005) Firstly during the carbonization, porous structure is formed. Then for the duration of the activation step, this formed porous structure is developed. The volume is enhanced and diameters of the pores are enlarged during the activation process. The nature of starting material and the carbonization influence the pore structure and the pore size distributions. Disorganized carbon removed from structure during activation step and this leads to the improvement of a microporous structure. (Bansal and Goyal, 2005).

> "The activated carbons in general have a strongly developed internal surface and are usually characterized by a polydisperse porous structure consisting of pores of different sizes and shapes. Several different methods used to determine the shapes of the pores have indicated ink-bottle shaped, regular slit shaped, V-shaped, capillaries open at both ends, or with one end closed, and many more." (Bansal and Goyal, 2005)

The dimensions of pores which comprises active carbon surface are variable. Dubinin (1960) categorized the pores and this classification has been approved by "International Union of Pure and Applied Chemistry (IUPAC)". The classification is on the basis of their width (w), which denotes the distance between the walls of the radius of a cylindrical pore or slit-shaped pore. The pores are categorized into three groups: "the macropores, the mesopores (transitional pores) and the micropores". (IUPAC, 1985)

The schematic representation of micropores, mesopores and macropores can be seen in Figure 2.6.

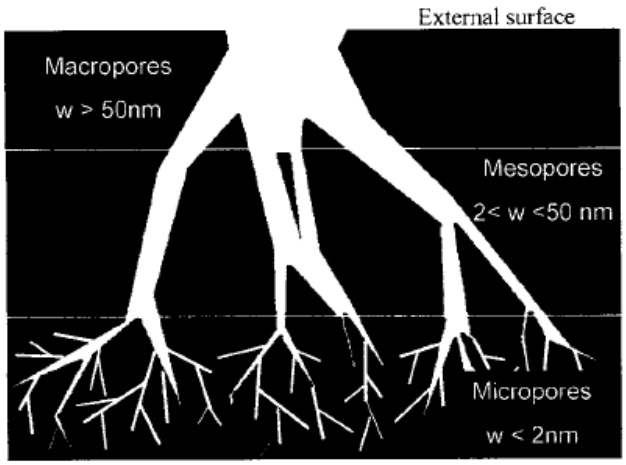

Figure 2.6. Schematic representation of pore network of activated carbon (Bandozs, 2006)

Micropores have pore diameters less than 20 Å (2 nm). "Micropores can be further divided into supermicropores (with a size of 0.7-2 nm) and ultramicropores (<0.7 nm in size)". (Bandozs, 2006) "The adsorption in these pores occurs through volume filling and there is no capillary condensation taking place." (Bansal and Goyal, 2005) They usually have a pore volume range between 0.15 and 0.70 cm^3/g. Micropores contribute about 95 % of the total surface area of the active carbon.

Mesopores, also known as “transitional pores” have pore diameters in the range between 20 Å and 500 Å (2 nm and 50 nm) and mesopore volume generally ranges between 0.1 and 0.2 cm^3/g. “The surface area of these pores does not exceed 5% of the total surface area of the carbon.” (Bansal and Goyal, 2005) Mesopores are characterized by capillary condensation.

Macropores have not considerable significance in the adsorption process since their contribution to the total surface area of the activated carbon is very small and does not exceed 0.5 m^2/g. They have pore diameters greater than 500 Å (50 nm) with a pore volume of 0.2 to 0.4 cm^3/g. Macropores have function as “transport channels” for the adsorbate into the micropores and mesopores. Macropores are characterized by mercury porosimetry and not filled by capillary condensation. (Bansal and Goyal, 2005)

These pores have different roles in adsorption process.

> “Micropores are filled at low relative vapor pressure before the commencement of capillary condensation. The mesopores, on the other hand, are filled at high relative pressures with the occurrence of capillary condensation. The macropores enable adsorbate molecules to pass rapidly to smaller pores situated deeper within the particles of active carbons.” (Bansal and Goyal, 2005)

Pore structure of activated carbon using scanning electron microscopy (SEM) is shown in Figure 2.7.

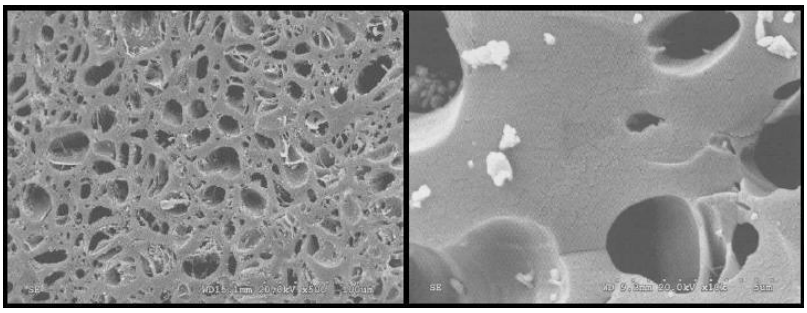

Figure 2.7. Scanning electron micrographs of an activated carbon (Marsh and Rodriguez-Reinoso, 2006)

2.1.7. Chemical Structure of Activated Carbon

Besides the physical and porous structure, the active carbon surface also has a chemical structure (Bansal and Goyal, 2005). Not only the physical and porous structure, but also chemical composition strongly influences the adsorptive properties of active carbon (Smisek and Cerny, 1970).

Activated carbon involves two types of constituent. These are ash and chemically counded elements. Ash inorganic part of the active carbon; whereas and chemically bounded elements organic part of the activated carbon which build up the organic structure with the carbon atoms (Smisek and Cerny, 1970). The chemically bounded structures compose of chiefly oxygen and hydrogen elements, but they may include nitrogen, sulfur, halogens atoms. These heteroatoms are originated from the precursor used and take part in the chemical structure because of imperfect carbonization or they bond chemically to the surface during activation or after treatments (Bansal and Goyal, 2005).

X-ray diffraction studies have revealed that these heteroatoms are bonded to the elementary graphitic crystallites and to carbon atoms, so create surface groups (Bansal and Goyal, 2005). “All of these heteroatoms influence the properties of the carbons in several ways but the greatest influence comes from the presence of oxygen, in particular edge-bonded-oxygen.” (Marsh and Rodriguez-Reinoso, 2006)

Oxygen surface groups are the most significant surface groups, because they effect “the surface characteristics such as acidity, polarity and wettability”; and “the physicochemical properties such as chemical, catalytic and electrical reactivity”. (Bansal and Goyal, 2005) Oxygen-surface groups are widespread surface groups in the active carbon structure. The unsaturated carbon atoms at the edges of the crystallite basal planes are connected with high concentrations of unpaired electrons, which have a significant role in chemisorption. The area of the

edges of basal planes is high, because of the disordered structure of active carbon that caused strong tendency for oxygen chemisorption. Moreover the basal planes of crystallites can have several imperfections and dislocations. These are active centers of oxygen chemisorption and leads to the formation of oxygen functional groups. Oxygen function groups are formed not only by reaction with oxygen but also by reaction with other oxidant gases such as O_3, N_2O, CO_2 and with oxidizing solutions such as HNO_3, H_2O_2. The amount and nature of oxygen functional groups will depend on the surface area and the preparation method. Oxygen can only be removed from surface as CO and/or CO_2 at temperatures above 120 ºC. (Kwiatkowski, 2011)

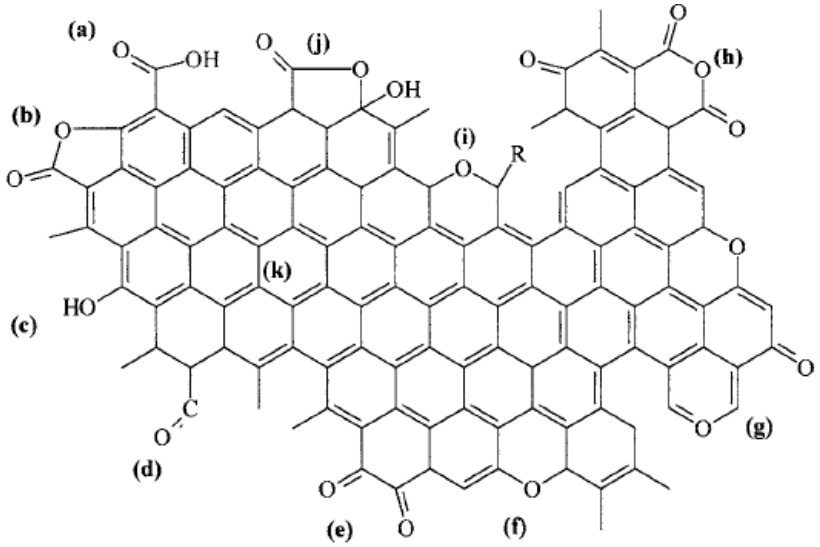

Figure 2.8. Oxygen surface groups found on activated carbon surface: "(a) carboxyl groups,(b) lactone, (c) hydroxyl, (d) carbonyl, (e) quinone, (f) ether, (g) pyrone, (h) carboxylic anhydride, (i) chromene (j) lactol and (k) π electron density on carbon basal planes" (Bandozs, 2006)

Hydrogen is usually present on activated carbons as chemisorbed water, as a part of other surface groups like phenols, carboxylic acids, amines; or bonded to carbon atoms as a part of aliphatic or aromatic structure. "The carbon-hydrogen bond is very stable." (Bandozs, 2006) Complete desorption of hydrogen only

occurs above 1000 ºC so that carbon-oxygen bond breaks on heating at this temperature (Kwiatkowski, 2011). According to Kipling (1956), hydrogen and oxygen are important constituents of an activated carbon for adsorptive properties.

Nitrogen functionalities can also be present in active carbon structure. The nitrogen content is usually very small in active carbon. Depending on the starting material content such as nitrogen-enriched polymers, carbazole, melamine or acridine; or introduced by treatment with nitrogen containing reagents such as urea, melamine, ammonia, types of nitrogen surface groups existing on the carbon structure.

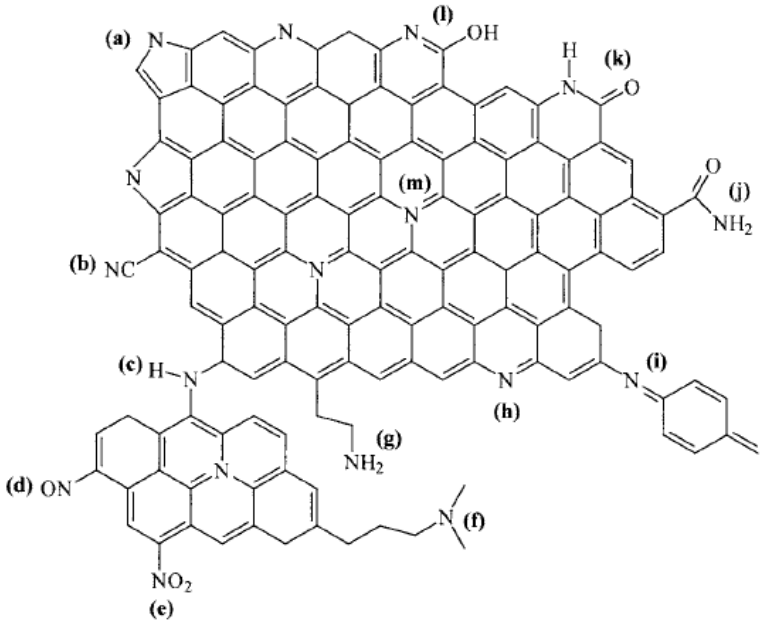

Figure 2.9. Nitrogen surface groups found on activated carbon surface: "(a) pyrrole- like group, (b) nitrile, (c) secondary amine, (d) nitro group, (e) nitroso group, (f) terciary amine, (h) pyridine-like group, (i) imine, (j) amide, (k) lactam, (1) pyridone and (m) quaternary amine" (Bandozs, 2006)

Sulfur can be found in activated carbons as the element itself or as sulfur compounds in low amounts. Carbon-sulfur surface groups can be strongly stable

and might not be removed completely even above 1000ºC, unless the heating is performed in a reducing hydrogen atmosphere.

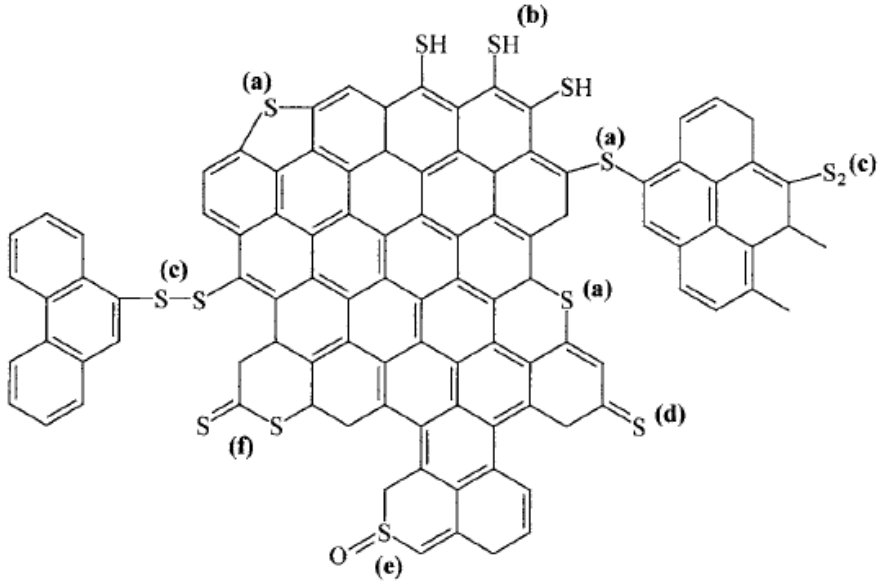

Figure 2.10. Sulfur surface groups found on activated carbon surface: "a) sulfide, b) thiophenol, c) disulfide, d) thioquinone, e) sulfoxide, f) thiolactone" (Bandozs, 2006)

Phosphorous surface groups are contained in active carbon, if phosphoric acid is used as an activating agent in the preparation step. Carbon-phosphorous surface groups can be stable between 500 ºC and 1000 ºC and can be found as red phosphorous and/or in chemically bounded forms. These groups can be formed during the carbonization step at low temperature. (Kwiatkowski, 2011)

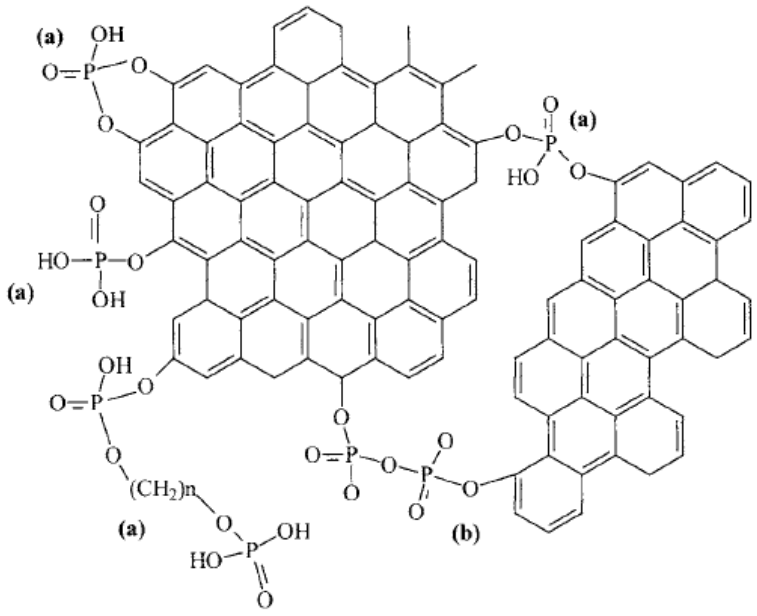

Figure 2.11. Phosphrous surface groups found on activated carbon surface: "a) phosphocarbonaceous esthers, b) pyrophosphate species" (Bandozs, 2006)

2.2. ACTIVATED CARBON PRODUCTION

Properties of activated carbons depend on both the physical and chemical properties of starting material and the production conditions and the type of the production method (Bota et al., 1997). Steps of the activated carbon production are mainly raw material selection, pyrolysis (carbonization) and activation.

2.2.1. Raw Material

Activated carbons are produced from a wide variety of carbonaceous materials such as coal, lignite, wood and cokes. The selection of raw material mostly depends on "its availability, cost and purity". (Kirk Othmer, 2003) Thus attention on biomass is increased worldwide because it is widely available, renewable, low cost and eco-friendly (Karagöz et al., 2008). There are various biomass resources, such as agricultural residues, low grade plants, municipal solid wastes and forest

residues. Due to high carbon content agricultural wastes are good raw materials for production of activated carbon with a “high adsorption capacity”, “low ash content” and “considerable mechanical strength” (Kılıç et al., 2012; Savova et al., 2001; Mohammad Nor et al., 2013).

Agricultural by-products are rich resources of lignocellulosic material which consists of three main components containing cellulose, hemicellulose and lignin. In general, average composition of lignocellulosic biomass is “40-50% of cellulose”, “20-30% of hemi-cellulose”, “20-25% of lignin” and “1-5% of ash” (Rafatullah et al., 2013). In the lignocellulose structure, as hemicellulose surrounds cellulose which is formed from microfibrils (McKendry, 2002). Hemicellulose is linked to cellulose by non-covalent bonds, cellulose binds to lignin as shown in the Figure 2.12 (Xu et al., 2013).

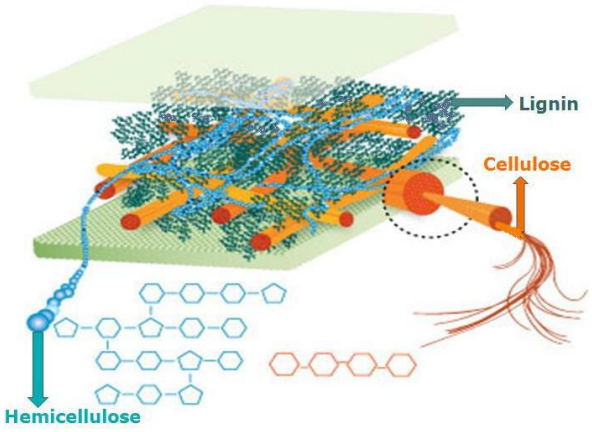

Figure 2.12. Structure of the lignocellulosic biomass (Özmak, 2010)

Any cheap material with a low ash and high carbon content can be a starting material for the preparation of activated carbon. There have been many efforts to produce low cost active carbons from agricultural residues such as corn straw, corn cob, wheat, bagasse, olive stones, almond shells, apricot stones, peach stones, nut shells, hazelnut shells and etc. (Ioannidou and Zabaniotoui 2007). Table 2.2 and Table 2.3 give the proximate and ultimate analysis of some typical sources for the activated carbon production.

Table 2.2. Proximate analysis of some typical sources for activated carbon production (McKendry, 2002)

Material	**Moisture (wt. %)**	**Volatiles (wt. %)**	**Fixed Carbon (wt. %)**	**Ash (wt. %)**
Wood	20	82	17	1
Barley Straw	30	46	18	6
Wheat Straw	16	59	21	4
Bituminous Coal	11	35	45	9
Lignite	34	29	31	6

Table 2.3. Ultimate analysis of some typical sources for activated carbon production (McKendry, 2002)

Material	**C (wt %)**	**H (wt %)**	**O (wt %)**	**N (wt %)**	**S (wt %)**	**Ash (wt %)**
Wood	51.6	6.3	41.5	-	0.1	1
Barley Straw	45.7	6.1	38.3	0.4	0.1	6
Wheat Straw	48.5	5.5	3.9	0.3	0.1	4
Lignite	56.4	4.2	18.4	1.6	-	5
Bituminous Coal	73.1	5.5	8.7	1.4	1.7	9

2.2.1.1. Horse Chestnut Kernel as a Raw Material

The Horse Chestnut (Aesculus Hippocastanum L.) is an endemic species inhabiting the South part of the Balkan Peninsula. Horse chestnut trees are stable and important elements of urban and rural landscapes. In the seventeenth century, it was cultivated to whole of Europe. Since then, it has been used as an ornamental and shade tree in parks and the center of cities. (Cukanovic at al., 2011; Karlinski et al., 2014)

Currently, seeds of horse chestnut kernel are used for ornamental purposes (Castano et al., 2014). Besides, horse chestnut seeds are used in production β-escin, which used in pharmaceutical and cosmetic fields (Marton and Bakan, 1995).

Biochemical composition of the horse chestnut seed was studied by Cukanovic et al. (2011). The horse chestnut seed includes biologically active matters in different amounts depending on time duration of seed preservation. Starch which is organic matter has the highest ratio in the seed. Fats which have a significant role in the pharmaceutical industry come second in the seed composition. Proteins which are organic matter have the lowest ratio. Table 2.4 shows chemical composition of horse chestnut seed according to the two different researchers.

Table 2.4. Chemical composition of horse chestnut seed

	Component	**wt. %**
According to Cukanovic et al. (2011)	Moisture	33.78 – 36.91
	Starch	34.10 – 34.38
	Fat	5.65 – 6.39
	Protein	5.95 to 5.96
According to Marton and Bakan (1995)	Water Soluble Saccharides	6.64
	Non-water Soluble Saccharides	18.10
	Lignin	9.72
	Hemicellulose	10.83
	Cellulose	3.60
	Ash	3.00
	Lipids	13.07
	Proteins	34.37

2.2.2.Pyrolysis

Pyrolysis is a crucial process in biomass combustion and gasification (Fu et al., 2009). Pyrolysis which is thermo-chemical process is one form of energy recovery operation (Demirbaş, 2001; Pütün et al., 2005). Biomass is converted into oil, char and non-condensable gases during the pyrolysis at elevated temperatures about 750 K in the absence of air (Demirbaş, 2001). This thermal process eliminates the moisture and the volatile matters of the biomass. The residual solid char shows different properties than the starting biomass. The significant differences are chiefly in surface area, porosity, pore structure, elemental analysis, composition and ash content (Haykırı Açma et al., 2005). So the char becomes an attractive by product for activated carbon production (Fan et al., 2004).

In general, pyrolysis and carbonization terms are used without any difference, because these processes are almost the same. The thermal degradation of a carbonaceous material under an inert atmosphere where the gaseous and volatiles contents are removed from the material occurs in both pyrolysis and carbonization process. However, there are differences between these processes. Pyrolysis focuses on generation of gaseous and volatile compounds without regard to final char, whereas carbonization focuses on the final char product and its properties and to enrich the carbon content of the material without regard to gaseous compounds (Bandosz, 2006; Mohammad Nor et al., 2013).

The first step of the active carbon production is the carbonization of the starting material. Carbonization occurs in the temperature range of 500-600 ºC under nitrogen atmosphere. Permanent gases and tars which are primary pyrolysis gases are removed during the process. The remaining matter of the process is the char, the base material of the activation process. Temperature, heating rate and residence time effect the char generation and its properties (Rafatullah, 2013). In general, increasing carbonization temperature causes decreasing yield of char and active carbon. In addition, ash content and fixed carbon content is increased,

whereas volatile compound is decreased with temperature rising. So, char with improved quality can be produced at higher temperatures (Ioannidou and Zabaniotou, 2007).

2.2.3. Activation

The char produced in the carbonization process has a developing porous structure and its adsorption properties are not enough for adsorption processes. This porous structure is needed to be enhanced for use as an adsorbent. So, the carbonization step should be followed by activation step for further porosity. (Bandozs, 2006)

The purpose of the activation step is to enlarge the diameter of the pores, increase the pore volume and enhance the porosity of activated carbon. During the activation step, firstly disordered carbon is removed from the structure due to exposure of lignin with activating agents. This causes an improvement of the microporosity. Then the walls between the pores are completely burnt-off, so micropores are widened. This leads to the increasing volume of mesopores and macropores. (Mohammad Nor et al., 2013)

Generally, activation process can be carried out by two main methods; “physical activation” and “chemical activation”. Physical activation uses an oxidizing gas for activation of the chars. The chemical activation uses dehydrating agents for chemical treatment of raw material. (Rafatullah et al, 2013)

2.2.3.1.Physical Activation

Physical activation process is carried out in two steps and involves carbonization of a starting material and activation of the produced char at higher temperature under oxidizing gases.

The raw material is carbonized at temperatures between 400 to 800 ºC under an inert atmosphere to produce char in the carbonization step of the physical

activation. This resulting char has only some microporosity. Thus, a second heat treatment is required to obtain well-developed micropore structure in the presence of oxidizing gases at temperature between 600 to 1000 ºC. This second step is activation. Physical activation is the combination of these two steps and sometimes is called thermal activation. (Kwiatkowski, 2012)

Oxidizing or gasification agents are O_2, CO_2, steam and their mixture. O_2 is uncommonly used in the physical activation. Oxygen reacts with carbon atoms in the precursor surface at high temperatures as follows:

$$2C + O_2 \rightarrow 2CO \quad (1)$$

$$C + O_2 \rightarrow CO_2 \quad (2)$$

These reactions are exothermic and difficult to control. These reactions occur at surface so that improvement of microporosity is insignificant (Kwiatkowski, 2012). The most commonly used oxidizing agents are CO_2, steam and their mixture. With the gasification reaction, carbon atoms extract from the char via reaction of carbon with steam and CO_2 and porous structure with wide range of pores (mainly micropores) produced (Lim et al., 2010). The reactions of carbon with steam and CO_2 can be carried out as follows (Marsh and Rodriguez-Reinso, 2006):

$$C + CO_2 \rightarrow 2CO \qquad \Delta H = +159\ kJ/mole \quad (3)$$

$$C + 2H_2O \rightarrow CO_2 + 2H_2 \quad \Delta H = +75\ kJ/mole \quad (4)$$

$$C + 2H_2O \rightarrow CO_2 + 2H_2 \quad \Delta H = +75\ kJ/mole \quad (5)$$

These reactions are endothermic and slow. Thus, activation process can be easily controlled with these gases, CO_2 and steam (Marsh and Rodriguez-Reinso, 2006).

CO_2 can be easily handled and largely available in different degree of purity, while steam is less expensive for the activation process (Kwiatkowski, 2012). CO_2 and steam influence differently the improvement of microporosity. CO_2 creates and widens small micropores. As a result, activated carbons produced by physical activation with CO_2 represent larger micropore volume and small micropore size (Molina-Sabio et al, 1996). On the other hand, steam widens present micropores. Thus, produced active carbon exhibits larger mesopore and macropore structure (Rafatullah et al., 2013).

2.2.3.2.Chemical Activation

In chemical activation process, the carbonization and activation step is performed together. The raw material is mixed with chemical activation agent and it is followed by heat treatment under inert atmosphere (Ioannidou and Zabaniotou, 2007). Chemical activation provides dehydration and degradation of the lignocellulosic materials and the removal of the organic content (Mohammad Nor et al., 2013; Rafatullah et al., 2013). Chemical activation has a number of advantages; “single step activation”, “low activation temperatures”, “higher yields”, “low activation time” and “better porous structure” (Ioannidou and Zabaniotou, 2007; Rafatullah et al., 2013). Chemical activation has higher carbon yield than physical activation, because chemical activation agents prevent the formation of tar and other undesirable products through the carbonization process (Hayashi et al., 2000).

During the impregnation step, chemical activating agents causes hydrolysis and swelling of carbon structure. Also activation agent occupies some volume which leads to prevention of shrinkage of the structure during heat treatment. When the activating agent is washed from the material after the process, some porosity is formed in the structure (Rafatullah et al, 2013).

In the chemical activation, potassium hydroxide, phosphoric acid and zinc chloride are the mostly used activating agents. During the carbonization, each of activation agents effects activating mechanism and porosity in different way (Kwiatkowski, 2012).

Raw materials with high amount of volatiles such as lignocellulosic materials are preferred in the chemical activation with zinc chloride. Impregnation with $ZnCl_2$ causes hydrolysis reaction that leads to weakening of the structure during the evaporation. As a result, there is an increase in elasticity and swelling of the structure. Also, $ZnCl_2$ prevent the tar formation and the shrinkage of the structure. Thus, impregnation with $ZnCl_2$ provides wide and open microporosity. However, low recovery efficiencies, corrosion problems, the presence of remain zinc in carbon matrix and the need for control of plant emissions are the disadvantages of the chemical activation with $ZnCl_2$ (Bandozs, 2006).

Chemical activation with potassium hydroxide uses a raw material with low volatile content and high carbon content such as high rank coal and petroleum coke. The mechanism of the KOH is different from the other activating agents. KOH reacts with carbon in the structure and produce solid and gaseous products. Hydrogen, metallic potassium, CO, CO_2 and potassium oxide are formed as a result of the reaction.

$$6\,KOH + C \leftrightarrow 2K + 3H_2 + 2K_2CO_3 \qquad (6)$$

Potassium carbonate also decomposes to K_2O and CO_2. With the reaction, a carbon is burnt-off leading to increase porosity. In general, chemical activation with KOH provides activated carbon with high adsorption capacity, narrow microporosity and no mesopores. Activation with KOH is performed under inert atmosphere generally. Air cannot be used because air burn up the raw material and react with the metallic potassium. The porosity developed by steam

atmosphere is lower than by nitrogen. Also, activation under carbon dioxide produces activated carbon with no porosity (Bandozs, 2006).

Raw materials with high volatile content are used in the phosphoric acid chemical activation. Activated carbons produced by phosphoric acid activation have a lower density and more developed mesoporosity. Moreover, the recovery of phosphoric acid can be possible by multiple stage extraction. Materials impregnated with phosphoric acid become elastic since acid separate the cellulose fibers and causes de-polymerization of lignin and hemicellulose. Therefore, tar is formed on the surface of the particle and structure of particle swell. After the de-polymerization of cellulose, dehydration and condensation occurs. These reactions lead to formation of tar and cross-linked structure. The product is washed with water after activation to recover the acid. Water hydrolyzes the phosphate crosslinks and removes the phosphoric acid leaving behind unoccupied volume which causes formation of some porosity in the structure (Marsh and Rodriguez-Reinoso, 2006; Bandosz, 2006; Kwiatkowski, 2011).

During early stage of heat treatment, phosphoric acid firstly attacks lignin and hemicellulose because acid can easily reach lignin and hemicellulose than cellulose. At the intermediate temperatures, removal of volatile compounds and formation of water-soluble product with polymerization cause a significant weight loss. The stabilization and enlargement of the structure result in pore development while the crosslinking, bond cleavage and de-polymerization reactions carry on. The enlargement of the structure provides porosity development. Phosphoric acid inhibits volatile component formation and decreases weight loss. Phosphoric acid also inhibits shrinking through thermal treatment by occupying material surface; due to formation of phosphate and polyphosphate bridges that crosslinked to bio-polymer particles. At higher temperatures carbon skeleton starts to shrink because of the breakage of the phosphate linkages between the cellulose fibers. The micropores widen and the mesoporosity is developed (Jagtoyen and Derbyshire, 1998).

The use of nitrogen as an atmosphere provides the best results for porosity and carbon yield in activation with phosphoric acid. The use of air also gives good results in terms of porosity but lower yield achieved. The use of CO_2 and steam provide active carbons with lower adsorption capacity (Bandozs, 2006).

> "An important factor in chemical activation is the degree of impregnation. This weight ratio of the activation agent to the raw materials is defined as the impregnation ratio. The effect of the degree of impregnation on the porosity of the resulting product is apparent from the fact that the volume of salt in the carbonized material is equal to the volume of pores, which are freed by its extraction. For small impregnation ratios, a small increase in impregnation amount causes an increase in the total pore volume of the product showing an increase in the volume of smaller pores. When the impregnation ratio is further raised, the number of larger diameter pores increases and the volume of the smallest pores decreases." (Balcı, 1992)

Another factor that influences the development of the microporosity during activation is the nitrogen flow rate. The suggested action for its influence on the activation performance is the physical removal of the produced H_2O which in its vapor form is also an activating agent. The higher nitrogen flow rate provides the faster removal of H_2O from the reacting medium (Alcaniz-Monge and Illan-Gomez, 2008).

2.3. CHARACTERIZATION METHODS OF ACTIVATED CARBONS

Characterization of porous materials like activated carbon has been great interest for many decades. The significant development of different methods is observed to describe microporous solids due to their important promotion to improving adsorption capacity.

Because activated carbon has a complex pore network involving micropores, mesopores and macropores, their characterization is a main task to the surface chemist (Marsh and Rodriguez-Reinso, 2006) Thus, a combination of different methods is used for characterization. For a comprehensive characterization of activated carbon porous structure, the structural properties such as the distribution

of pores, pore volumes, surface are of pores and total surface area are necessary to be known. “The adsorption of gases and vapors by standard gravimetric or volumetric techniques and mercury porosimetry” are traditional and suitable methods for the activated carbon characterization. (Özsin, 2011) Transmission electron microscopies, small angle scattering (X-rays or Neutrons) which are the complementary techniques are also used for the characterization of pores (Marsh and Rodriguez-Reinso, 2006; Şenel, 1994).

2.3.1. Adsorption Phenomena and Standard Isotherms

Gas adsorption is one of the most widely used methods for porous materials characterization.

The fundamentals of adsorption phenomena involve definitions. “In experimental adsorption systems, the gas or vapor of a gas phase, or the solute in a solution, is termed adsorptive. An adsorbed phase within a solid is called the adsorbate, and the solid is named the adsorbent.” (Marsh and Rodriguez-Reinso, 2006)

> “In the real adsorption system, the adsorbent is in contact with the bulk phase and the so-called interfacial layer. This layer involves two regions: the part of gas presented in the force field of the solid surface and the surface layer of the solid. The penetration by the adsorbate molecules into the bulk solid phase is determined as ‘adsorption’. The adsorption isotherm is the equilibrium relation between the amount of the adsorbed material and the pressure or concentration in the bulk phase at constant temperature.” (Dabrowski, 2001)

Adsorption process begins with surrounding of solid (adsorbent) by the gas (adsorbate). The forces between the solid surface and adsorbate cause transfer and accumulation of adsorbate gas molecules in the interfacial layer (Yahşi, 2004).

Analysis of adsorption and desorption isotherms of gases and vapors give information about porous structure of adsorbents. Gases such as N_2, Ar, Kr, CO_2 and vapors of low-boiling aliphatic hydrocarbons, benzene, alcohols, water and carbon tetrachloride can be used as adsorbate. Although adsorption of polar

adsorbates gives information about both surface and structural properties of adsorbates, analysis of isotherm data is more difficult than in the case of non-polar adsorbates. Therefore, nitrogen and argon are the most used adsorbates for characterization of porous structure.

Adsorption isotherms of gases and vapors can be determined volumetrically or gravimetrically using various adsorption analyzers.

Gas adsorption isotherms are classified into six shapes with respect to the molecular interactions between the adsorbent surface and gas. After Brunauer et al. (1940) explained 5 isotherms, the types of adsorption isotherms published by IUPAC (1985). Also Gregg and Sing (1982) stated the differences between them with an additional isotherm. Typical shapes of isotherms are given in Figure 2.13.

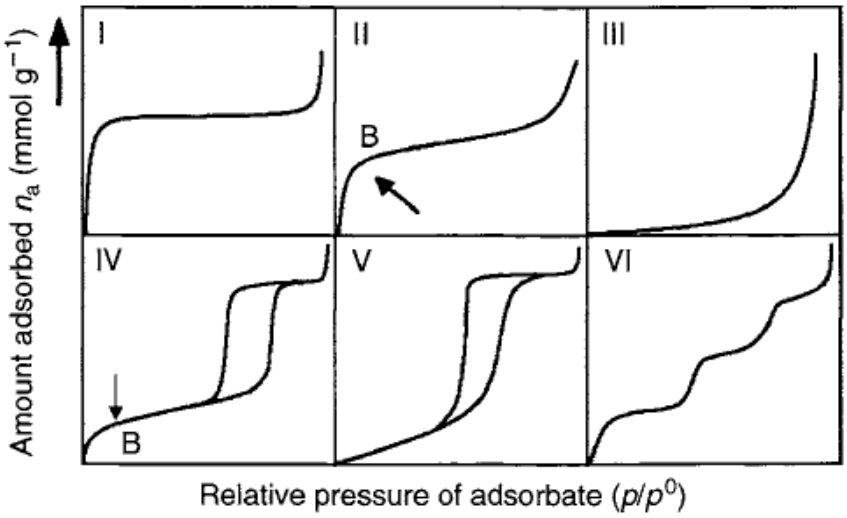

Figure 2.13. The lUPAC classification of adsorption isotherm shapes

Type I isotherms shows a plateau that is nearly horizontal and parallel to the relative pressure axis. This type of isotherms is observed for monolayer (unimolecular) adsorption. The isotherms of most microporous adsorbents are also of Type I. This is because with such adsorbents there is definite saturation limit

corresponding to complete filling of micropores. This isotherm is common to chemisorption and all active sites are covered at the limiting value.

Type II isotherms conform to multilayer physical adsorption. This type of isotherm shows an inflection point in the region of p/p0> 0.1 and p/p0 >0.9. After these inflection points, amount of adsorption increase very rapidly. The adsorption and desorption curves coincide and adsorption desorption hysteresis does not occur between adsorption and desorption curves for Type II and III isotherms. Macroporous and non-porous solids show reversible type II isotherms characteristically.

Type III and Type V isotherms shows convex shape in the whole relative pressure range. The convexity of Type III isotherms continues through the isotherm, whereas the convexity reaches a plateau at high pressure for Type V isotherms. The convexity of the isotherms indicates that the adsorbate-adsorbate interactions are more important than adsorbate-adsorbent interactions. The weak adsorbate-adsorbent interaction causes small adsorption at low pressures. Type III isotherms usually belong to non-porous or highly macroporous adsorbents. Type V isotherms is showed in adsorption of mesoporous or microporous adsorbents.

Type IV isotherms are attained for multilayer adsorption of mesoporous solids. Type IV isotherms is similar to Type II isotherm. Type IV and Type V isotherms show adsorption-desorption hysteresis. After filling mesopores by capillary condensation, the adsorption isotherms levels off. “The amount adsorbed is always greater at any given relative pressure along the desorption branch than along the adsorption branch.” (Bansal and Goyal, 2005) This difference results in hysteresis loop.

Type VI isotherm is a special case and show multilayer adsorption of surfaces with extremely uniform structure.

2.3.1.1.The Brunauer, Emmet and Teller Theory (BET)

Brunauer, Emmet and Teller (1938) derived an equation for multi-molecular adsorption by using Langmuir concept which uses uni-molecular adsorption approach. They generalized Langmuir theory to multi-molecular adsorption. The derived equation is known as BET equation. BET equation has a important role for adsorption studies since it fits the actual isotherms shapes.

Concept of Langmuir is based on some assumptions. The important assumptions are as follows;

- Monolayer adsorption occurs during the adsorption process.
- The adsorbed molecules are attached to certain localized sites and each site holds only one adsorbed molecule.
- The energy state of adsorbed molecules is the same at all localized sites. There is no lateral interaction between the adsorbate molecules. Thus, the surface is homogeneous and smooth in the Langmuir theory.

The BET theory assumes that the Langmuir isotherms are applicable to the every adsorption layer. So, the first layer of adsorbed molecules pretends a base for the second layer of molecules. And this second layer of adsorbed molecules pretends as a base for the third layer and so on. In addition, BET theory assumes the interactions among the adsorbed molecules are negligible as in the Langmuir theory. (Bansal and Goyal, 2005)

The BET equation is derived as;

$$\frac{P}{V(P_o - P)} = \frac{1}{V_m C} + \frac{C-1}{V_m C}\frac{P}{P_o} \tag{7}$$

where; “V is the volume adsorbed at the relative equilibrium pressure P/Po”, “Vm is the monolayer capacity” and “C is a constant”:

$$C = \exp\left[\left(\frac{q_1 - q_2}{RT}\right)\right] \tag{8}$$

where; "q_1 is the heat of adsorption of the first layer", "q_2 is the heat of adsorption of the second and following layers".

The BET theory is presently a standard way to determine specific surface area of solid. A plot of $\frac{P}{V(P_o - P)}$ versus $\frac{P}{P_o}$ gives a straight line with "slope" and "intercept".

$$S = \frac{(C-1)}{V_m C} \quad \text{and} \quad I = \frac{1}{V_m C} \tag{9}$$

Rearrangement of slope and intercept equations gives us;

$$V_m = \frac{1}{(S+I)} \quad and \quad C = \frac{S}{I} + 1 \tag{10}$$

Thus, the two constant Vm and C could be calculated from the slope and intercept, as shown above. If the molecular area Am is known, the specific surface area can be calculated by using following equation.

$$S_{BET} = \frac{V_m A_m N_A}{V_{mol}} \tag{11}$$

The BET equation isotherms are often linear in the relative pressure range between 0.05 and 0.35. The equation fails above and below this region. Because of the surface heterogeneity of the adsorbent, the equation fails at low relative pressures below 0.05. At higher relative pressures, the thickness of the adsorbed layer is limited by narrow micropores. Since capillary condensation occurs with physical adsorption, the equation is not valid above relative pressure of 0.35.

Nitrogen, argon, krypton and carbon dioxide are used as an adsorbate for the characterization of porous structure. But, nitrogen at 77 K is commonly regarded as a suitable adsorbate for surface area determination. “C value of nitrogen at 77 K is small enough to obstruct localized adsorption and large enough to prevent the adsorbed layer from behaving as a two dimensional gas.” (Özsin, 2011) Also, in the multilayer adsorption, nitrogen is not very sensitive to variances in adsorbent structure. Thus, the specific surface area of adsorbents is determined by nitrogen adsorption at 77 K with molecular cross sectional area of 0.162 nm^2. The properties of the gasses used for adsorbent characterization are given in Table 2.5.

Table 2.5. Values of molecular cross sectional areas of adsorbate gases (Marsh and Rodriguez-Reinso, 2006; Özmak, 2010)

Adsorbate Gas	**Temperature (K)**	**Molecular Surface Area (nm^2)**
Nitrogen	77	0.162
Carbon dioxide	195	0.163 – 0.206
Krypton	77	0.152
	195	0.297
Argon	77	0.142 – 0.15

2.3.1.2.Pore Analysis by Adsorption / Desorption Isotherms

The adsorption process on mesoporous adsorbents often shows hysteresis loop among the adsorption and desorption isotherms. The hysteresis loops give information about porous texture of adsorbent.

The adsorption process is reversed by lowering pressure. The desorption step is slower than adsorption since activation energy of desorption is higher (Marsh and Rodriguez-Reinso, 2006). Presence of mesoporosity causes differences in curve on adsorption and desorption and hysteresis loop is formed. The hysteresis is commonly based on thermodynamic and network effects. The capillary condensation or evaporation may be retarded and occurred at lower or higher pressures, this is the thermodynamic effect.

> "The hysteresis may also be caused by pore connectivity (network) effects, which are expected to play an important role in desorption processes. Namely, if larger pores have access to the surrounding only through narrower pores, the former cannot be emptied at the relative pressure corresponding to their capillary evaporation since the latter are still filled with the condensed adsorbate. So the larger pores may actually be emptied at the relative pressure corresponding to the capillary evaporation in the smaller connecting pores (or at the relative pressure corresponding to the lower limit of adsorption−desorption hysteresis)." (Kruk and Jaroniek, 2001)

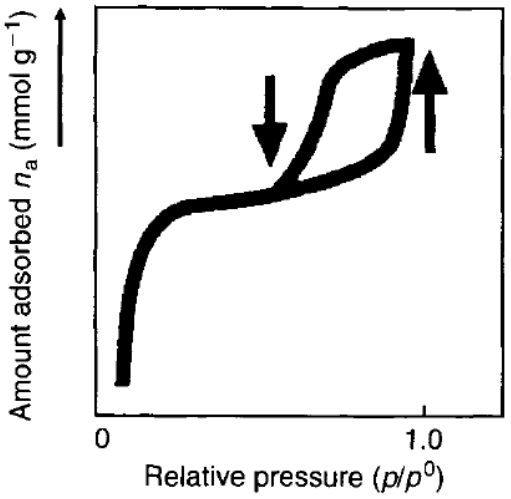

Figure 2.14. The phenomenon of hysteresis in adsorption (Marsh and Rodriguez-Reinso, 2006)

According to the IUPAC, hysteresis loops are categorized into four types that are shown in Figure 2.15.

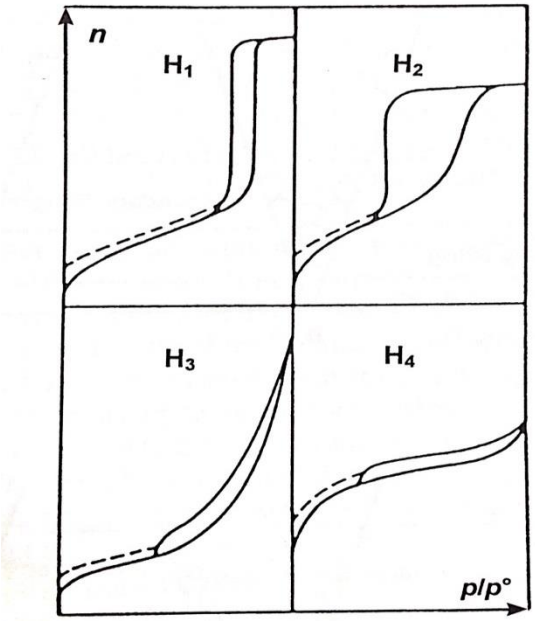

Figure 2.15. Classification of hysteresis loops (Sing et al., 1985)

Type H1 loop shows parallel and almost vertical curves. Adsorbents with cylindrical pore geometry and uniform pore size exhibit H1 hysteresis loops. The shape of H2 loop is triangular and desorption curve is steep. The H2 loops were observed for adsorbent with ink-bottle pores. In the type H3 loops, isotherm do not level-off and do not show limiting value of adsorption at $P/P_0=1$. Porous materials have slit-like pores shows type H3 hysteresis loops. Type H4 loop braches are parallel and nearly horizontal. Adsorption of materials with narrow slit-like pores exhibits this type of loop.

Occurrence of the hysteresis along the isotherms is evidence for existence of the mesopores. The shape and situation of the isotherm connected with the pore

geometry, owing to evaporation and condensation phenomena. These can be defined by “Kelvin's capillary condensation equation” as;

$$r_P = \frac{-2\,\sigma\,V_{mol}\,\cos\theta}{R\,T\,\ln\left[{}^{P}/_{P_o}\right]} \tag{12}$$

where, “r_p is the mean radius of the liquid meniscus”, “σ is the surface tension”, “θ is the angle of contact between the condensed phase and the surface of the solid”, “R is the gas constant”, “T is the absolute temperature”. To find the pore radius by using Kelvin equation it is required to consider “the thickness t of the adsorbate layer”. “The actual pore radius r_p” is given by,

$$r_P = r_k + t \tag{13}$$

The term “r_k is named as the Kelvin radius or the critical radius at which condensation takes place at the required relative pressure”. This radius is not the actual pore radius. “During desorption, an adsorbed film remains on the pore wall when evaporation of the center core takes place.” (Özsin, 2011) A useful analytical expression was developed for “the thickness of the layer t” by Halsey (1948) as a function of the relative pressure,

$$t = t_m\left[\frac{5}{\ln\left({}^{P}/_{P_O}\right)}\right]^{1/3} \tag{14}$$

Here, “t_m is the thickness of the monolayer”. Thus, substituting equation (12) and equation (14) into equation (13) for nitrogen as the adsorbate at its normal boiling point of -195.6°C, with t_m as 0.354 nm, the following equation is found:

$$r_P = \frac{4.15}{\log\left({}^{P}/_{P_O}\right)} + 3.54\left[\frac{5}{2.303\,\log\left({}^{P}/_{P_O}\right)}\right] \tag{15}$$

For the derivation of equation (15), nitrogen molecules are assumed to have closely packed hexagonal liquid structure.

> "For a symmetrical pore geometry, calculation of the size distribution of the mesopores from the adsorption or desorption data permits a simple determination of the mesopore surface area. The gas volumes adsorbed or desorbed upon a change of the relative pressure are taken from the isotherms, and Equation (15) is used to calculate the corresponding mesopore radius. Assuming certain pore geometry, the contribution to the surface area from the pores of various sizes can be found from the pore radius distribution." (Çuhadar, 2005)

2.3.1.3.Methods for Determination of Porous Structure

"Due to non-uniform structures of porous materials which include micropores, mesopores and macropores together, several methods have been developed to determine the porous texture of materials by several investigators." (Özsin, 2011)

Gas adsorption gives information about both of the surface area and pore volume, porous structure, pore shape of the material. This data are gained from the isotherms. Different theories are applied through the isotherm shown in Figure 2.16.

Pore structure of the material is determined by using different methods such as αs method, t–plot, Dubinin Astakhov (DA), Dubinin Radushkevich (DR), Saito Foley (SF), Horvath-Kawazoe (HK), Barrett, Joyner, Halenda (BJH) methods and Density Functional Theory (DFT).

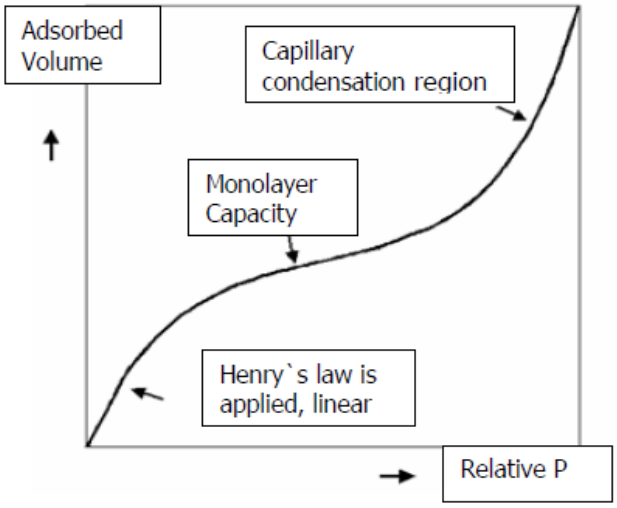

Figure 2.16. Region of physisorption isotherms (Ok, 2005)

2.3.1.3.1. The t-plot method

"The t-plot method is used in the determination of micro and mesopores based on modeling a multilayer formation. In this method statistical layer thickness is calculated as a function of relative pressure according to the several mathematical expressions like de Boer, Halsey and Harkins methods. t-plot curve is obtained as a graphical representation of the relationship between volume adsorbed and statistical thickness at each relative pressure value. The linear range occurs between monolayer formation and capillary condensation. Hence, it is possible to estimate the complete micropore filling and initiation of the mesopore filling by the plot. Also the external area of the porous material (area of mesopores, macropores with the outside surface area) and micropore volume and area can be derived from the plot." (Özsin, 2011)

2.3.1.3.2. α_s Method

"In the αs method, a comparison between the tested isotherm and a normalized reference isotherm obtained from a sample of known surface area, is carried out. Without any assumption or calculation of statistical thickness as it is been in t-plot method, a plot of the amount adsorbed versus αs values is obtained. Similar to t-plot, linear range of plot occurs between monolayer and capillary condensation. Assessment of microporosity with mesoporosity is also possible." (Özsin, 2011)

2.3.1.3.3. Dubinin Radushkevich (DR) Method

"Dubinin and Radushkevich proposed an equation that is based on the Polanyi's potential theory and micropore filling." (Özsin, 2011)

The equation is as follow;

$$\log W = \log W_O - k \left[\log\left(\frac{P}{P_O}\right)\right]^2 \quad (16)$$

k and W_o are defined as;

$$k = 2.303\, K \left(\frac{RT}{\beta}\right)^2 \quad (17)$$

and

$$W_O = V_O\, \rho \quad (18)$$

"'W', 'ρ' and 'Vo' are weight adsorbed, liquid adsorbate density and micropore volume, respectively. An identical degree of filling of the volume of adsorption space is stated by Dubinin and Raduskevich and called the affinity coefficient, 'β', which is a constant as the ratio of adsorption potentials of any two vapors. The term 'K' is also a constant that was determined by the shape of the pore size distribution." (Özsin, 2011)

2.3.1.3.4. Dubinin Astakhov (DA) Method

"DA method is related with DR method. In the case of non-homogeneous surface and texture, DA method is more preferable. This method is also based on the micropore filling mechanism. Dubinin-Astakhov parameter and average adsorption energy are considered in the method. Dubinin-Astakhov parameter depends on surface heterogeneity and effects the width of the resulting pore size distribution." (Özsin, 2011)

2.3.1.3.5. Horvath-Kawazoe (HK) Method

"Horvath-Kawazoe (HK) method is a semi-empirical, analytical method which is based on micropore filling mechanism. The calculation depends on slit-shaped pore model assumption for activated carbons. HK method considers the effect of pore geometry and the strength of the attractive adsorptive-adsorbent

interaction on the adsorption potential. But imperfection of this method comes from that it does not differentiate the thermo-physical properties of bulk fluid from the fluid in the pores. Also, mesopore analysis is not applicable by this method. Calculation of pore size distributions from the low relative pressure region of adsorption isotherms is possible by an expression derived which is a relationship between pore size and relative pressure and this expression also includes magnetic susceptibility of adsorbent and adsorbate molecules." (Özsin, 2011)

2.3.1.3.6. Saito-Foley (SF) Method

"Since HK method has been developed for slit-shaped pores, another expression like HK was developed for cylindrical pore geometry. Calculation of SF method is also restricted to micropore region as it was in HK method." (Özsin, 2011)

2.3.1.3.7. Barrett, Joyner, Halenda (BJH) Method

"BJH method is also cited as the modified form of Kelvin equation and measures mesopore size distribution. This method is based on a combination of physical adsorption and capillary condensation mechanism (Kelvin equation for hemispherical meniscus). It includes the analysis of desorption isotherm instead of adsorption isotherm. But, some studies with this method includes the study of both desorption and adsorption branch of isotherms although it can't be justified theoretically.

The deficiency of this method is that it does not consider the fluid-solid interactions on capillary condensation. But it is still a convenient method and it is considered one of the main methods in the pore size distributions despite the questions raised about its validity and limitations." (Özsin, 2011)

2.3.1.3.8. Density Functional Theory (DFT)

"Instead of other methods used in determination of pore structure, DFT is based on statistical thermodynamics on a molecular level. This method associates microscopic properties of the system such as fluid-fluid and fluid-solid interaction parameter, pore size, pore geometry and temperature with the adsorption isotherms. Complex modeling of microscopic system properties results in more realistic density profiles as a function of pressure and temperature. By this way, amount adsorbed, transport properties of the system and heat of adsorption can be derived from density profiles closely to the actual value. In summary, DFT method includes constructing an equation called a

grand potential functional of the average density of the adsorbate and find equilibrium density profile to obtain quantity of adsorbed at each pressure that yields isotherms.

For a wide variety of materials, pore geometries and analysis conditions for individual isotherms have created for specific adsorbent/adsorbate pairs and these isotherms are available by software programs. Hence, it is possible to find pore size distribution of materials such as activated carbon by matching the isotherm with the tested material. Although DFT is an important achievement in the determination of pore size distribution, isotherms used require an improvement to incorporate the surface heterogeneity effect." (Özsin, 2011)

2.4. PREVIOUS STUDIES DONE ON THE PRODUCTION AND CHARACTERIZATION OF ACTIVATED CARBON

There have been various studies on the activated carbon preparation and characterization over the years. This part presents some recent works and studies on influences of different parameters on preparation and characterization of activated carbon.

2.4.1. Physical Activation Studies

Valente Nabais et al. (2011) prepared activated carbon by physical activation with carbon dioxide, CO_2 from almond shell. The precursor, almond shell was first carbonized at 400 ºC for 1 hour under nitrogen flow. Then almond shell was activated under CO_2 atmosphere at 700 ºC for 1, 2, 3, 5 and 7 hours and 800 ºC for 0.5, 1, 2, 3 and 5 hours to get burn-off between the range of 12 - 70 wt.%. The burn-offs of samples were determined. To characterize produced activated carbons, nitrogen adsorption at 77 K analysis was performed and the isotherms were examined by using BET, DR and αs methods. The nitrogen isotherms showed that isotherms of produced activated carbons conformed to Type I. It is concluded from the isotherms that mesoporosity did not influenced by the

temperature and time and the mesopore volume remained low through the activation. Pore size distributions showed that products had a well-developed microporous structure. Pore distribution got wider, a small band showed up in the mesopore region with increasing burn-off degree. BET surface area is increase with burn-off degree. The BET surface area values of products were between 364 and 745 m^2/g for activation temperature of 700 ºC, 548 and 1138 m^2/g for activation temperature of 800 ºC. The maximum BET surface area was reached as 1138 m^2/g for activation temperature of 800 ºC and activation time of 5 hours.

Demiral et al. (2011) worked activated carbon production from olive bagasse by physical activation with steam and characterization. Pyrolysis of olive bagasse was carried out at 500 °C under nitrogen flow rate to obtain char product. Then, the char was activated at temperatures of 750, 800, 850 and 900 °C for 30, 45 and 60 minutes using steam as activation agent. When the temperature increased from 750 to 900 °C, weight loss of the products were increased due to releasing of volatiles and removal of carbon through the carbon-steam oxidation. Produced activated carbons were characterized through nitrogen adsorption at -196 °C. All shapes of isotherms exhibited Type I indicating mainly microporous structure; form of pores were ink bottle that were determined from adsorption-desorption isotherms. Pore size distributions also confirmed that activated carbon samples had micro and mesoporous structure. The present pores were developed and new pores were generated with increasing the activation temperature and time except activation temperature at 900 °C. They considered that increasing activation time 45 to 60 min for 900 °C activating temperature could cause conversion of some micro and mesopores to macropores due to over burn-off. It was concluded that activated carbons produced from olive bagasse by steam activation were mainly microporous. In this work, a maximum BET surface area was attained as 1106 m^2/g at activation temperature of 900 °C for activation time of 45 minutes.

Effects of activation time, activation temperature and CO_2 gas flow rate on activated carbon from date palm tree fronds by one step physical activation were studied by Shoaib and Al-Swaidan (2015). Pyrolysis and activation of raw material were performed together. Pyrolysis of the precursor carried out under nitrogen gas. After reaching chosen activation temperature, the gas atmosphere was switched with CO_2 which was activation gas. At the end of activation, cooling was done under nitrogen atmosphere. To investigate effect of activation temperature, the physical activation was performed in temperature range of 700 to 1000 K. The BET surface area of the samples increased with increasing temperature up to 850 K due to the formation of new pores. After this temperature, a decreasing trend of surface area was observed. The effect of activation time was also determined for activation time between 15 to 60 minutes at 850 K. Similarly, the BET surface areas were increased initially with raising activation time up to 30 minutes than decreased. They came up with that enlargement of existing pores and merging of pores owing to collapse of pore walls could cause decreasing surface area at higher temperatures and longer contact times. Also impact of CO_2 gas flow rate on the pore characteristics of active carbon was examined under gas flow rate of 25 to 250 cm^3/min. The BET surface area reached maximum value at 50 cm^3/min CO_2 flow rate. It was concluded that, higher flow rates reduce diffusion of molecules in the pore structure and lead to decreasing the BET surface area. From nitrogen adsorption-desorption isotherms, it was seen that activated carbons are mainly microporous and smaller mesoporous with slit-shape pores. as a conclusion, the suitable conditions for preparation of activated from date palm tree fronds by physical activation were determined as activation temperature of 850 K, activation time of 30 minutes and CO_2 flow rate of 50 cm^3/min. The produced activated carbon under these conditions had the BET surface area of 1094 m^2/g with mainly microporous structure with a little mesoporosity.

2.4.2. Chemical Activation Studies

Xu et al. (2014) obtained activated carbon from reedy grass leaves by chemical activation with phosphoric acid. Sieved reedy grass leaves were impregnated with 60 wt. % H_3PO_4 at impregnation ratio of 0.88:1 for impregnation time of 4 h. Chemical activation was performed at 400, 500, 600, 700 and 800 ºC, for 1, 2, 3 and 4 hours under nitrogen atmosphere. Characterization of produced active carbons was determined by nitrogen adsorption. The results showed that BET surface area and micropore volume increased first then reduced with increasing temperature. When the temperature reached 500 ºC, the new micropores formed; then after this temperature existing micropores enlarged. They explained this that phosphorous species may tent to boil and lead to enlargement of the structure during the carbonization. Changing of activation time also affected of the porous structure same as temperature. When the activation time raised 1 hour to 2 hours, again BET surface area and micropore volume increased. But, increasing the activation time from 2 to 5 hours effected the BET surface area and micropore volume negatively. They connected this effect with that the longer activation times lead to enlargement and collapse of pores. They determined the ideal conditions of activated carbon production from reedy grass leaves by phosphoric acid activation as activation temperature of 500 ºC and activation time of 2 hours. Produced activated carbon under these conditions had 1474 m^2/g BET surface area, 0.560 cm^3/g micropore volume. Also, the pore size distribution showed that obtained activated carbon structure is predominantly micro and mesoporous.

A study for production and characterization of activated carbon by chemical activation was done by Al Bahri et al. (2012). They used grape seeds as a raw material in their study. Chemical activation agent was chosen as phosphoric acid. Grape seed impregnated with phosphoric acid at different ratios of 1:1, 2:1, 3:1 and 4:1 (H_3PO_4:sample) for 2 hours. Chemical activation was conducted under nitrogen atmosphere at temperature ranging between 350 and 550 ºC for 2 hours

activation time. Prepared activated carbons were characterized by nitrogen adsorption at 77 K. Activated carbon prepared at lower temperatures showed predominantly microporous structure, whereas activated carbon prepared at higher temperatures showed mainly microporous with developing mesoporous structure. Pore size distributions showed that increasing temperature cause to widening pores up to 500 ºC and then pore volume was slightly decreased. This effect lead to increasing up to 500 ºC and then decreasing of The BET surface area. Also effect of impregnation ratio was studied at activation temperature of 500 ºC. Nitrogen adsorption isotherms showed type II which indicating to microporous structure with small mesoporosity. The increasing impregnation ratio 1:1 to 3:1 led to increase BET surface area and widening porous structure. A further increase in the ratio up to 4:1 caused mesoporosity with ultra-micropores. This was attributed to that excess of phosphoric acid could result in formation of surface group in the pore mouths, leading to creation of narrower pores. The maximum BET surface area and mesopore volume were attained as 1139 m^2/g and 0.24 cm^3/g for conditions of 3:1 impregnation ratio and 500 ºC activating temperature. Produced by phosphoric acid activation of grape seeds had microporous structure with a significant support of mesoporosity.

Hayashi and co-workers (2000) studied the effect of chemical activation agent on activated carbon pore structure. Activated carbons prepared from lignin by chemical activation at activation temperature between 500 to 900 ºC for 1 hour of activation time under nitrogen atmosphere. $ZnCl_2$, H_3PO_4 and alkali metals compounds of K_2CO_3, Na_2CO_3, KOH, NaOH were used as a chemical activating reagents. The activated carbons were characterized by nitrogen adsorption at 77 K. The results of the nitrogen adsorption analysis showed that the maximum BET surface areas of produced activated carbons by $ZnCl_2$ and H_3PO_4 activation observed at 600 ºC and these activated carbons were well developed microporosity. In contrast, the maximum BET surface area of activated carbon produced by alkali metal compounds activation was achieved at 800 ºC. The

mesopore volume of these activated carbons increased with activation temperature. They suggested that these results indicated that at temperature greater than 600 ºC, alkali metals works efficiently as activating agent; but $ZnCl_2$ and H_3PO_4 did not. The activated carbon produced by K_2CO_3 activation has a surface area of about 2000 m^2/g. It was concluded that $ZnCl_2$ work efficiently as dehydration agents below 600 ºC whereas K_2CO_3 works effectively above 600 ºC.

Gomez-Serrano et al. (2004) used chestnut wood as a raw material for production of activated carbon by phosphoric acid chemical activation. The influence of phosphoric acid concentration (by weight 1:1, 1:2, 1:3 water/ 85 wt % H3PO4) and activation temperature (300, 400, 500 and 600 ºC) on activated carbon structure were investigated. Carbonization and activation were carried out under nitrogen atmosphere for 4 hours of activation time. The products were characterized by nitrogen adsorption at -196 ºC. Results of the N_2 adsorption analysis showed that BET surface areas increased with phosphoric acid concentration, whereas increased first with activation temperature 300 to 500 ºC and then decreased at 600 ºC. This result was linked with that stabilization of phosphorous thermally lead to effect undesirably porous texture. N_2 adsorption desorption isotherms which belonged to Type I showed activated carbons were nearly microporous. Micropore volumes were much higher than mesopore volume for all prepared activated carbons. Micropore region in the pore size distribution of both activated carbon activated at 400 and 500 ºC were similar for different phosphoric acid concentrations. On the other hand, the micropore structure of activated carbon which activated at 300 ºC was more heterogeneous at highest phosphoric acid concentration, whereas that of activated at 600 ºC was more heterogeneous at lowest acid concentration. In this study, the highest BET surface area was achieved as 783 m^2/g for activated carbon produced at 500 ºC for 1:3 water/phosphoric acid concentration.

Kılıç and friends (2012) produced activated carbon from Euphorbia rigida by chemical activation with different activating agents ($ZnCl_2$, K_2CO_3, NaOH and

H_3PO_4) and different impregnation ratios (25, 50, 75 and 100 wt. %). Chemical activation was conducted at 700 ºC for 1 hour activation time under nitrogen. N_2 adsorption at 77 K was used for characterization of activated carbons. It was found that, yields of carbon decreased with increasing impregnation ratio due to the gasification of char by chemicals. N_2 adsorption – desorption isotherms showed that the highest nitrogen uptakes attained for activated carbon produced by K_2CO_3 activation. N_2 adsorption - desorption isotherms also exhibit hysteresis loop which indicate mesoporosity. The maximum BET surface area was attained as 2613 m^2/g for K_2CO_3 activation with 75 wt. % of impregnation ratio; 1115 m^2/g for $ZnCl_2$ activation with 75 wt. % impregnation ratio; 396 m^2/g for NaOH activation with 100 wt. % impregnation ratio; 790 m^2/g for H_3PO_4 activation with 100 wt. % impregnation ratio. It was seen that NaOH has insignificant effect on activated carbon producing with high surface area. Pore structures of activated carbons were also determined. Activated carbons by K_2CO_3 and $ZnCl_2$ activation showed developed microporosity, whereas H_3PO_4 chemically activated carbons were mainly mesoporous structure. It was concluded that K_2CO_3 was more effective activation agent in terms of high BET surface area and porosity development.

Timur et al. (2010) prepared activated carbon from oak cups pulp by chemical activation. They studied the effect of impregnation time (2 h to 24 h at 110 ºC), impregnation ratio (0.4:1 to 1:1 chemical agent/sample by weight) and chemical activation agent ($ZnCl_2$ and $H3PO_4$). Chemical activation experiments were carried out under nitrogen at 600 ºC of activation temperature for 2 hours of activation time. Nitrogen adsorption analyses were done for characterization. They observed that the surface area slightly increased with impregnation time from 2 to 4 hours and then remained nearly constant. Thus, it was concluded that impregnation time had no effect on activated carbon. The BET surface area increased with increasing impregnation ratio for both activating agent of $ZnCl_2$ and H_3PO_4. The highest BET surface area obtained for $ZnCl_2$ activation. When the

ash contents of activated carbon were considered, lowest impregnation ratio gave the lowest ash content. On the other hand, the ash contents of activated carbons activated by $ZnCl_2$ were notably lower than activated by H_3PO_4. Zinc salts contained in carbon mass are soluble and easily removed during washing process. In contrast, impregnation with phosphoric acid leads to formation of insoluble phosphates which connected and cross-linked to carbon matrix. Adsorption isotherms and pore size distributions also indicated that both of activated carbon prepared by $ZnCl_2$ and H_3PO_4 were microporous, but activated carbon prepared by H_3PO_4 showed more developed mesoporosity. The suitable conditions for preparation of high surface area activated carbon from oak cups pulp in this study was found as 1:1 of impregnation ratio, 4 hours of impregnation time and $ZnCl_2$ of chemical agent. The best BET surface area was obtained as 1152 m^2/g for these conditions.

Anas Nahil and Williams (2012) studied pore characteristics of activated carbon produced by phosphoric acid chemical activation of cotton stalks. Chemical activation was performed under nitrogen at various temperatures between 500 and 800 ºC and at various impregnation ratios between 0.3 and 3 (H_3PO_4 to cotton stalks). Characteristics of prepared activated carbons were examined by nitrogen adsorption at 77 K. When impregnation ratio increased from 0.3 to 1.5, the surface area increased. However, when impregnation ratio reached to 3, the surface area decreased. On the other hand, mesopore volume increased continually with increasing impregnation ratio. They thought that when large amount of acid impregnated, the presence of phosphate and polyphosphate species in the carbon matrix might block some of created pores after washing. The effect of activation temperature was evaluated for impregnation ratio of 1.5. As the temperature increased from 500 to 700 ºC, the BET surface area decreased and then increased at 800 ºC. This might be due to the collapse of pores at high temperatures which lead to increase in porosity. But increase in BET surface area at 800 ºC might due to the partial gasification of the carbon by P_2O_5 and

elimination of $H_2PO_4^{-1}$ and $H_2P_2O_7^{-2}$. Adsorption isotherms and pores size distributions showed that when impregnation ratio increased, isotherms shows hysteresis loops. At lower impregnation ratio, produced activated carbon was mainly microporous. At higher impregnation ratio, the hysteresis loops showed pores were slit-shaped. Adsorption desorption exhibit hysteresis loop which appeared to combination of type I and type IV. Produced activated carbons were microporous and developed mesoporous with slit-shape pores. Mesoporosity developed with increasing activation temperature. The maximum BET surface area was attained as 1720 m^2/g for activated carbon produced at 500 ºC and 1.5:1 impregnation ratio. This activated carbon was microporous and developed mesopore with slit-shape pores.

2.4.3. A Study Done with Horse Chestnut Kernel

There is only one study performed with horse chestnut kernel to produce activated carbon.

Momcilovic et al. (2011) prepared activated carbon from horse chestnut kernel by phosphoric acid chemical activation. 85 % phosphoric acid was used with impregnation ratio of 1:1 by weight (phosphoric acid/horse chestnut kernel). Two phase temperature regimes were applied to impregnated sample for carbonization and activation processes. Carbonization and activation process was performed under nitrogen atmosphere to inhibit oxidation of the product. Firstly, impregnated sample was heated room temperature to 170 ºC with heating rate of 6 ºC/min and held at 170 ºC for 1 hour. Then, heating was continued from this temperature to 500 ºC with heating rate of 8 ºC/min. After reaching temperature of 500 ºC, temperature was held constant for 1 hour. Obtained product was washed with hot distilled water until residual activating agent was removed and dried at 110 ºC for 24 hours. The product was characterized by nitrogen adsorption at -196 ºC. The surface area was determined by using the BET; the mesopore volume and surface area determined by using BJH; the micropore volume was determined by

using DR equation. Methylene Blue adsorption was also performed to get information about adsorption capacity of produced activated carbon. In this study, a surface area of 663.9 m^2/g, a bulk density of 1.41 g/ml, a yield of 47.7 % and methylene blue number of 157.7 mg/g was attained with horse chestnut kernel. Produced activated carbon showed mainly mesoporous structure. Results were shown that horse chestnut kernel is a good precursor as an agricultural waste for production of activated carbon.

CHAPTER 3

MATERIALS AND METHODS

3.1. MATERIALS

3.1.1. Raw Material Preparation

In this work, horse chestnut kernels (seeds) were used as a raw material for activated carbon production. Horse chestnuts were gathered from Middle East Technical University Ankara Campus in the year of 2013. Air –dried horse chestnut kernels were not subjected to chemical treatments like washing with chemicals. After separation of kernels from shells, kernels crushed and sieved to a particle size between 18 and 10 mesh (1 and 2 mm). All the milled and sieved horse chestnut kernels were saved in a sealed plastic box at the room temperature.

The moisture, volatile matter and ash contents of the air-dried horse chestnut kernel were determined from proximate analysis by using the ASTM standards of E871, E872 and D1102.

Table 3.1. The proximate analysis of the air-dried horse chestnut kernel

Content	**Percentage (wt. %)**
Ash	2.04
Volatile Matter	85.66
Moisture	6.03
Fixed Carbon	6.27

Elemental analysis of air-dried raw material was also performed through CHNS-932 (LECO) elemental analyzer located in Central Laboratory at METU. Result of elemental analysis given in Table 3.2.

Table 3.2. The elemental analysis of the air-dried horse chestnut kernel

Content	**Percentage (wt. %)**
Carbon	42.89
Hydrogen	7.32
Nitrogen	1.02
Sulfur	-
Oxygen (by difference)	48.77

3.1.2.Activation Agent

Chemical activation experiments were carried out with 50 wt. % phosphoric acid. 50 wt. % H_3PO_4 was prepared by diluting of 85 wt.% ortho-phosphoric acid (J.T. Baker) with deionized water.

3.2. EXPERIMENTAL METHODS

3.2.1. Experimental Set-up

All the carbonization and activation experiments were performed in a horizontal tubular furnace, “Lenton Unit C2”. A quartz tube with diameter of 30 mm and length of 90 cm was placed into the furnace to hold the sample. An oval quartz boat with diameter of 17 mm and length of 50 cm and a quartz rod were used for locating the sample in the process zone.

The inlet and the outlet of quartz tube connected with quartz fittings, to inhibit the entering of air to the furnace. Also a flowmeter was placed to the inlet of furnace to N_2 flow rate.

The outlet gases were kept in a cooling bath and the non-condensable gases were gave off from the system. Figure 3.1 shows experimental set-up used for production of activated carbon.

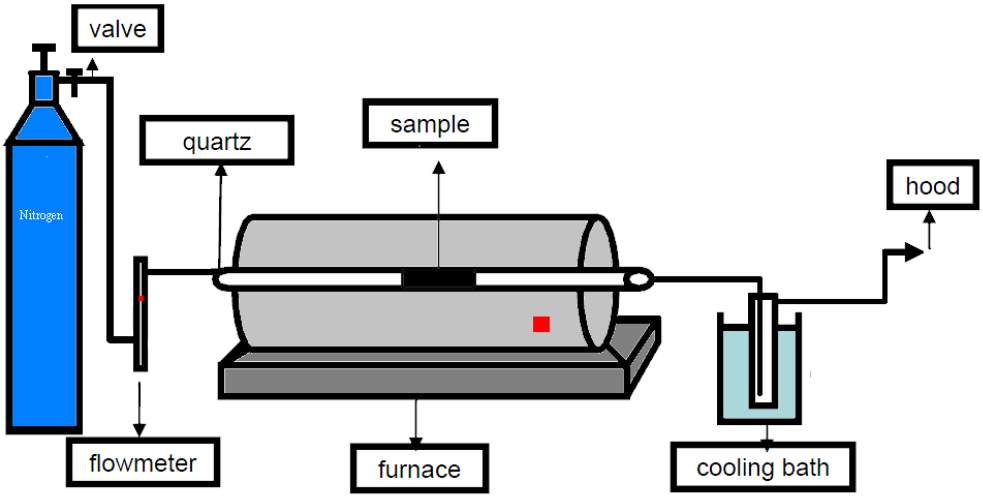

Figure 3.1. Experimental set-up

3.2.2. Carbonization and Activation Process

To produce activated carbon from the horse chestnut kernels, air-dried raw material were impregnated with 50 wt. % phosphoric acid at room temperature in two different impregnation ratios as 1:1 and 1:2 (weight of H_3PO_4 / weight of kernels) by weight Mixtures of phosphoric acid and horse chestnut kernels were impregnated for 24 hours at room temperature. Finally, samples were ready for carbonization and activation process.

In this study, activated carbons were produced by chemical activation method. Thus, carbonization and activation steps were performed simultaneously. For this purpose, phosphoric acid impregnated samples were heated from room temperature to the chosen activation temperatures under nitrogen atmosphere with a heating rate of 10 ºC/min. Activation temperatures ranged between 300 to 800 ºC. After reaching desired activation temperature, temperature was kept constant for activation time of 1 hour. Process conditions which were constant are shown in Table 3.3.

Table 3.3 . Process conditions of carbonization and activation experiment

Particle Size	10 -18 mesh
N_2 Flow Rate	100 cm^3/min
Heating Rate	10 ºC/min
Activation Time	1 hour

After carbonization and activation experiment, samples were cooled down. Carbonized and activated samples were washed with hot distilled water to remove excess phosphoric acid and derivatives until neutral pH. Washed products were filtered and dried in an oven at 105 ºC for 24 hours to remove moisture. They were saved in sealed plastic boxes for characterization tests and coded according to experimental conditions. Coding of the product are given in Table 3.4.

Table 3.4. Experimental variables and samples coding

Raw Material	Impregnation Ratio (w/w)	Temperature (°C)	Sample Code
Horse Chestnut Kernel	1:1 (H_3PO_4:Kernels)	300	AC-1-300
		400	AC-1-400
		500	AC-1-500
		600	AC-1-600
		700	AC-1-700
		800	AC-1-800
	2:1 (H_3PO_4:Kernels)	300	AC-2-300
		400	AC-2-400
		500	AC-2-500
		600	AC-2-600
		700	AC-2-700
		800	AC-2-800
Reproducibility Experiments			
Horse Chestnut Kernel	**2:1 (H3PO4:Kernels)**	500	AC-2-500-R
		700	AC-2-700-R

Entire processes applied for the production of activated carbons are presented in the Figure 3.2.

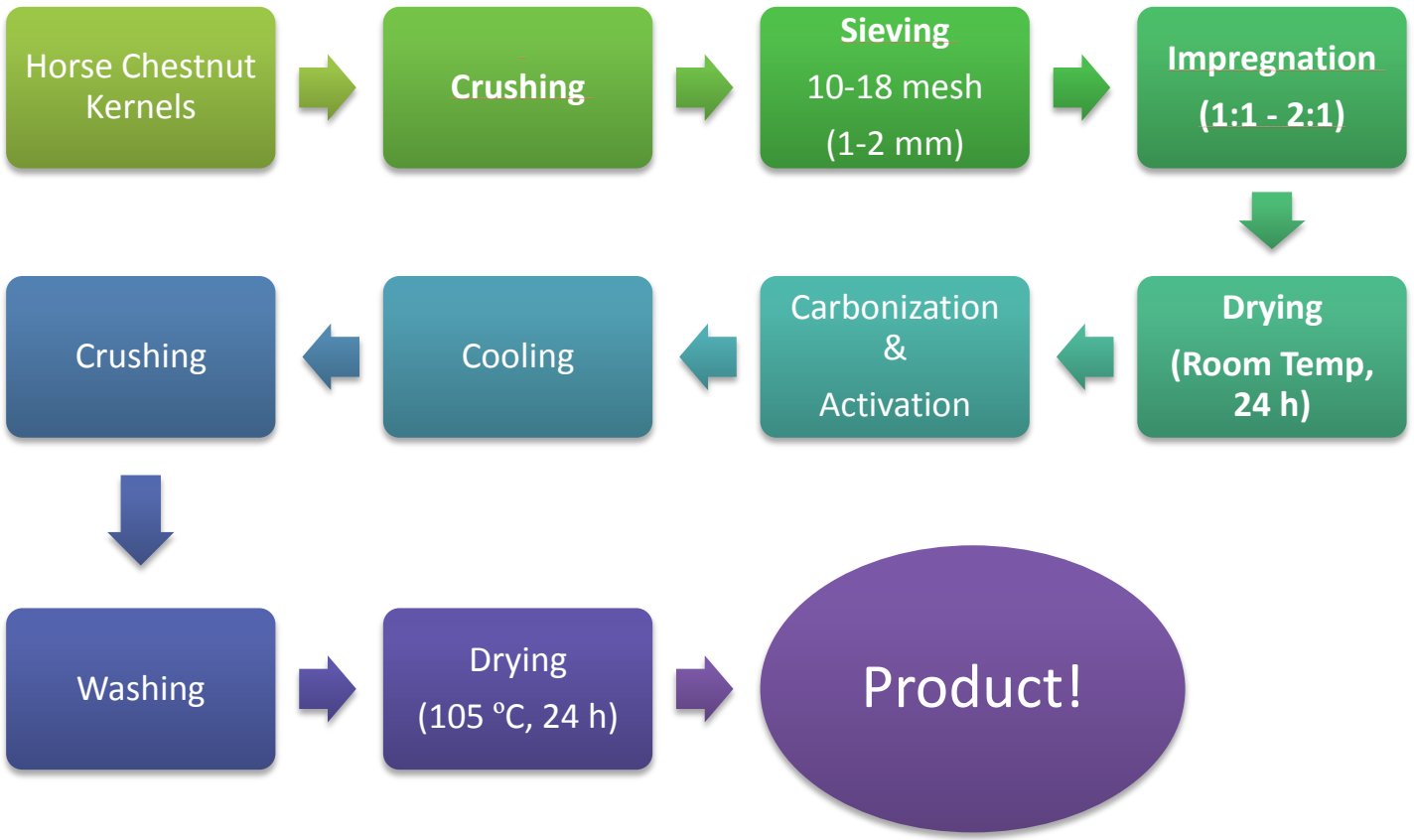

Figure 3.2. Schematic representation of production of activated carbon from horse chestnut kernel

3.3. CHARACTERIZATION OF THE PRODUCTS

Characterization of activated carbons was carried out by nitrogen gas adsorption at -195.6 ºC (77 K) in terms of surface area, isotherm and pore size distribution. Nitrogen gas adsorption analyses were conducted Autosorb-6 (Quantachrome Corporation) apparatus located in METU Central Laboratory. This device is capable of simultaneously measuring N_2 adsorption for 6 sample chamber. The apparatus has a degas unit with 6 degas chamber for heating the samples under vacuum (degas) for removal of moisture before measurement of the samples. All activated carbon samples were outgassed at 100 ºC for 4 h, which would not lead any significant structural changes on the samples.

Figure 3.3. Surface area and pore size analyzer (right) and degassing unit (left) (Central Laboratory, METU)

Thermal gravimetric analyses were conducted to determine the thermal behavior of air-dried raw horse chestnut kernel, phosphoric acid impregnated horse chestnut kernels. In TGA analyses, Perkin Elmer Pyris 1 Thermogravimetric Analysis apparatus in METU Central Laboratory was used. TGA experiments

were performed at the same experimental conditions for temperature in range between room temperature to 950 ºC and heating rate of 10 ºC/min.

Elemental compositions of produced activated carbons (carbon, hydrogen, nitrogen and sulphur contents) were also analyzed by using an elemental analyzer (CHNS-932, LECO Corporation, Central Laboratory, METU).

The adsorption of methylene blue on activated carbon products was studied. Methylene blue numbers (MBN) of obtained activated carbon products were determined to get information about decolorizing properties of them. 100 mg/L stock solution was prepared by stirring 0.1 g of methylene blue trihydrate, $C_{16}H_{18}ClN_3S^* xH_2O$ (Color index 52015) supplied by Merck with 1 L of deionized water. For methylene blue adsorption, 0.1 g of each activated carbon sample was added to 50 mL of 100 mg/L methylene blue solution. Solutions containing activated carbon sample was mixed in water bath shaker at 120 rev/min (rpm) at the 25 ºC for 24 hours to reach equilibrium. Concentrations of methylene blue solutions were measured by a UV-Visible spectrophotometer (Shimadzu UV-2550) at a wavelength of 664.5 nm. "The area of methylene blue molecule was assumed as 1.62 nm^2." (Akgün, 2005) Surface areas of activated carbons which were covered by methylene blue were calculated.

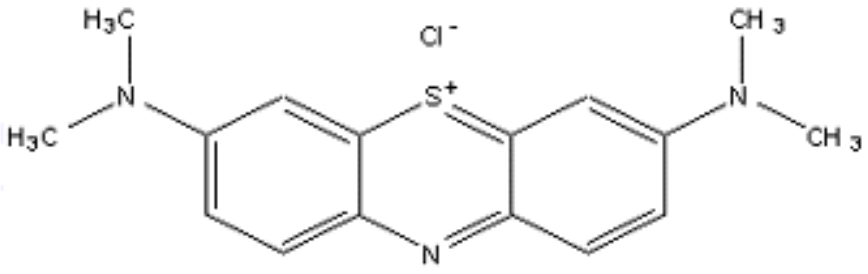

Figure 3.4. Chemical structure of methylene blue

CHAPTER 4

RESULTS AND DISCUSSION

Activated carbon from horse chestnut kernel has been produced by the chemical activation method using phosphoric acid as activating agent. For different carbonization temperature and impregnation ratio, activated carbons have been obtained. The products were characterized by thermogravimetric analysis, N_2 gas adsorption for BET surface area, isotherm and pore size distribution, elemental analysis and methylene blue adsorption.

4.1. THERMOGRAVIMETRIC ANALYSIS

Thermogravimetric (TG) analysis is useful for characterizing activated carbon precursors and intermediate and final products. TG analysis is performed to get information about thermal behavior of raw horse chestnut kernel sample.

TG analysis also was carried out on phosphoric acid impregnated samples to determine the nature of biomass to carbon transformations involved and to find out the product yields. TGA experiments were performed at the same experimental conditions in terms of impregnation ratio, N_2 flow rate, heating rate, carbonization temperature and carbonization time.

Figure 4.1 shows the thermal behavior of raw horse chestnut kernel. As it can be seen from the TGA curve the weight of horse chestnut kernel decreased gradually with temperature up to around 800 ºC. Above this temperature there is no weight loss. The decomposition of the horse chestnut kernel takes place in three stages. The initial weight loss at 25-120 ºC corresponds to the evaporation of moisture that was originally contained in the horse chestnut kernel was about 7.4%. In the

second stage, there is a significant weight loss which is about 77.5% was observed between 120 ºC and 500 ºC. Weight loss between these temperatures was considered to be due to the vaporization of volatile organic compounds which resulted in carbonization of the horse chestnut kernel. In the second stage mainly hemicellulose, cellulose and starch decompose. Finally, at 500-800 ºC rate of weight loss was decreased due to the consolidation of the char structure. At about 800 ºC the mass loss is close to 90.3% and thermal degradation was almost completed.

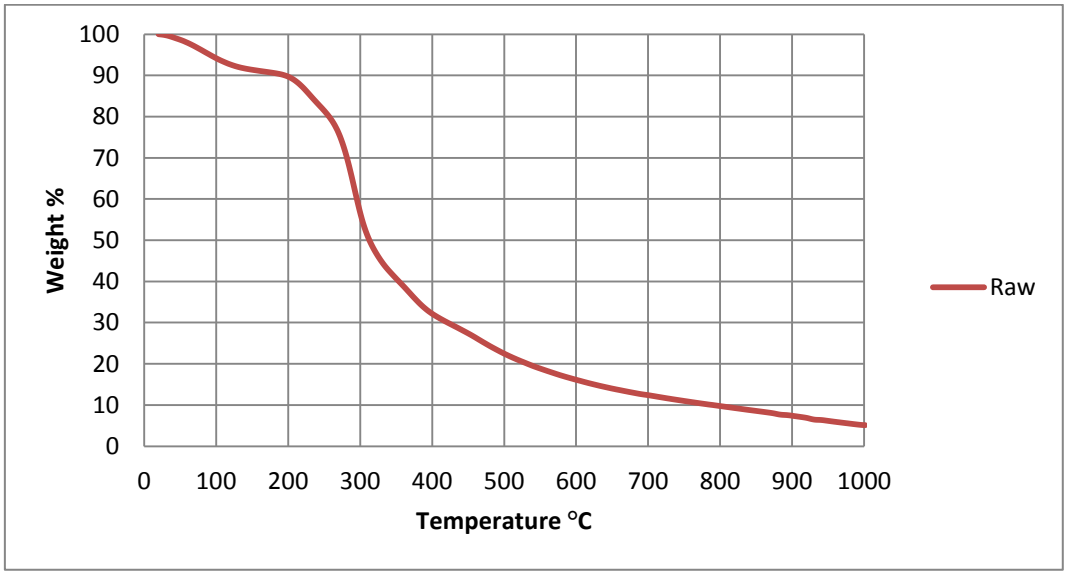

Figure 4.1. TGA curve of raw horse chestnut kernel under N_2 atmosphere at heating rate of 10 °C/min

Figure 4.2 shows that the plot of weight loss of phosphoric acid impregnated samples is shifted to higher temperatures by comparison with raw horse chestnut kernel. TGA curves of both of phosphoric acid impregnated samples shows a significant weight loss up to 200 ºC, then slight weight loss in the range of 200-500 ºC and in the range of 500-800 ºC. The initial weight loss at 25-200 ºC was

observed mainly due to the evaporation of water which comes from phosphoric acid solution and the moisture in sample. In temperature range of 200-500 ºC, the mass be as a result of phosphate and polyphosphate esters formation by crosslinking phosphoric acid with organic species in raw material. Formation of these linkages expands the structure and leads to forming pores. The third weight loss at 500-800 ºC may be assigned due to the volatilization of phosphorous compounds. That can produce new pores and lead to increase in porosity.

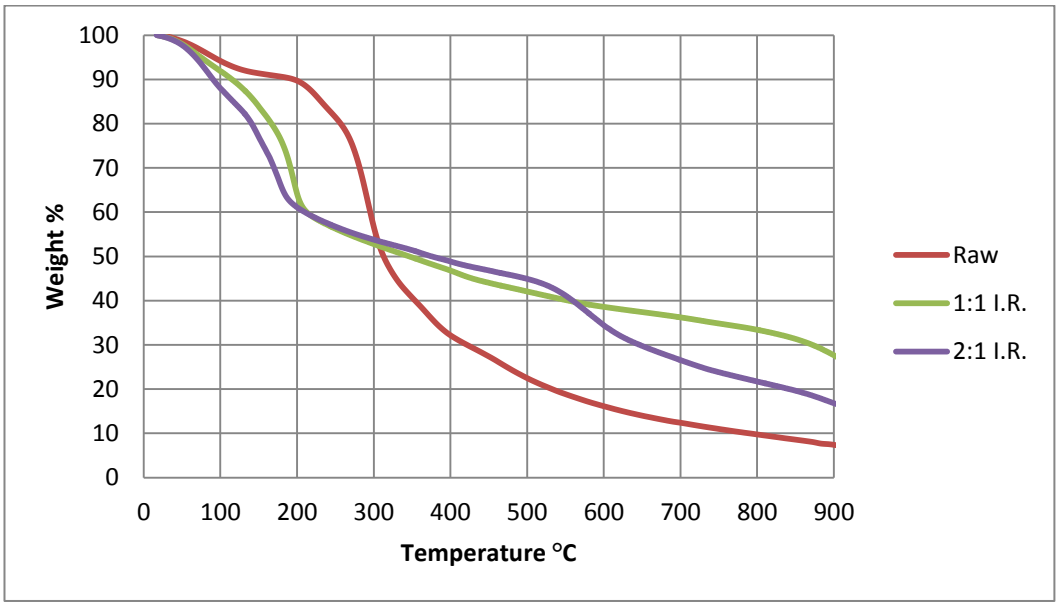

Figure 4.2. TGA curves of raw horse chestnut kernel and phosphoric acid impregnated horse chestnut kernels under N_2 atmosphere at heating rate of 10 °C/min

Yield can be defined as final weight of material divided by initial weight of raw material as received. Product yield is calculated as follows;

$$Yield\ (\%) = \frac{W_f}{W_i} \times 100 \tag{19}$$

Yields were calculated by using TGA data; sample calculation and product yields were given in Appendix A. Product yield values which were found out using the TGA data are given in the Table 4.1 for the horse chestnut kernel and phosphoric acid impregnated samples. The Figure 4.3 shows that yield values of phosphoric acid impregnated samples are higher than the yield of raw horse chestnut kernel. It was due to the tar restriction of phosphoric acid during the pyrolysis. Volatiles could not vaporize easily so that higher yields were observed. When compared impregnated samples. up to temperature 540 ºC, product yields of phosphoric acid impregnated sample with 2:1 impregnation ratio were higher than 1:1 impregnation ratio. But above 540 ºC, product yields of 1:1 impregnation ratio were higher.

Table 4.1. Yield values (%) of raw horse chestnut kernel and phosphoric acid impregnated horse chestnut kernel

	Yield %						
Temperature ºC	**300**	**400**	**500**	**600**	**700**	**800**	**900**
Raw	56.7	32.2	22.5	16.1	12.4	9.7	7.4
Impregnation Ratio 1:1	52.8	46.8	42.1	38.6	36.2	33.4	27.6
Impregnation Ration 2:1	53.8	48.8	44.9	34.4	26.5	21.7	16.8

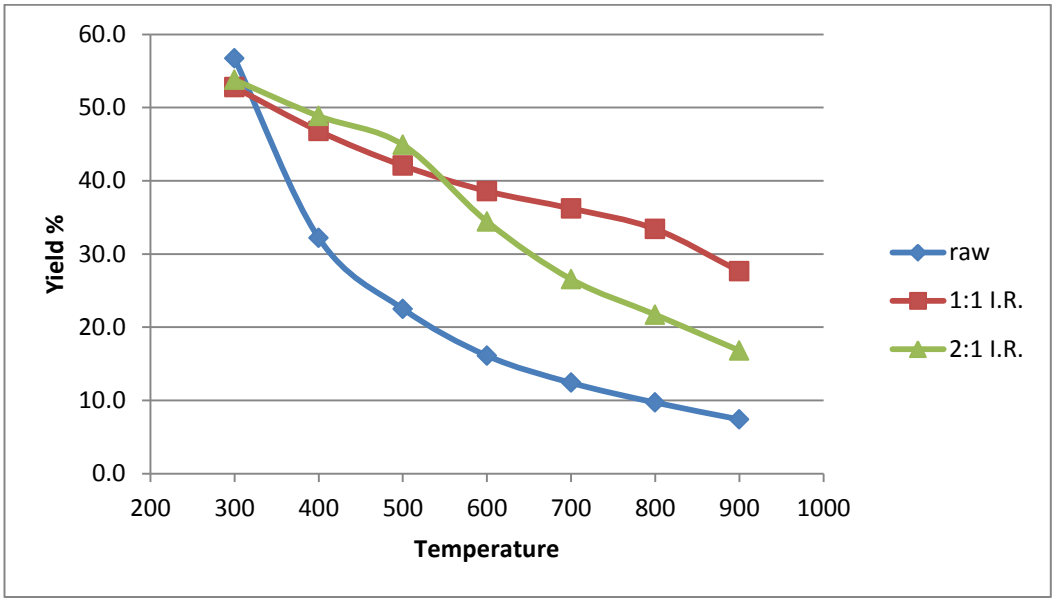

Figure 4.3. Yield (%) of raw horse chestnut kernel and phosphoric acid impregnated horse chestnut kernel

These results verify that the pyrolysis of the precursor without impregnation is not efficient with regards to carbon production yield.

4.2. NITROGEN ADSORPTION MEASUREMENTS

The physical characterization of the produced activated carbons was carried out by nitrogen adsorption at 77 K. The samples were characterized by the determination of BET surface areas, nitrogen adsorption isotherms and pore size distributions.

4.2.1.Bet Surface Area Analysis of the Activated Carbons

BET surface area values of horse chestnut kernel based activated carbons are shown in the Figure 4.4. It was seen that activated carbon obtained by an impregnation ratio of 2:1 and activation temperature of 800 ºC has the highest BET surface area, 862.4 m^2/g.

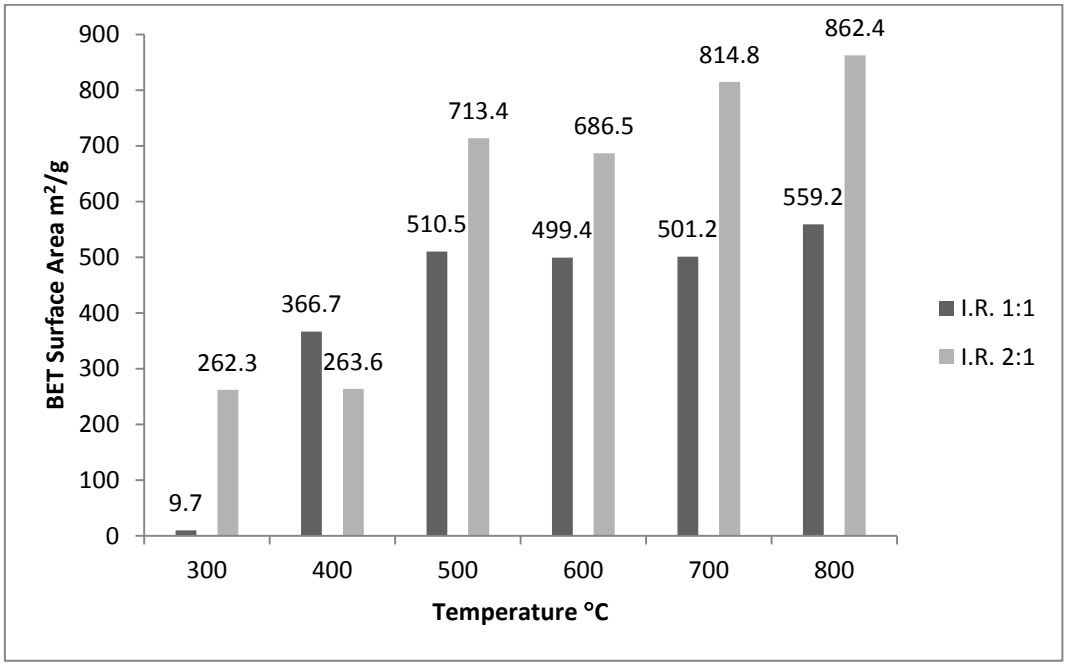

Figure 4.4. BET surface area values of the produced activated carbons

To our knowledge, there is only one study conducted with horse chestnut kernel to produce activated carbon. Momcilovic et al. (2011) studied production of activated carbon from horse chestnut kernel by phosphoric acid activation. They used 85 wt. % phosphoric acid and the impregnation ratio is 1:1 by weight. BET surface area of the produced activated carbon was 663.9 m^2/g at 500 ºC.

In Figure 4.5 the effect of activation temperature and phosphoric acid impregnation ratio to BET surface areas can be seen more clearly. BET surface area increases up to 500 ºC. At temperatures below 500 ºC new micropores are created in the structure. Thus, surface area of the structure increases. But at higher temperatures, created micropores are widened. For temperatures between 500 and 600 ºC, widening micropores in the structure might have caused a decrease in surface area. For temperatures between 600 and 800 ºC, surface area increased by increasing temperature.

For impregnation ratio of 1:1, there is not a significant increase in BET surface areas in the temperature range 500 – 800 °C. For impregnation ratio of 2:1, BET surface areas increase in the temperature range 600 – 800 °C.

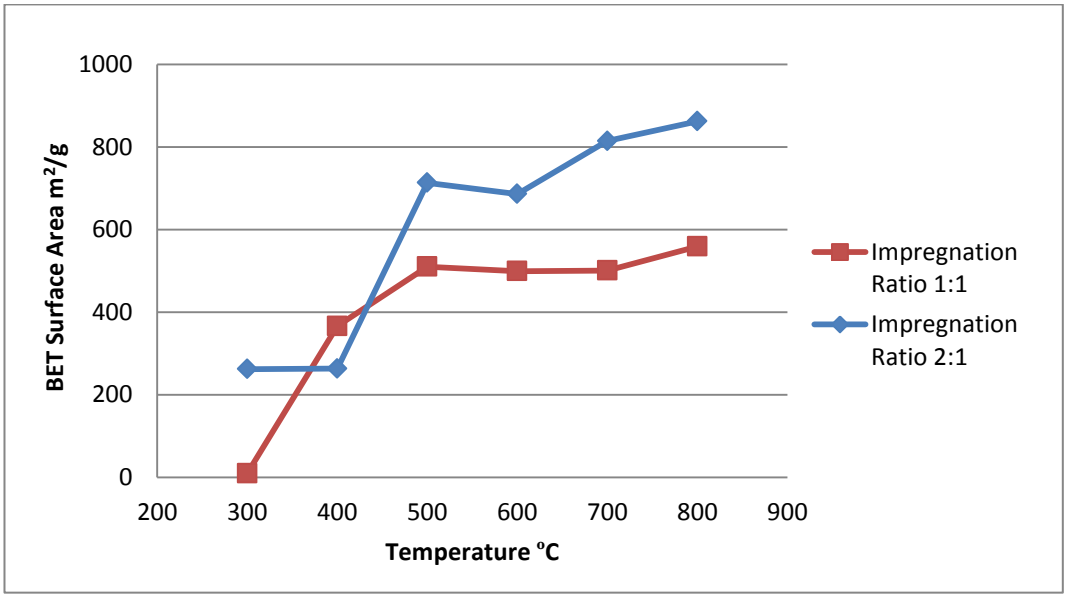

Figure 4.5. Effect of activation temperature and impregnation ratio on BET surface area of horse chestnut kernel based activated carbons

As it can be seen from the Figure 4.5, BET surface area increased at all temperatures except 400 ºC with increasing impregnation ratio from 1:1 to 2:1. Girgis and El Hendawy (2001) stated that impregnation ratio has almost no effect on pore development at lower temperatures. Above the activation temperature of 500 ºC, the effect of impregnation ratio can be significant. Phosphoric acid inhibits the shrinking through the thermal treatment by occupying material surface. After washing of activated carbon, phosphoric acid and its derivatives are removed from the structure leaving behind free void or pores. Thus, increasing phosphoric acid amount may provide porosity development. But at higher amount of phosphoric acid, excess phosphoric acid may cover the surface and inhibit conduction with atmosphere.

Table 4.2. Comparison of BET surface area and yield values of activated carbons

PA/HCK Impregnation Ratio	Temperature °C	BET Surface Area m^2/g	Yield % (TGA)
1:1	300	9.7	52.8
	400	366.7	46.8
	500	510.5	42.1
	600	499.4	38.6
	700	501.2	36.2
	800	559.2	33.4
2:1	300	262.3	53.8
	400	263.6	48.8
	500	713.4	44.9
	600	686.5	34.4
	700	814.8	26.5
	800	862.4	21.7

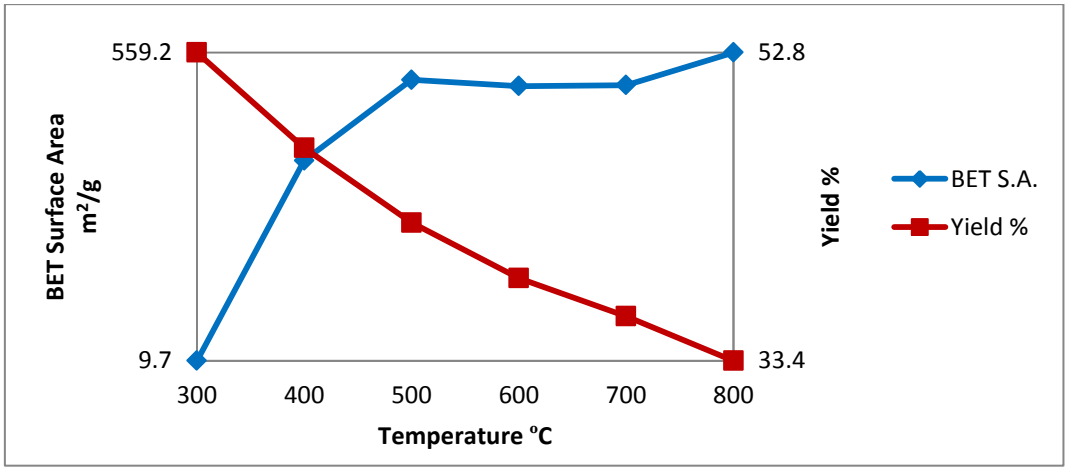

Figure 4.6. Comparison of BET surface area and yield values for impregnation ratio of 1:1

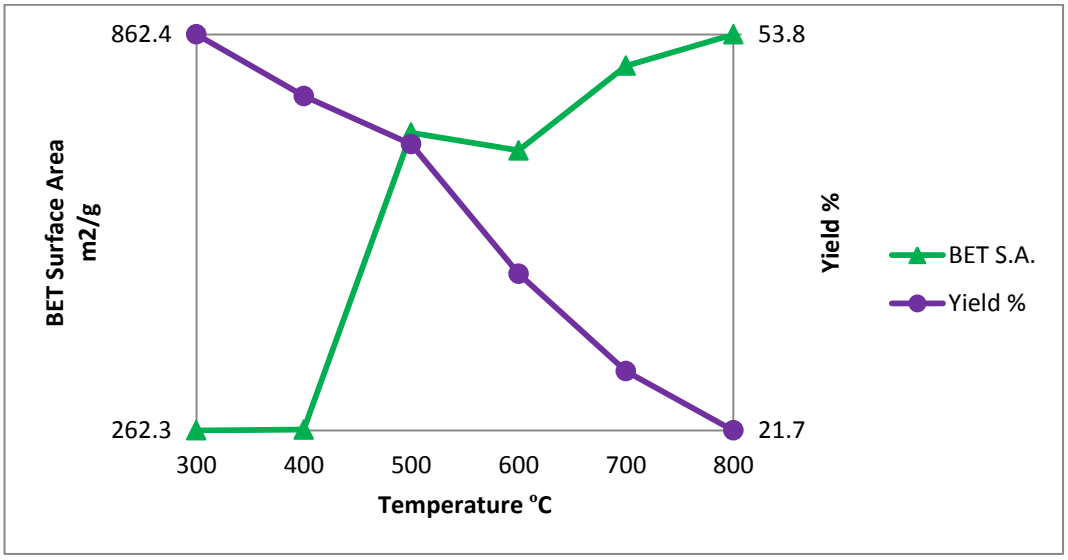

Figure 4.7. Comparison of BET surface area and yield values for impregnation ratio of 2:1

To find the suitable process condition for the activated carbon production, the activation temperature, the BET surface area and the yield must be evaluated together. BET surface area increased with increasing activation temperature. However, high activation temperatures are not desired from the point of process economy. The yield is also an important parameter for choosing suitable process conditions. The lower yield values are not desired. The yield values decreased with increasing activation temperature for both 1:1 and 2:1 impregnation ratio. Effect of impregnation ratio on the yield is different below above activation temperature of 500 ºC. For activation temperatures up to 500 ºC, yield increases with increasing impregnation ratio and yield values are about the same whereas for activation temperatures over 500 ºC yield values decreased with increasing impregnation ratio. Activated carbon produced at activation temperature of 800ºC and impregnation ratio of 2:1 which has the maximum BET surface area has the lowest yield value (21.7 %). Even though the activated carbon produced at 800ºC and 2:1 impregnation ratio has the maximum BET surface area, it is not favored

due to low yield value. In this study, activation temperature of 500 ºC and impregnation ratio of 2:1 seemed to be the suitable conditions for activated carbon production from horse chestnut kernel. When the activation temperature increased from 300 to 500 ºC for 2:1 impregnated samples, the yield decreased slightly, but BET surface area increased slightly. When the activation temperature is continued to increase from 500 to 800 ºC, the BET surface area showed slight increase whereas the yield showed dramatic decrease. If AC-1-500 and AC-2-500 are compared, it shows that AC-2-500 has grater BET surface area and yield value. Besides, when AC-1-400 and AC-2-500 are compared, BET surface area increased almost two times and yield decreased slightly for AC-2-500.

4.2.2. Comparison of BET Surface Area of Horse Chestnut Kernel Based Activated Carbon and Commercial Activated Carbons

The BET surface areas of some commercial activated carbons and with activated carbon produced in this study compared and summerized in Table 4.3.

Table 4.3. BET surface areas of commercial activated carbons

Commercial Activated Carbon	**BET Surface Area m^2/g**	**Reference**
Carbochem	950	Guo et al. (2008)
Microcarb	1150	Guo et al. (2008)
Filtracarb	1150	Guo and Lua (2003)
Calgon OLC Plus 12x30	1113	Lua and Jia (2007)
BDH from Merck	1118	Tan et al. (2007)
Filtrasorb F300	957	Tan et al. (2007)
BPL from Calgon Corporation	972	Tan et al. (2007)
AC-2-500	713.4	

When activated carbon produced at activation temperature of 500°C and impregnation ratio of 2:1 (weight of H_3PO_4/ weight of raw material) which was found to be suitable conditions of this study is considered, BET surface area of this activated carbon was found as 714.3 m^2/g. Even if BET surface area of AC-2-500 is not high as commercial activated carbon, it is close to commercial ones.

4.2.3. Porous Texture of the Produced Activated Carbons

The t-plot approach was applied to examine the mesopore area, micropore area and micropore volume. Total pore volume was determined by using Horvath-Kawazoe (HK) method.

Table 4.4. Surface characteristics of products

Products Sample	**BET Surface Area m^2/g**	**Micropore Area m^2/g (t-plot)**	**Mesopore Area m^2/g (t-plot)**
AC-1-300	9.7	0	9.7
AC-1-400	366.7	246.9	119.9
AC-1-500	510.5	415.2	95.3
AC-1-600	499.4	416.9	82.5
AC-1-700	501.2	427.3	73.8
AC-1-800	559.2	480.4	78.98
AC-2-300	262.3	208.5	53.89
AC-2-400	263.6	140.2	123.4
AC-2-500	713.4	402.6	310.8
AC-2-600	686.5	420.1	266.4
AC-2-700	814.8	556.6	258.3
AC-2-800	862.4	609.0	253.5

When activation temperature increases, micropore area increases for 1:1 impregnation ratio. On the other hand, for 2:1 impregnation ratio, micropore area decreased when activation temperature increased from 300 to 400 ºC. It can be seen from the Table 4.4, when amount of activation agent H_3PO_4 increased (impregnation ratio changed from 1:1 to 2:1), mesopore area increased.

Table 4.5. Pore volumes of products

Products Sample	Total Pore Volume cm^3/g (HK)	Micropore Volume cm^3/g (t-plot)
AC-1-300	0.0033	0
AC-1-400	0.1493	0.1039
AC-1-500	0.2078	0.1775
AC-1-600	0.2029	0.1776
AC-1-700	0.2036	0.1809
AC-1-800	0.2272	0.2040
AC-2-300	0.1063	0.0929
AC-2-400	0.1071	0.0639
AC-2-500	0.2932	0.1750
AC-2-600	0.2822	0.1816
AC-2-700	0.3330	0.2374
AC-2-800	0.3539	0.2659

Micropore volume increases with increasing activation temperature for 1:1 impregnation ratio. But also, increasing activation temperature from 300 to 400 ºC caused decreasing micropore volume for impregnation ratio of 2:1. At higher activation temperatures greater than 400ºC, micropore volume increased with increasing temperature for 2:1 impregnation ratio. Changing impregnation ratio from 1:1 to 2:1 caused increasing total pore volume except activation temperature of 400ºC.

It can be said that the products are mainly microporous except AC-1-300. On the other hand, sample AC-1-300 showed mesopore structure.

Because most gaseous molecules have 0.4 - 0.9 nm diameter range, gas phase adsorbents generally have microporous structure. Conversely, liquid phase adsorbents have mesoporous structure due to the large size of liquid molecules and low diffusion coefficients in liquid phase (Rafatullah et al., 2013). In this study, nitrogen adsorption results showed that products are mainly microporous structure except AC-1-300. Product AC-1-300 showed mesopore structure, has insignificant BET surface area. Activated carbons obtained in this work can be used in gas phase applications due to the microporic structure of products.

4.2.4.Nitrogen Adsorption – Desorption Isotherms

Nitrogen adsorption isotherm shows quantity of nitrogen adsorbed at any given relative pressure at liquid nitrogen temperature (77 K). These isotherms give information about pore structure and adsorption behavior of adsorbents.

Figure 4.8 shows nitrogen adsorption desorption isotherms of products for different activation temperatures and impregnation ratio of 1:1.

As it can be seen from the Figure 4.8, sample AC-1-300 which was produced at activation temperature of 300ºC and impregnation ratio of 1:1 has insignificant adsorption capacity. This resulted in a very low BET surface area, 9.7 m^2/g. The activated carbons produced at temperatures higher than 400 ºC for 1:1 impregnation ratio similar to Type I and Type II isotherms according to the IUPAC classification. Quantity of volume adsorbed cannot reach a limiting value with the increasing pressure. After initial steep region of adsorption isotherm, the slope of adsorption branch decreases. Low slope region of the isotherm shows first few multilayers on external surface including mesopores. Besides,

appearance of hysteresis loops on nitrogen adsorption and desorption isotherm shows the presence of mesopores in the structure. These isotherms showed activated carbons are mainly microporic structure with mesopores.

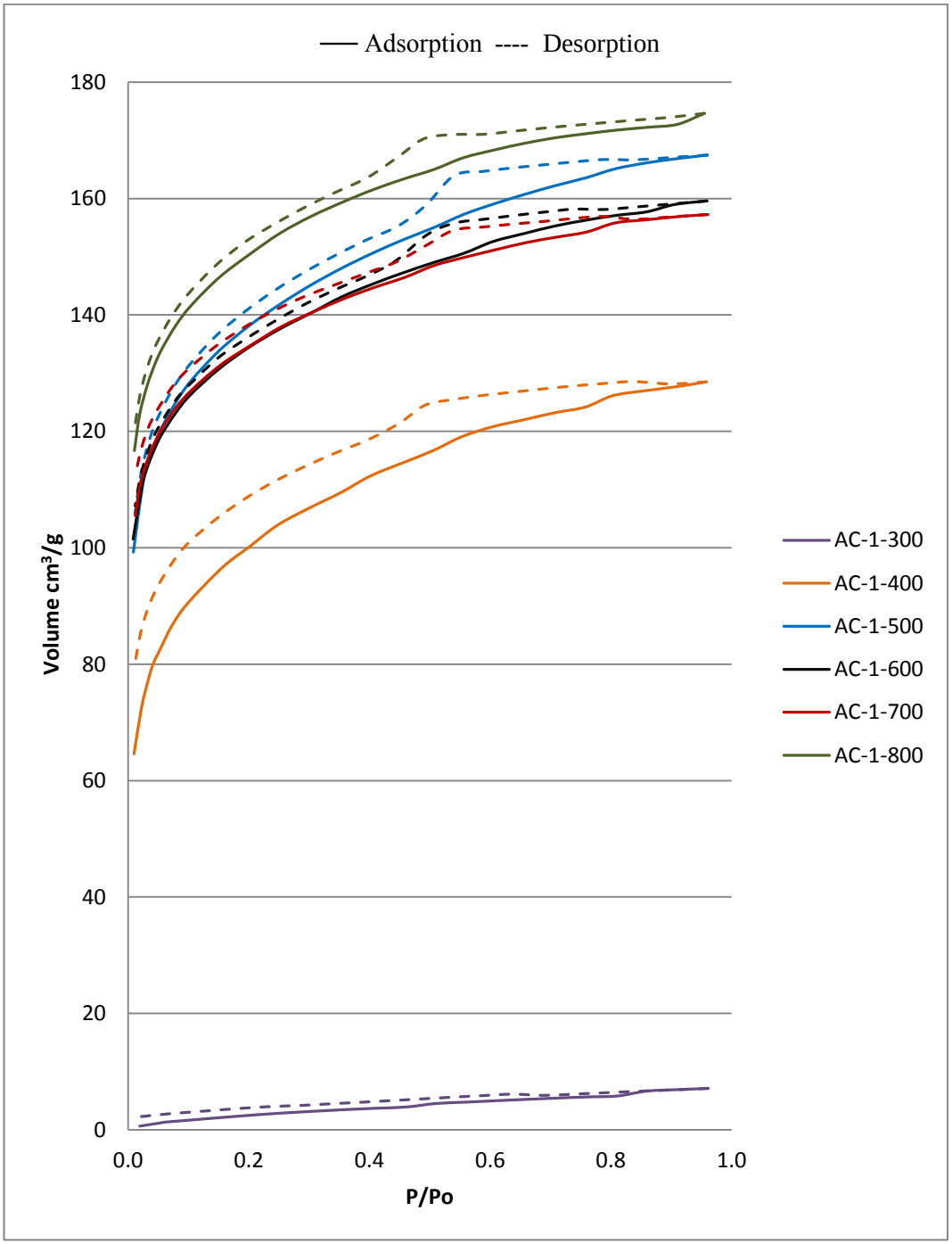

Figure 4.8. Nitrogen adsorption-desorption isotherms of activated carbon produced at different temperatures for impregnation ratio of 1:1

Figure 4.9 shows nitrogen adsorption desorption isotherms of products for different activation temperatures and impregnation ratio of 2:1. After initial steep region of adsorption isotherms, the slope of adsorption branches decrease. Low slope region of the isotherm shows first few multilayers on external surface including mesopores. Besides, presence of hysteresis loop indicates the existence of mesopores in the structure. These isotherms show activated carbons consist of micropores with mesopores.

It was observed from Figure 4.9 that the nitrogen adsorption isotherm of sample AC-2-800 which was produced at activation temperature of 800ºC and impregnation ratio of 2:1 shows the maximum adsorption.

The shape of adsorption and desorption isotherms provides information about porous texture and pore geometries of adsorbents.

It seems to be H4 hysteresis for samples produced at lower temperatures than 400 ºC for both impregnation ratio of 1:1 and 2:1, the adsorption and desorption branches are nearly parallel to each other and this H4 loop indicates slit-shape pores. At higher activation temperature than 400 ºC for both impregnation ratio of 1:1 and 2:1, hysteresis loop seems to convert into H2 loop. H2 loop is broad with long and almost flat plateau and steep desorption branch. This type of loop is attributed to mainly the presence of ink-bottle pores.

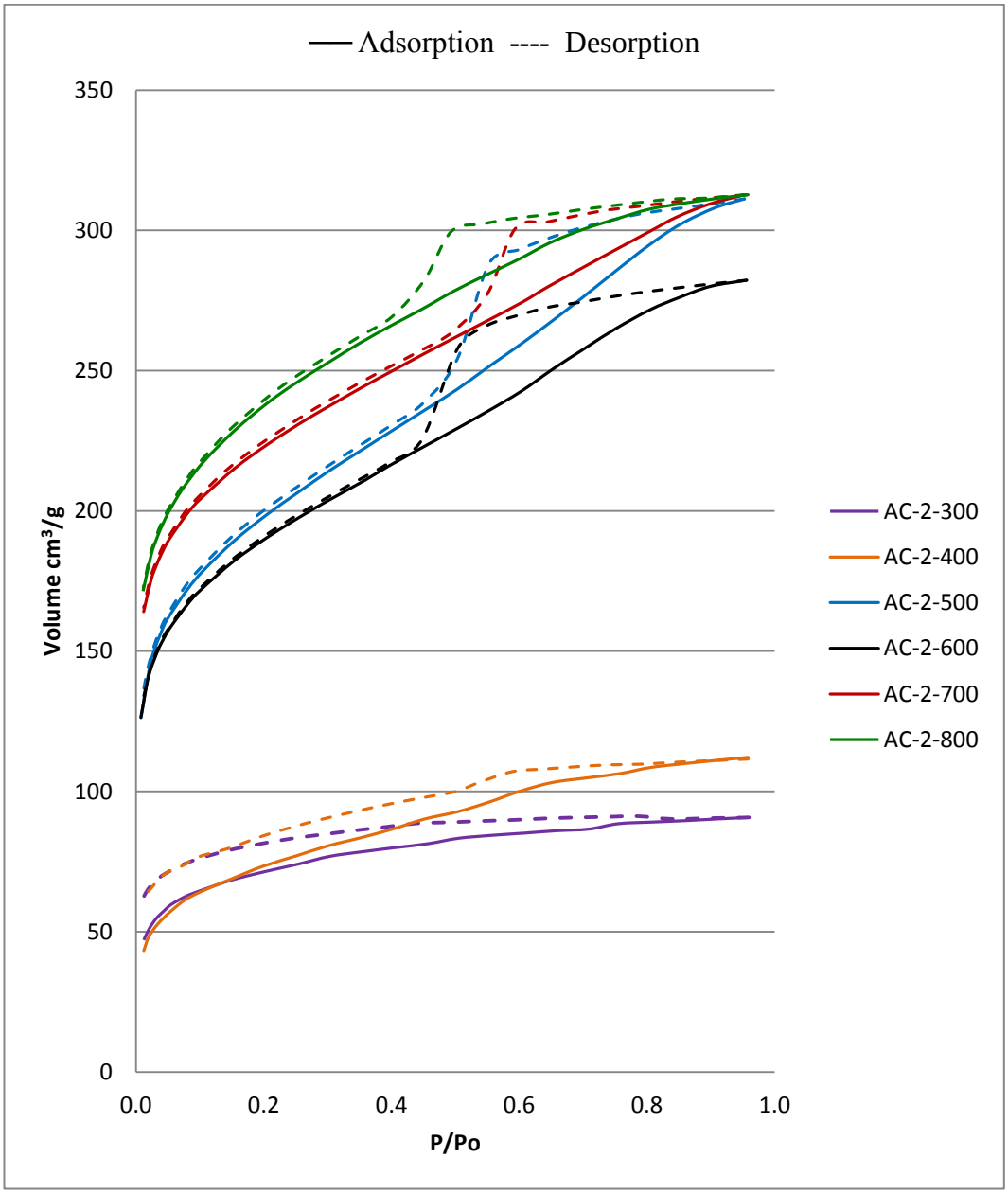

Figure 4.9. Nitrogen adsorption-desorption isotherms of activated carbon produced at different temperatures for impregnation ratio of 2:1

4.2.5.Pore Size Distributions

The structural heterogeneity of porous material is usually characterized in term of pore size distribution. The nitrogen adsorption data with DFT analysis is used to determine pore size distribution.

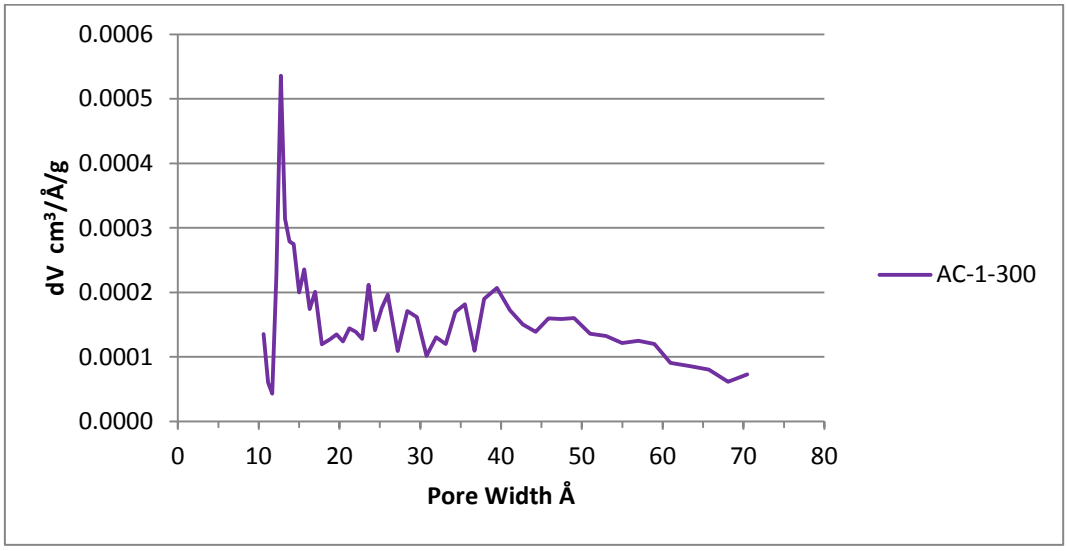

Figure 4.10. Pore size distribution of activated carbon produced at activation temperature of 300 ºC and impregnation ratio of 1:1

As it can be seen in Figure 4.10, the activated carbon produced at 300 ºC for 1:1 impregnation ratio has surface heterogeneity. If BET surface area 9.7 m^2/g considered, it can be said that AC-1-300 activated carbon has an insignificant adsorption capacity.

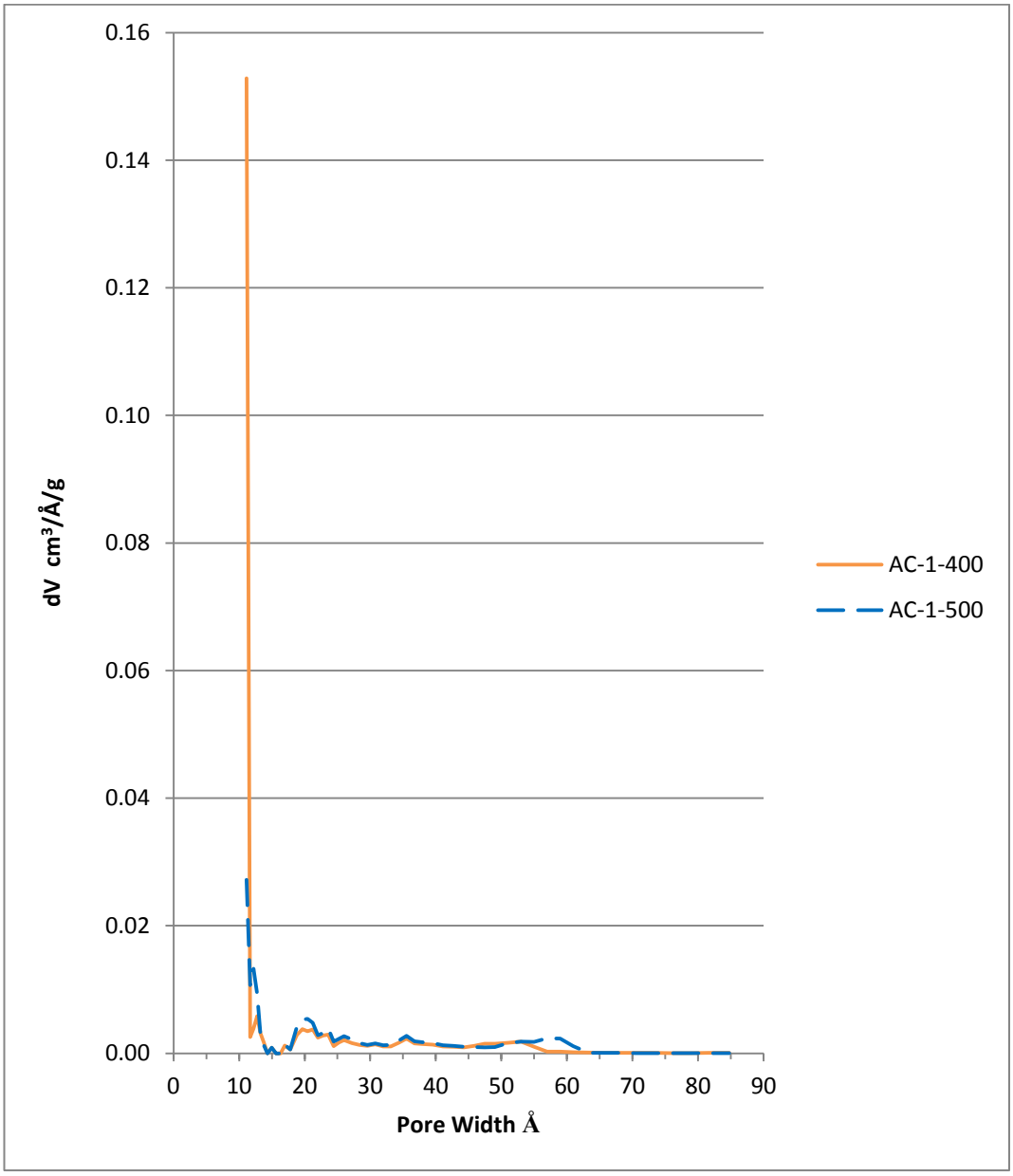

Figure 4.11. Effect of temperature on pore size distribution of activated carbon produced at activation temperature of 400 and 500 ºC and impregnation ratio of 1:1

As it is seen from the Figure 4.11, samples AC-1-400 and AC-1-500 include both micro and mesopores. Increasing activation temperature from 400 to 500 ºC causes pore improvement.

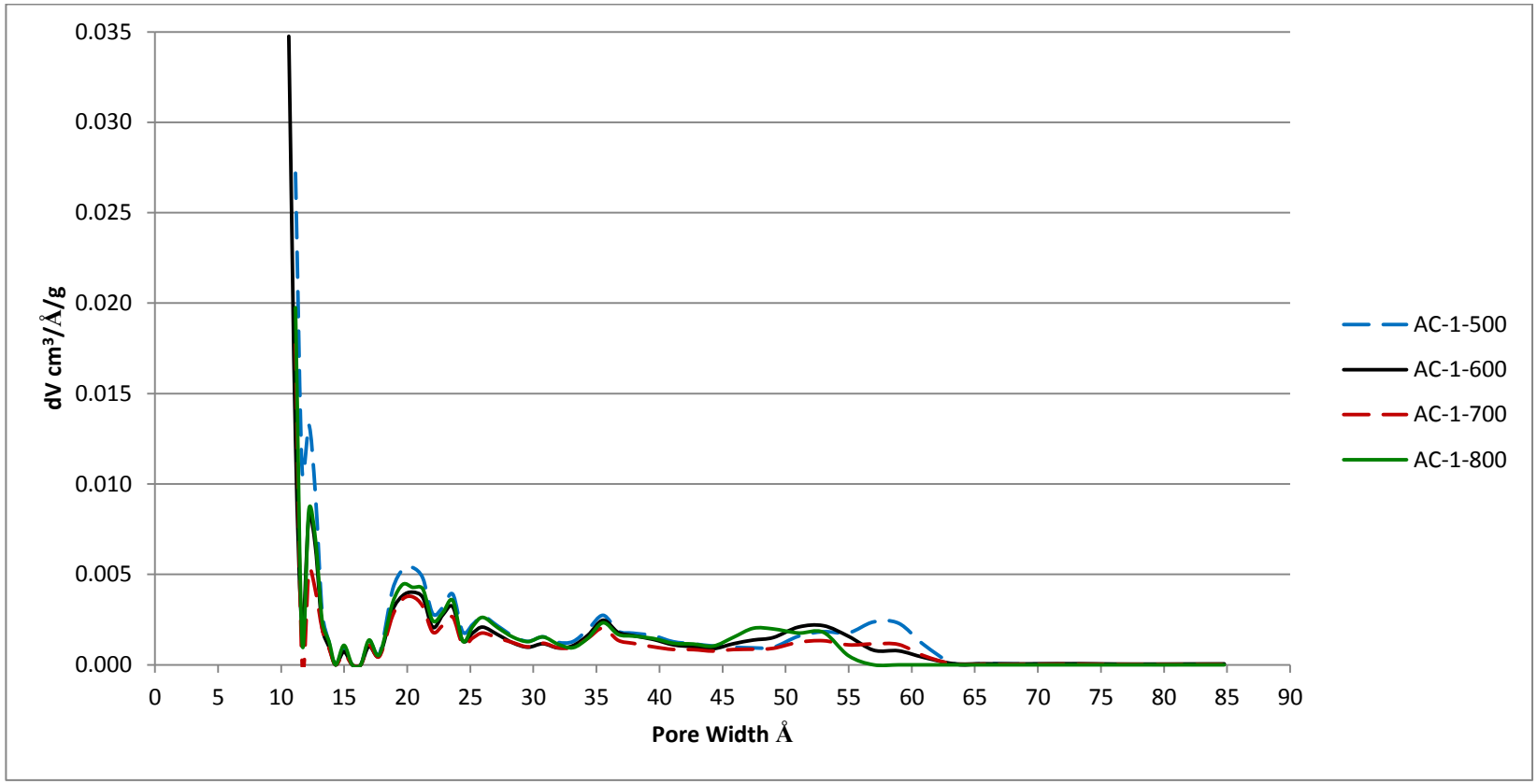

Figure 4.12. Effect of temperature on pore size distribution of activated carbon produced at activation temperature of 500, 600, 700 and 800 ºC and impregnation ratio of 1:1

Comparison of different activation temperatures of 500, 600, 700 and 800 ºC for 1:1 impregnation ratio is shown in Figure 4.12. Samples show both micro and mesopore structure. If the peaks around 12 Å, 20 Å, 23 Å, 26 Å and 36 Å considered, pore width does not change with increasing temperature. It can be said that pore size distributions resembles to each other.

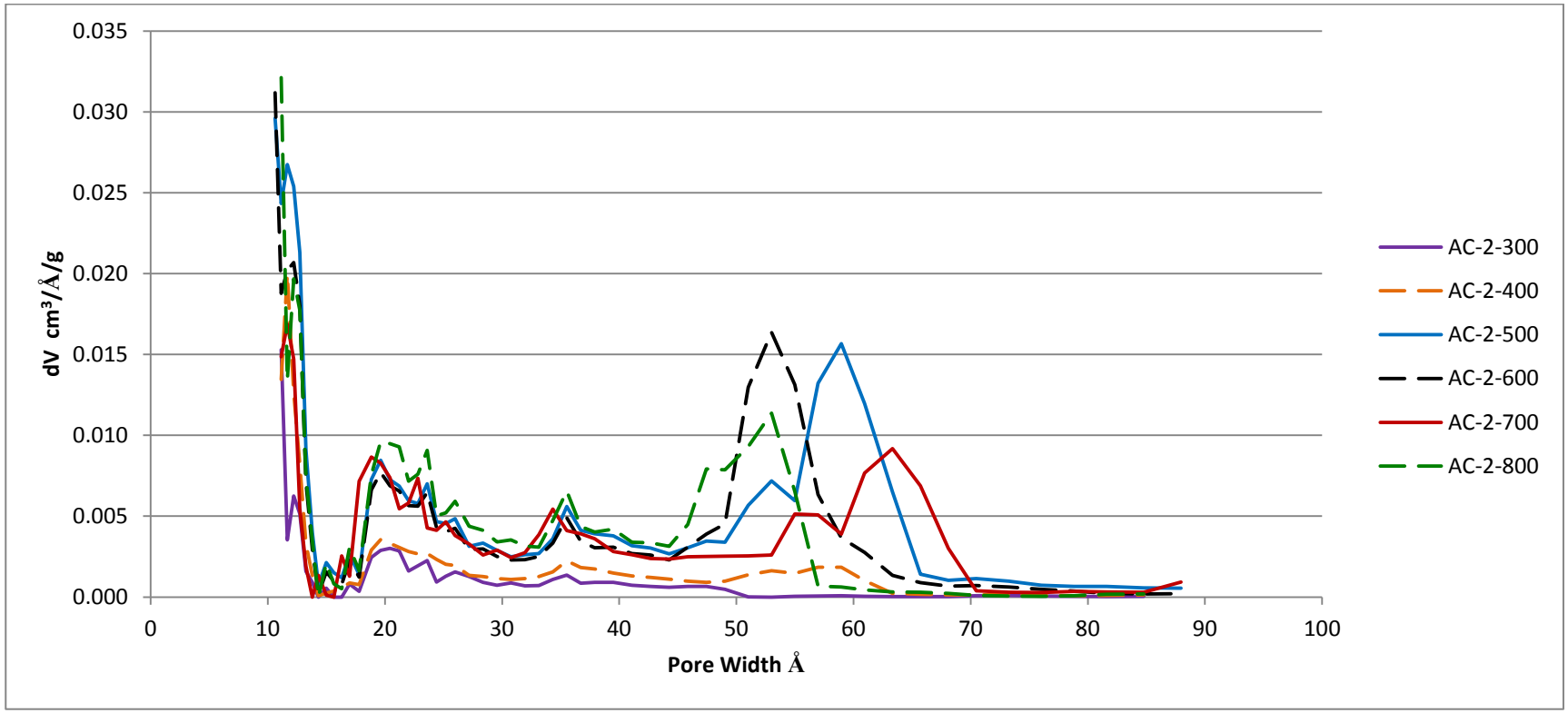

Figure 4.13. Effect of temperature on pore size distribution of activated carbon produced at activation temperature of 300, 400, 500, 600, 700 and 800 ºC and impregnation ratio of 2:1

As it can be seen from the Figure 4.14, at higher temperatures than 300 ºC, new peak is appeared in mesopore region around 50 – 70 Å.

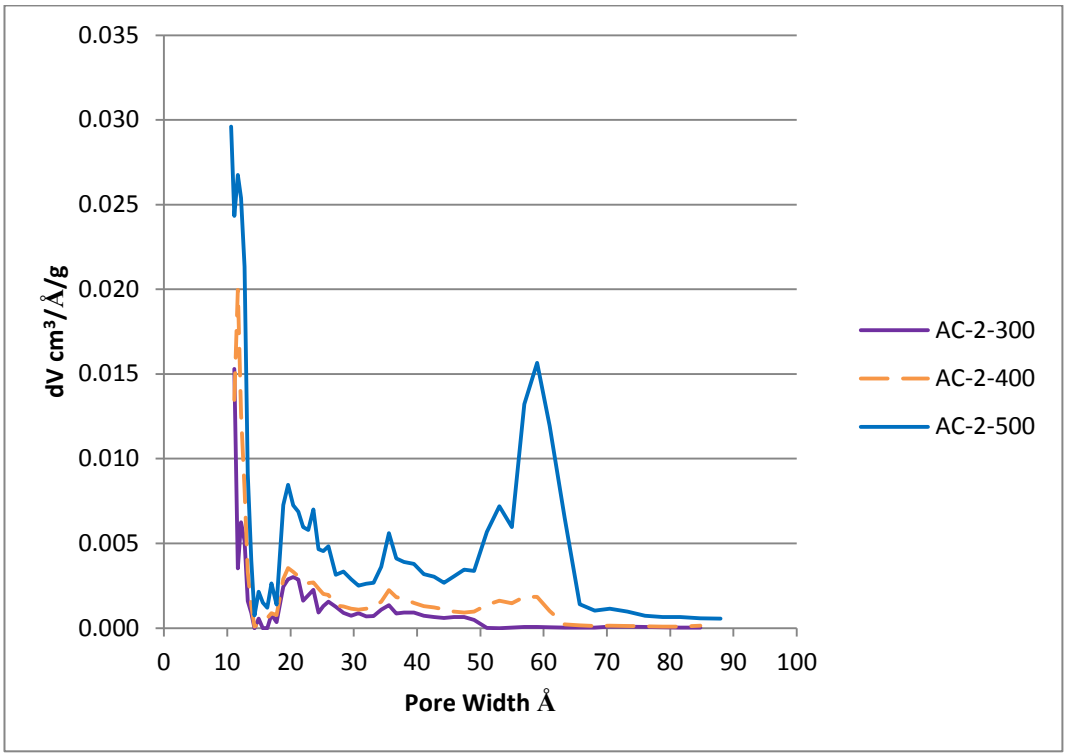

Figure 4.14. Effect of temperature on pore size distribution of activated carbon produced at activation temperature of 300, 400 and 500 ºC and impregnation ratio of 2:1

When pore size distribution of AC-2-300 and AC-2-400 considered, the slight peak appeared in mesopore region showed development of porosity. On the other hand, changing of activation temperature from 400 to 500 ºC caused appearing of sharp peak in micro and mesopore region around 10 20, 35 and 60 Å. These sharp peaks indicate pore development for AC-2-500. These effects resulted in noticeable increase in BET surface area.

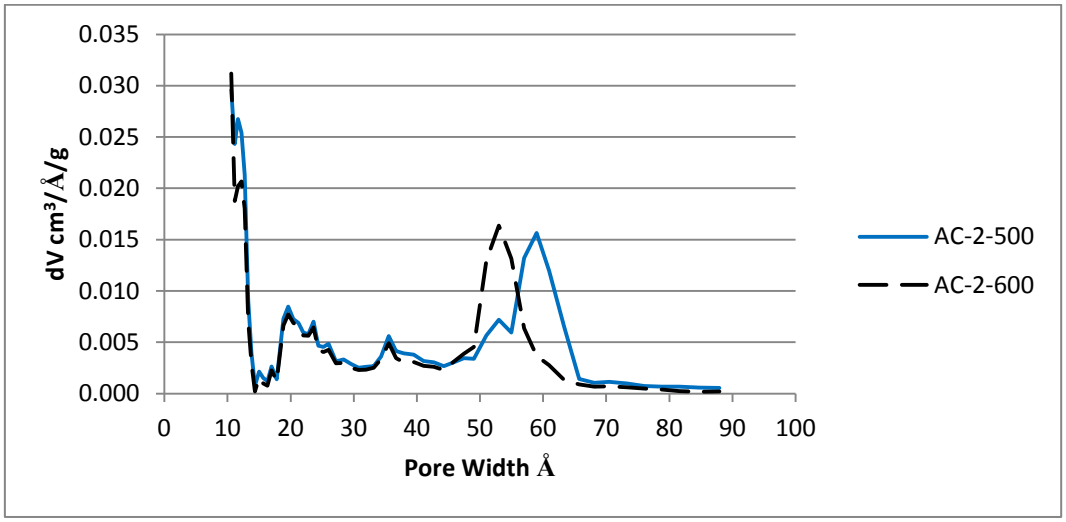

Figure 4.15. Effect of temperature on pore size distribution of activated carbon produced at activation temperature of 500 and 600 ºC and impregnation ratio of 2:1

As we can see from the Figure 4.15, when temperature increases 500 to 600 ºC, the peak around 60 Å seems to be shifting to around 50 Å.

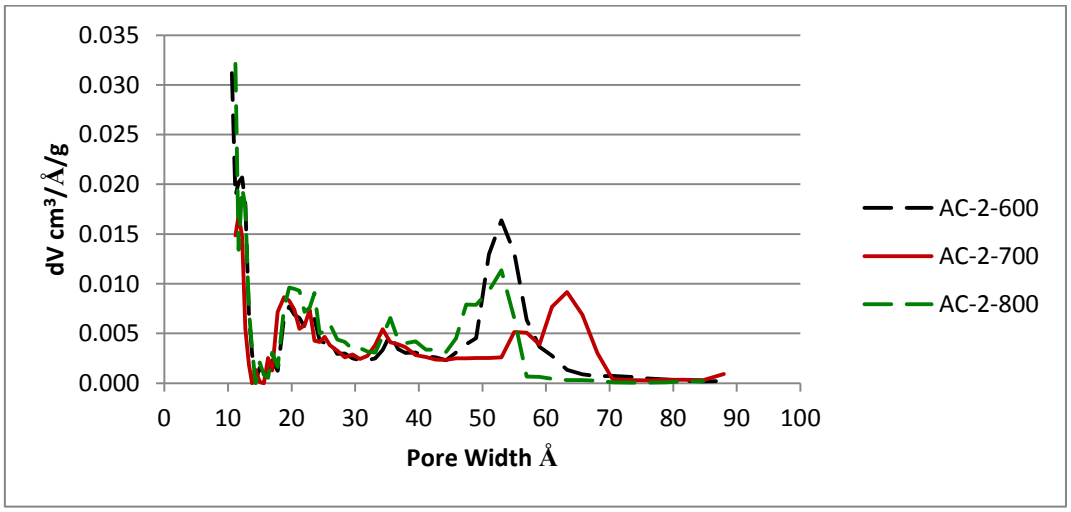

Figure 4.16. Effect of temperature on pore size distribution of activated carbon produced at activation temperature of 600, 700 and 800 ºC and impregnation ratio of 2:1

The peak around 50 Å shifted to 65 Å with temperature increasing 600 to 700 ºC. When temperature raised 700 to 800 ºC, the peak around 50 Å shifted to 50 Å.

The Figure 4.17, 4.18, 4.19, 4.20, 4.21, 4.22 show effect of impregnation ratio on pore development. Increasing phosphoric acid amount caused pore development except activation temperature of 400 ºC.

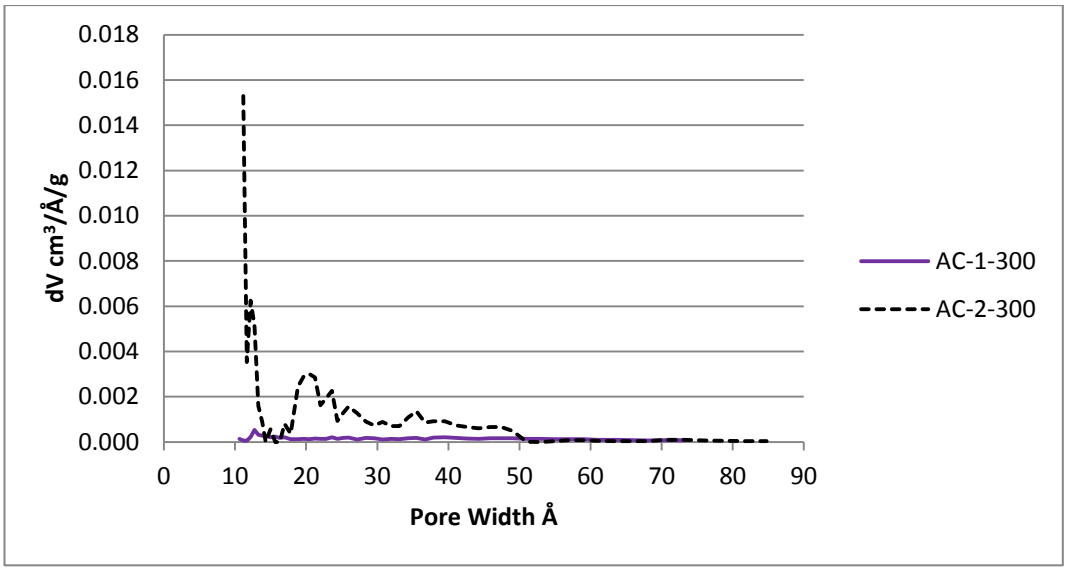

Figure 4.17. Effect of impregnation ratio on pore size distribution of activated carbon produced at activation temperature of 300 ºC

For activation temperature of 300 ºC, there is a significant pore development with phosphoric acid increasing. Pores in micro and mesopore region developed for 2:1 impregnation ratio.

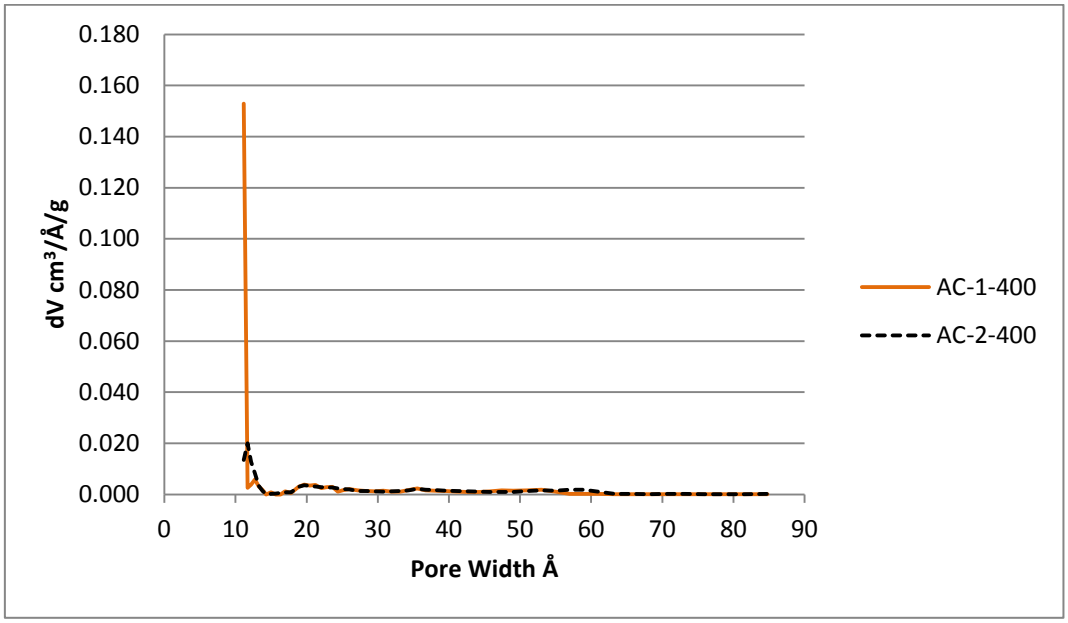

Figure 4.18. Effect of impregnation ratio on pore size distribution of activated carbon produced at activation temperature of 400 ºC

For activation temperature of 400 ºC, the peak in the micropore region which is about 11 Å decreased with changing impregnation ratio 1:1 to 2:1.

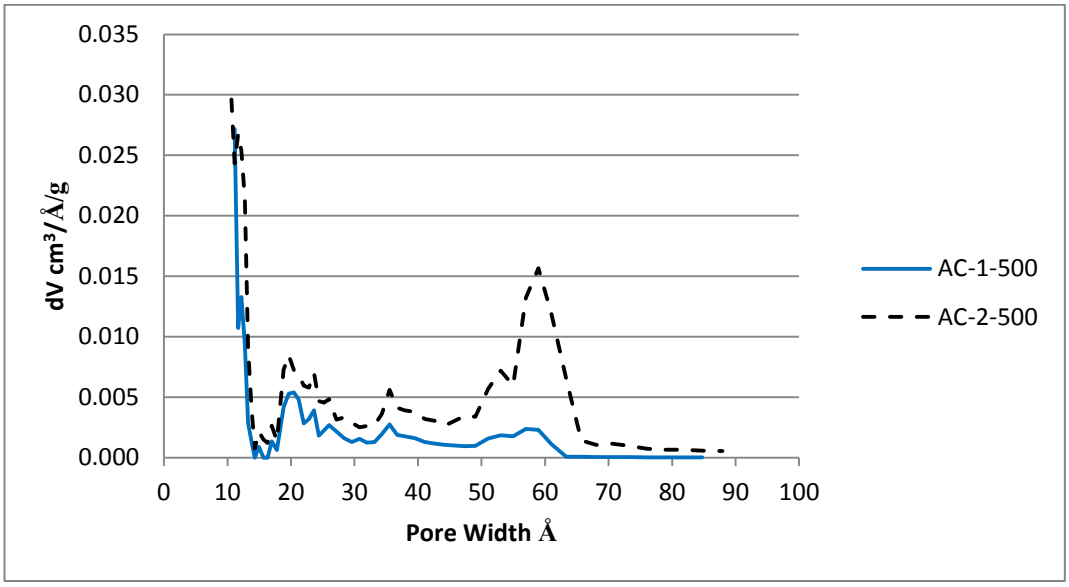

Figure 4.19. Effect of impregnation ratio on pore size distribution of activated carbon produced at activation temperature of 500 ºC

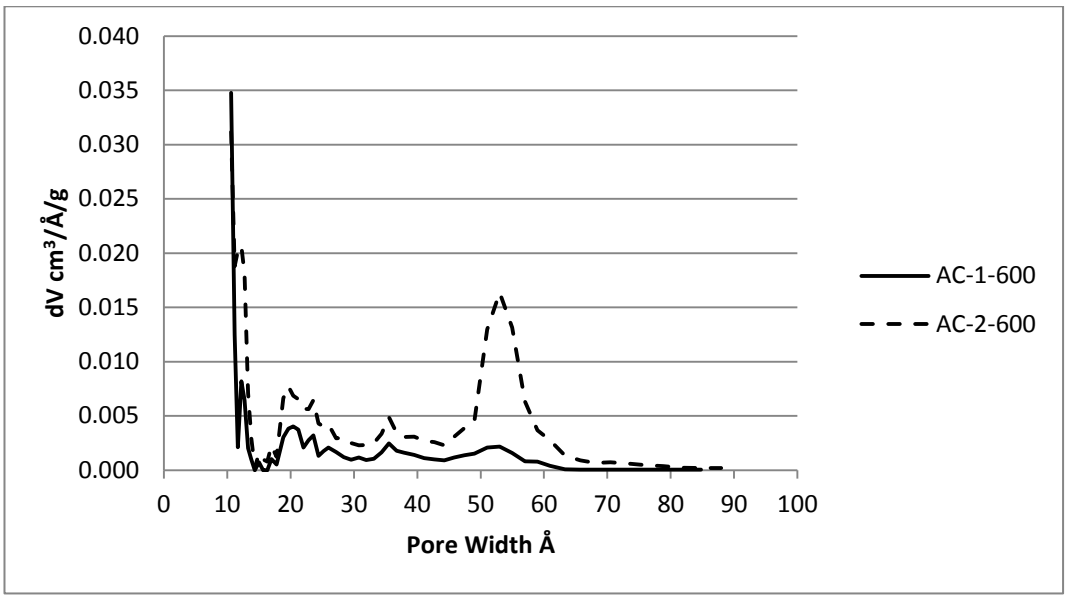

Figure 4.20. Effect of impregnation ratio on pore size distribution of activated carbon produced at activation temperature of 600 ºC

For activation temperature of 500 ºC and 600 ºC, increasing impregnation ratio caused significant change in mesopore region. Micropores and mesopores seem to be developed for 2:1 impregnation ratio.

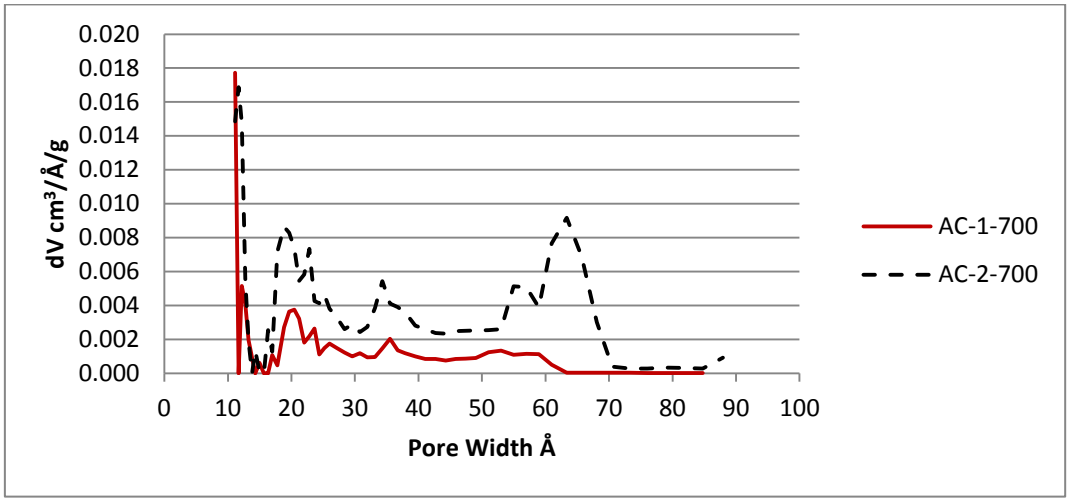

Figure 4.21. Effect of impregnation ratio on pore size distribution of activated carbon produced at activation temperature of 700 ºC

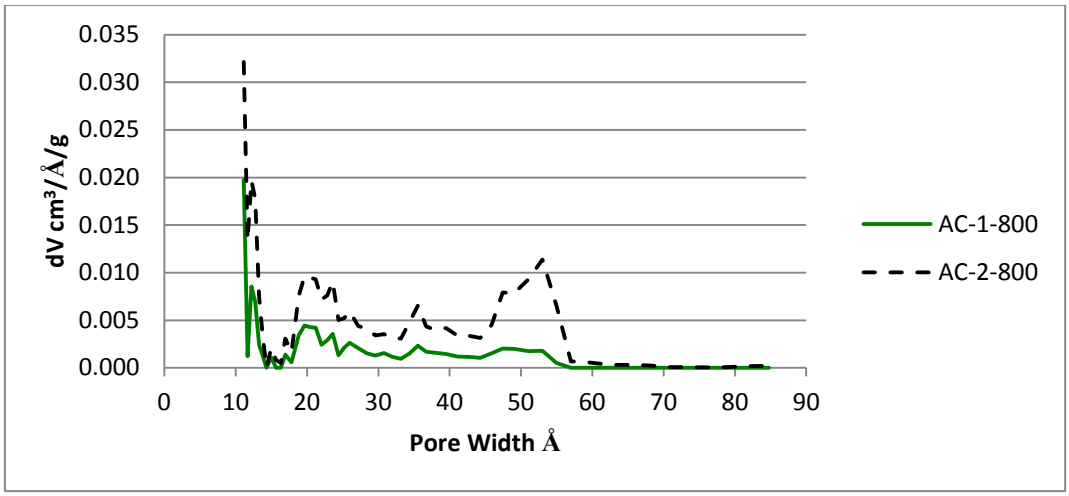

Figure 4.22. Effect of impregnation ratio on pore size distribution of activated carbon produced at activation temperature of 800 ºC

For activation temperature of 700 ºC and 800 ºC, changing impregnation ratio 1:2 to 2:1 caused notable improvement both micropores and mesopores.

4.2.6. Reproducibility Experiments

The reproducibility of the experiments was done for by reproducing activated carbon at activation temperature of 500 and 700 ºC for impregnation ratio of 2:1 at the same process conditions. The physical characterization of the reproduced activated carbons was done by nitrogen adsorption. Table 4.6 shows physical characteristics of reproduced activated carbons.

Table 4.6. Physical characteristics of AC-2-500, AC-2-500-R, AC-2-700, AC-2-700-R

Activated Carbon Sample	**BET S.A. m^2/g**	**Micropore A. m^2/g (t-plot)**	**Mesopore A. m^2/g (t-plot)**	**Total P.V. cm^3/g (HK)**	**Micropore V. cm^3/g (t-plot)**
AC-2-500-R	651.6	343.1	308.5	0.2680	0.1506
AC-2-700-R	830.4	536.2	294.2	0.3407	0.2317
AC-2-500	713.4	402.6	310.8	0.2932	0.1750
AC-2-700	814.8	556.6	258.3	0.3330	0.2374

Figure 4.23 and 4.24 show comparison of nitrogen adsorption and desorption isotherms of produced and reproduced activated carbons. Nitrogen adsorption and desorption isotherms of reproduced samples resembles to formerly produced samples

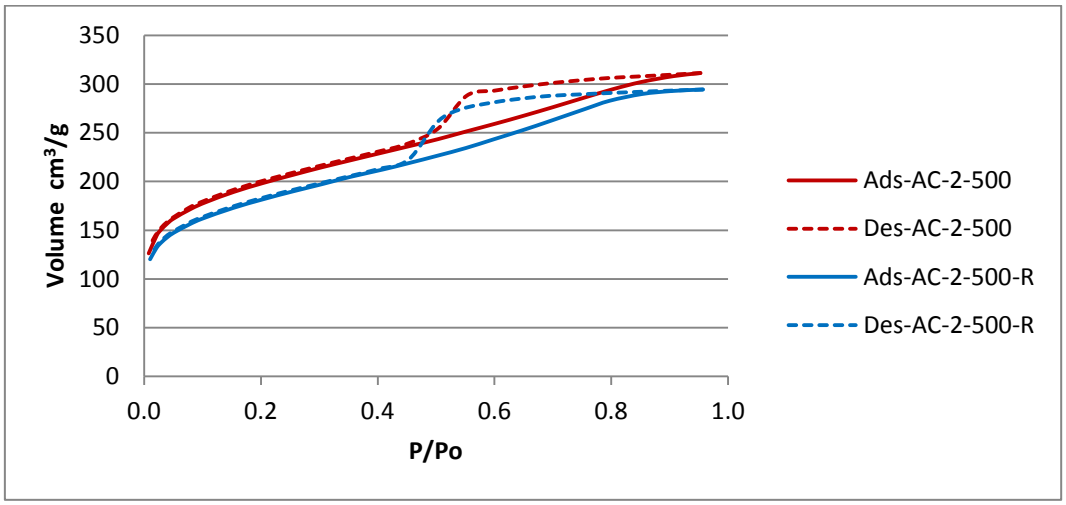

Figure 4.23. Nitrogen adsorption and desorption isotherms of AC-2-500 and AC-2-500-R

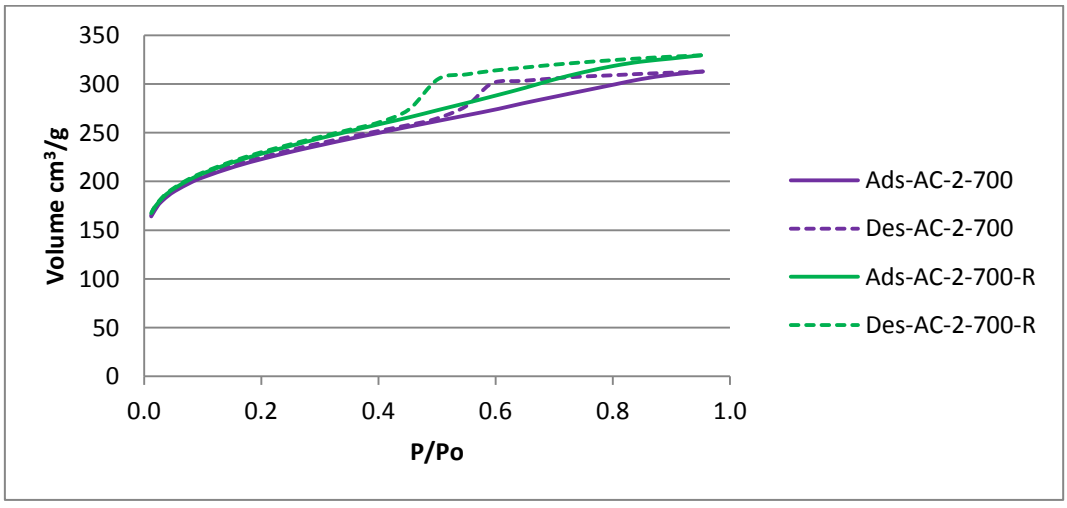

Figure 4.24. Nitrogen adsorption and desorption isotherms of AC-2-500 and AC-2-700-R

Figure 4.25 and 4.26 show comparison of pore size distributions of produced and reproduced activated carbons.

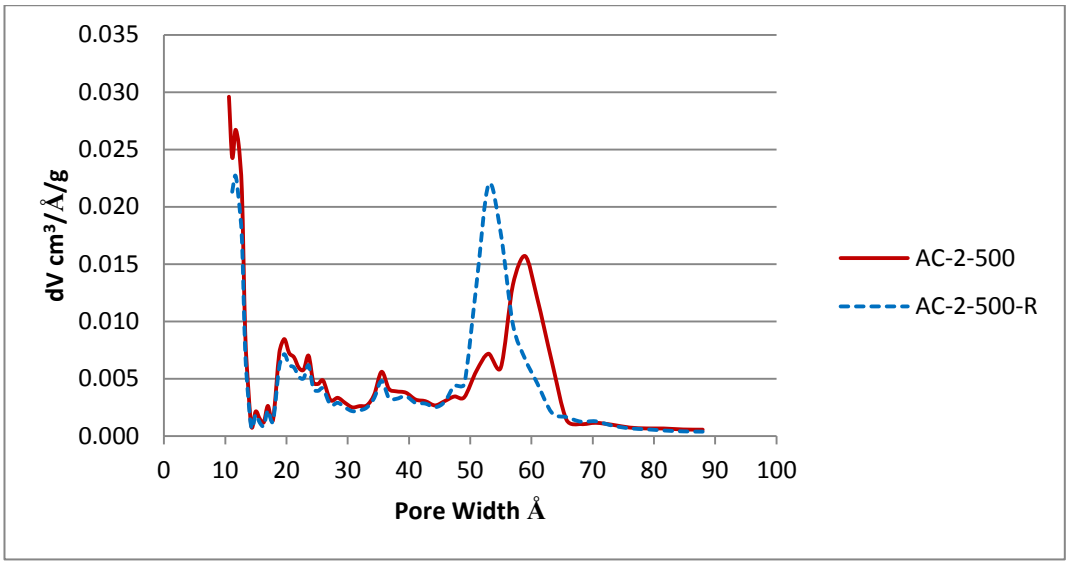

Figure 4.25. Pore size distribution of AC-2-500 and AC-2-500-R

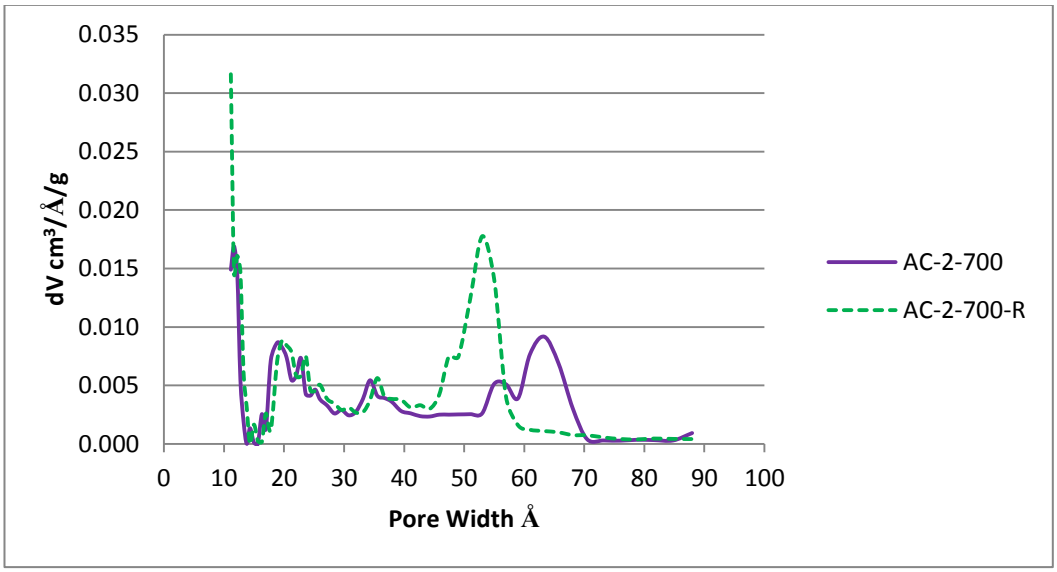

Figure 4.26. Pore size distribution of AC-2-700 and AC-2-700-R

As can be seen from the figures, there are deviations on pore size distributions. Despite these deviations, pore size distributions of reproducibility experiments are very similar.

Table 4.7. BET surface area values and deviation of reproducibility experiments

Impregnation Ratio (H_3PO_4/HCK)	Temperature ºC	BET Surface Area m^2/g		% Deviation
2:1	500	713.4	651.6	8.7
	700	814.8	830.4	1.9

Table 4.7 showed deviation values of the reproducibility experiments. Detailed calculations are given in Appendix C. These deviations are unavoidable due to random errors in both preparation and characterization steps. These results indicated that produced activated carbon at 700 ºC for 2:1 impregnation ratio has good reproducibility. On the other hand, sample produced at 500°C and 2:1 impregnation ratio does not have good reproducibility in terms of % deviation.

4.3. ELEMENTAL ANALYSIS OF PRODUCED ACTIVATED CARBONS

Elemental analysis of produced activated carbons was done to characterize products and to compare the elemental composition of products with the raw material horse chestnut kernel.

For comparison, elemental composition of raw horse chestnut kernel and the produced activated carbons were given in Table 4.8.

Table 4.8. Elemental composition of produced activated carbon

Activated Carbon Sample	**C %**	**H %**	**N %**	**O % (by diff.)**
AC-1-300	67.19	4.97	1.71	26.13
AC-1-400	78.00	3.99	1.57	16.44
AC-1-500	72.63	3.35	1.29	22.73
AC-1-600	65.78	3.01	1.51	29.70
AC-1-700	63.38	2.52	1.61	32.49
AC-1-800	61.33	2.35	1.66	34.66
AC-2-300	69.38	4.62	1.32	24.68
AC-2-400	80.52	3.96	1.18	14.34
AC-2-500	78.24	3.20	1.05	17.51
AC-2-600	76.21	2.81	1.27	19.71
AC-2-700	64.98	2.87	1.84	30.31
AC-2-800	67.52	2.31	2.22	27.95
	C %	**H %**	**N %**	**O % (by diff.)**
Raw Horse Chestnut Kernel	42.89	7.32	1.02	48.77

Elemental analysis results showed that all activated carbon samples have higher carbon content and lower hydrogen and oxygen content than raw material. Because, hydrogen and oxygen elements remove more easily than carbon element from the biomass structure during the heat treatment resulted in producing carbonaceous material (Tseng, 2007). There was a significant increase in carbon content of the material after carbonization and activation processes. Chemical activation has enhanced the removal of hydrogen and oxygen resulting increased carbon content as expected.

4.4. METHYLENE BLUE NUMBER EXPERIMENTS

"Methylene blue number is useful indicator of to estimate the adsorptive capacity of activated carbons. Methylene blue numbers of activated carbons related to the ability of adsorbent to adsorb on super micropores and mesopores." (Akgün, 2005)

Table 4.9. Properties of dehydrated methylene blue (Raposo et al., 2009)

Molecular weight	320 g /mol
Molecular width	14.3 Å
Molecular depth	6.1 Å
Molecular thickness	4 Å
Molecular volume	241.9 cm^3/ mol
Molecular diameter	0.8 nm

"Since surface area covered by methylene blue (S_{MB}) is used to estimate surface area of super micropores and mesopores, the ratio of S_{MB} to BET surface area (S_{BET}) represents the ratio of surface area of super micropores and mesopores to total surface area. When this ratio is higher, activated carbon is more desirable in adsorption of larger molecules or when this ratio is smaller, adsorption of smaller molecules should be chosen." (Akgün, 2005)

Results of methylene blue adsorption are showed in Table 4.10. Experimental data and sample calculations are given in Appendix D. Obtained products from phosphoric acid chemical activation had methylene blue numbers (MBN's) changing between 2.7 and 49.9. "It has been established that methylene blue can

measure the area accessible in pore diameters of ≥ 15 Å" (Attia et al., 2003). So that, the surface area of super micropores and mesopores could be estimated when surface area covered by methylene blue is known. Surface area covered by methylene blue of products were found as between 8.2 and 152.2 m^2/g. "The ratio of surface area covered by methylene blue to total surface area indicates that how much methylene blue can adsorbed on the surface of an adsorbent." (Özsin, 2011)

For activated carbon product AC-2-500, this ratio shows that approximately 20% of the total surface area was covered with methylene blue.

Table 4.10. Results of methylene blue experiments

Sample	**MBN mg/g**	**S_{MB} m^2/g**	**S_{BET} m^2/g**	**S_{MB}/S_{BET}**
AC-1-300	2.7	8.2	9.7	0.842
AC-1-400	30.2	92.2	366.7	0.251
AC-1-500	40.9	124.7	510.5	0.244
AC-1-600	35.7	108.8	499.4	0.218
AC-1-700	45.8	139.8	501.2	0.279
AC-1-800	49.7	151.6	559.2	0.271
AC-2-300	11.0	33.5	262.3	0.128
AC-2-400	18.8	57.3	263.6	0.217
AC-2-500	48.8	148.7	713.4	0.208
AC-2-600	49.8	151.7	686.5	0.221
AC-2-700	49.8	151.9	814.8	0.186
AC-2-800	49.9	152.2	862.4	0.176

"Also, the ratio of surface area covered by methylene blue to total surface area (BET surface area) provides initial information about the appropriate adsorbate molecule size that should be used in the adsorption on the activated carbon. Higher S_{MB}/S_{BET} ratios make activated carbon more preferable in the adsorption of large molecules because this high ratio indicates the amount of the pores greater than 1.5 nm is more than pores smaller than this size. On the other hand,

smaller S_{MB}/S_{BET} ratios of activated carbons are more suitable in the adsorption of small molecules." (Özsin, 2011)

The photos of methylene blue solutions before and after adsorption with activated carbon of AC-2-800 are shown in Figure 4.27.

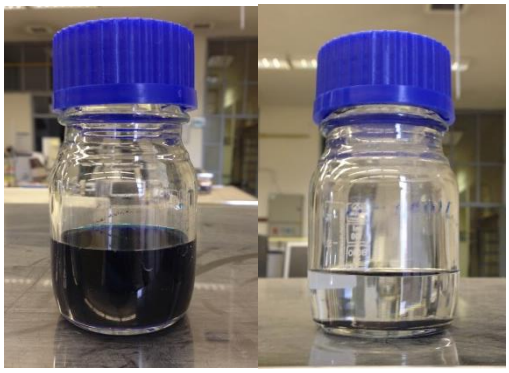

Figure 4.27. Methylene blue solutions before and after adsorption

Through nitrogen adsorption measurements, it was concluded that the products are mainly microporous except AC-1-300; whereas sample AC-1-300 showed mesopore structure in this study. Methylene blue experiments results showed that products have small S_{MB}/S_{BET} ratios except AC-1-300. Produced activated carbons are more suitable in the adsorption of small molecules. Methylene Blue experiments conform to nitrogen adsorption measurements. Activated carbons obtained in this work can be used in gas phase applications due to the microporic structure of products.

CHAPTER 5

CONCLUSION

In this present work, chemical activation with phosphoric acid was used to produce activated carbons from horse chestnut kernel. Products were characterized by nitrogen adsorption to measure BET surface areas. N_2 adsorption data were used for characterization of pore structure.

In this study, effect of activation temperature and impregnation ratio on production of activated carbon from horse chestnut kernel by phosphoric acid activation investigated. When the effect of activation temperature was investigated in phosphoric acid activation of horse chestnut kernel, it was seen that maximum BET surface areas were obtained at an activation temperature of 800 ºC which was 862.4 m^2/g. On the other hand, the product yield (21.7 %) was quite low. When the effect of impregnation ratio was examined, it was seen that increasing the amount of phosphoric acid caused increasing of BET surface areas except 400 ºC. Effect of impregnation ratio on the yield is different below activation temperature of 500 ºC and above activation temperature of 500 ºC. For activation temperatures up to 500 ºC, yield increases with increasing impregnation ratio whereas for activation temperatures over 500 ºC yield values decreased with increasing impregnation ratio.

To find the suitable process conditions for the activated carbon production from horse chestnut kernel, the activation temperature, the BET surface area and the yield were evaluated together. The activation temperature of 500 ºC and impregnation ratio of 2:1 were found as suitable conditions for activated carbon production from horse chestnut kernel in this study.

The BET surface area of activated carbon prepared by phosphoric acid activation method achieved a maximum value of 862.4 m^2/g for impregnation ratio of 2:1 by weight (H_3PO_4: g horse chestnut kernel) at an activation temperature of 800 ºC. Besides, the BET surface area of produced activated carbons achieved a suitable value of 713.4 m^2/g for impregnation ratio of 2:1 by weight (H_3PO_4: g horse chestnut kernel) at activation temperature of 500 ºC.

Nitrogen adsorption results showed that produced activated carbons except AC-1-300 which was produced at activation temperature of 300°C and impregnation ratio of 1:1 (weight of H_3PO_4/weight of raw material) were mainly microporous carbons with a significant contribution of mesopores. On the other hand, product AC-1-300 which was produced at activation temperature of 300°C and impregnation ratio of 1:1 (weight of H_3PO_4/weight of raw material) showed mesopore structure.

Results of reproducibility experiments showed that adsorption-desorption isotherms and pore size distributions were similar for produced and reproduced samples. On the other hand, when BET surface area is considered, activated carbon produced at 700°C and 2:1 impregnation ratio shows good reproducibility whereas activated carbon produced at 500°C and 2:1 impregnation ratio does not show good reproducibility.

Elemental analysis results showed that all activated carbon samples have higher carbon content and lower hydrogen and oxygen content than raw material. There was a significant increase in carbon content of the material after carbonization and activation processes. It can be said that chemical activation has improved the removal of hydrogen and oxygen resulting increased carbon as expected.

Methylene blue experiments results showed that products have small S_{MB}/S_{BET} ratios except one sample produced at 300°C for 1:1 impregnation ratio. This small

S_{MB}/S_{BET} ratio indicates that produced activated carbons are more suitable in the adsorption of small molecules.

Nitrogen adsorption measurements and methylene blue experiments showed that activated carbons obtained in this work can be used in gas phase applications due to the microporic structure of products.

The results of the study show that the horse chestnut kernel can be a goof precursor for activated carbon production.

CHAPTER 6

RECOMMENDATIONS

Activated carbon has been largely used in various applications due to its large surface area, the porous structure and adsorption capacity. Experiments should carry out under different experimental parameters such as impregnation ratio, heating rate, activation time etc. The experiment should be carried out with different impregnation ratio such as 3:1 (g H_3PO_4: g raw material). In this work, activated carbons were produced by phosphoric acid chemical activation method from horse chestnut kernel. Other chemical activation agents such as potassium hydroxide, sodium hydroxide and potassium carbonate should be examined to investigate effect of different activating agents on pore structure of produced activated carbon.

Chemical compositions of the prepared activated carbons were identified in terms of carbon, hydrogen and nitrogen content in this study. Besides that, ash content of the activated carbons should be identified for further information. The electron microscopy analysis should be also performed to observe surface morphology of activated carbons. It is recommended to characterize activated carbons by FTIR to determine surface properties of the carbons.

REFERENCES

- Akgün, A.M., "Sorption of Cadmium and Lead on Activated Carbons Produced from Resins and Agricultural Wastes", MSc. Thesis in Chemical Engineering, Middle East Technical University, Ankara, Turkey (2005)

- Alcaniz-Monge, J., Illan-Gomez, M.J., "Modification of activated carbon porosity by pyrolysis under pressure of organic compounds", Adsorption, 14, 93-100 (2008)

- Al Bahri, M., Calvo, L., Gilarranz, M.A., Rodriguez, J.J., "Activated carbon from grape seed upon chemical activation with phosphoric acid: Application to the adsorption od diuron from water.", Chemical Engineering Journal, 203, 348-356 (2012)

- Anas Nahil, M., Williams, P.T., "Pore characteristics of activated carbons from phosphoric acid chemical activation of cotton stalks", Biomass and Bioenergy, 37, 142-149 (2012)

- Attia, A. A., Girgis, B. S. and Khedr, S. A., "Capacity of activated carbon derived from pistachio shells by H_3PO_4 in the removal of dyes and phenolics", Journal of Chemical Technology and Biotechnology, 78, 611-619 (2003)

- Balcı, S., "Kinetics of Activated Carbon Production from Almond Shell, Hazelnut Shell and Beech Wood and Characterization of Products", Ph.D. Thesis in Chemical Engineering, Middle East Technical University, Ankara, Turkey (1992)

- Bandozs, T. J., “Activated Carbon Surfaces in Environmental Remediation”, 7, Interface Science and Technology, 1-571 (2006)

- Bansal, R. C., Goyal, M., “Activated Carbon Adsorption”, CRC Press, Boca Raton (2005)

- Biscoe, J., Warren, G.E., “An X-Ray Study of Carbon Black”, Journal of Applied Physics, 12(6), 364-371 (1942)

- Bokros, J.C., “Deposition, Structure, and Properties of Pyrolytic Carbon, Chemistry and Physics of Carbon”, 5, Marcel Dekker, New York (1969)

- Bota, A., Loszlo, K., Nagy, L.G., Copitzky, T., “Comparative study of active carbons from different precursors”, Langmuir, 13(24) 6502-9 (1997)

- Brunauer, S., Demming, L. S, Demming, W. S., Teller, E., “On a Theory of the Van Der Waals Adsorption of Gasses”, Journal of the American Chemical Society, 62, 1723–1732 (1940)

- Brunauer, S., Emmet, P. H., Teller, E., “Adsorption of Gases in Multimolecular Layers”, Journal of the American Chemical Society, 60, 309-19 (1938)

- Bussy, A., Journal of Pharmaceutical Sciences and Accessories, 8-257 (1822)

- Castano, J., Rodriguez-Llamazares S., Contreras K., Carrasco C., Pozo C., Bouza, R., Franco, C. M. L., Giraldo D., “Horse chestnut (Aesculus Hippocastanum L.) starch: Basic pyhsico-chemical characteristics and use as thermoplastic material”, Carbonhyrate Polymers, 112, 677-685 (2014)

- Cukanovic, J., Ninic-Todorovic, J., Ognjanov. V., Mladenovic, E., Ljubojevic, M., Kurjakov, A., "Biochemical Composition of The Horse Chestnut Seed (A. Hippocastanum L.)", Archives of Biological Sciences, Belgrade, 63 (2), 345-351 (2001)

- Çuhadar, Çiğdem, "Production And Characterization Of Activated Carbon From Hazelnut Shell And Hazelnut Husk", MSc. Thesis in Chemical Engineering, Middle East Technical University, Ankara, Turkey (2005)

- Dabrowski, A., "Adsorption – from theory to practice", Advances in Colloid and Interface Science, 93, 1333-224 (2001)

- Deitz, V.R., "Bibliography of Solid Adsorbents", U.S. Cane Sugar Refiners and Bone Char Manufacturers and National Bureau of Standards, Washington D.C.: History of adsorbent carbon, ix ff; Abstracts of reviews, histories and general discussions, 689-696 (1944)

- Demiral, H., Demiral, İ., Karabacakoğlu, B., Tümsek, F., "Production of activated carbon from olive bagasse by physical activation", Chemical Engineering Research and Design, 89, 206-213 (2011)

- Demirbaş, A., "Biomass resource facilities and biomass conversion processing for fuels and chemicals", Energy conversion and Management, 42, 1357-1378 (2001)

- Dubinin, M. M., Vishnyakova, M.M., Zhukovskaya, E.G., Leont'ev, E.A., Luk'yanovich, V.M., and Sarakov, A.I., "Investigation of the porous structure of solids by sorption methods. V. The structure of intermediate pores and macropores of activated carbon", Zhurnal Fizicheskoi Khimii, 34, 959-64 (1960)

- Fan, M., Marshall, W., Daugaard, D., Brown, R.C., "Steam activation of chars produces from oat hulls and corn stover", Biosource Technology, 93, 103-107 (2004)

- Franklin, R.E., "Crystallite Growth in Graphitizing and Non- graphitizing Carbons", Proceedings of Royal Society of London, 209, 196-218 (1951)

- Fu, P., Hu, S., Sun, L., Xiang, J., Yang, T., Zhang, A., Zhang, J., "Structural evolution of maize stalk/char particles during pyrolysis", Biosource Technology, 100, 4877-4883 (2009)

- Girgis, B. S., El-Hendawy, A.N.A., "Porosity Development in Activated Carbons Obtained from Date Pits Under Chemical Activation with Phosphoric Acid", Microporous and Mesoporous Materials, 52, 105–117 (2002)

- Gomez-Serrano, V., Cuerda-Correa, E.M., Fernandez-Gonzalez, M.C., Alexandre-Franco, M.F., Macias-Garcia, A., "Preparation activated carbons from chestnut wood by phosphoric acid-chemical activation. Study of microporosity and fractal dimension", Materials Letters, 59, 846-853 (2005)

- Gregg, S. J. and Sign, K.S.W., "Adsorption, Surface and Porosity", 2nd Edition", New York Academic Press, New York, USA (1982)

- Guo, J., Gui, B., Xiang, S.-X., Bao, X.-T., Zhang, H.-J., Lua, A. C., "Preparation of activated carbons by utilizing solid wastes from palm oil processing mills.", Journal of Porous Materials, 15, 535–540 (2008)

- Guo, J., and Lua, A. C., "Adsorption of sulphur dioxide onto activated carbon prepared from oil-palm shells with and without pre-impregnation.", Separation and Purification Technology, 30, 265–273 (2003)

- Hassler, J.W., "Purification with Activated Carbon", Chemical Publishing Co. Inc., Newyork, USA (1974)

- Haykırı Açma, H., Yaman, S., Küçükbayrak, S., "Gasification of biomass chars in steam-nitrogen mixture", Energy Conversion Management, Vol.47, 1004-1013 (2005)

- Hunter, J., Journal of Chemical Society, 18-285 (1865)

- Ioannidou, O., Zabaniotou, A., "Agricultural residues as precursors for activated carbon production – A Review", Renewable and Sustainable Energy Reviews, 11, 1966-2005 (2007)

- IUPAC (International Union of Pure and Applied Chemistry) Physical Chemistry Division Commission on Colloid and Surface Chemistry Including Catalysis, "Reporting Physisorption Data for Gas/Solid Systems with Special Referance to Determination of Surface Area and Porosity", Pure and Applied Chemistry, 57(4), 603-619 (1985)

- Jagtoyen M., Derbyshire F., "Activated Carbons from Yellow Poplar and White Oak by H_3PO_4 Activation", Carbon, 36, 1085- 1097 (1998)

- Karagöz, S., Tay, T., Ucar, T., Erdem, M., "Activated carbons from waste biomass by sulfuric acid activation and their use on methylene blue adsorption", Biosource Technology, 99(14), 6214-6222 (2008)

- Karlinski, L., Jagodzinski, A. M., Leski, T., Butkiewicz, P., Brosz, M., Rudawska, M., "Fine root parameters and mycorrhizal colonization of horse chestnut trees (Aesculus hippocastanum L.) in urban and rural environments", Landscape and Urban Planning, 127, 154-163 (2014)

- Kehl, D.M., "Observations et Journal sur la Physique, de chemie et d'Historie Naturelle et des arts", Paris, Tome XLII, 250 (1793)

- Kılıç, M., Apaydın Varol, E., Pütün, A.E., "Preparation and surface characterization of activated carbons from Euphorbia rigida by chemical activation with $ZnCl_2$, K_2CO_3, NaOH and H_3PO_4", Applied Surface Science, 261, 247-254 (2012)

- Kipling, J.J., "The Properties and Nature of Adsorbent Carbons", Quarterly Review of the Chemical Society, 10, 1–26, (1956)

- Kirk-Othmer, "Carbon, Activated", Volume 3, Encyclopedia of Chemical Technology, John Wiley and Sons Inc., 741-761 (2003)

- Klass, D.L., "Biomass for Renewable Energy, Fuels, and Chemicals", Elsevier Inc. (1998)

- Kruk, M., Jaroniec, M., "Gas Adsorption Characterization of Ordered Organic−Inorganic Nanocomposite Materials", Chemistry of Materials, 13, 3169-3183 (2001)

- Kwiatkowski, J. F., "Activated Carbon: Classifications, Properties and Applications", Nova Science Publisher, New York (2011)

- Lim, W.C., Srinivasakannan, C., Balasubramanian, N., "Activation of palm shells by phosphoric acid impregnation for high yielding activated carbon", Journal of Analytical and Applied Pyrolysis, 88, 181-186 (2010)

- Lipscombe, F., British Patent 2887 (1862)

- Lowitz, L., Crell's Chemical Annals, 1-211 (1786)

- Lua, A. C., and Jia, Q., "Adsorption of phenol by oil-palm-shell activated carbons.", Adsorption, 13, 129–137 (2007)

- Marsh, M., Rodriguez-Reinoso, F., "Activated Carbon", Elsevier (2006)

- Marton, G., Bakan, A., “Research and development on an integrated and wastefree utilization of horse chestnut (Aesculus Hippocastaneum) seeds”, Bioresearch Technology, 54, 197-200 (1995)

- McKendry, P., “Energy Production from Biomass (Part 1): Overview of Biomass”, Bioresource Technology, 83, 37-46 (2002)

- Mohammad Nor, N., Lee Chung, L., Teong, L.K., Mohammed, A.R., “Synthesis of activated carbon from lignocellulosic biomass and its applications in air pollution control- a review”, Journal of Environmental Chemical Engineering, 1, 658-666 (2013)

- Molina-Sabio, M., Gonzales, M., Rodriguez-Reinoso, F., Sepulveda-Escribano, A., “Effect of steam and carbon dioxide activation in the micropore size distribution of activated carbon”, Carbon, 34, 505-509 (1996)

- Momcilovic, M.Z., Purenovic, M.M., Miljkovic, M.N., Bojic, A.L., Zarubica, A.R., Randelovic, M.S., “Physico-chemical characterization of powdered activated carbons obtained by thermo-chemical conversion of brown municipal waste”, Hemijska Industrija, 65 (3), 242-247 (2011)

- Ok, S., “Adsorption Properties of Carbon Nanoparticles”, MSc. Thesis in Chemical Engineering, Middle East Technical University, Ankara, Turkey (2005)

- Ostrejko, R., British Patents 14224 (1900); 18040 (1900); German Patent 136, 792 (1901)

- Özmak, M., “Production of Activated Carbon From Biomass Wastes”, Ph.D. Thesis in Chemical Engineering, Ankara University, Ankara, Turkey (2010)

- Özsin, G., "Production And Characterization Of Activated Carbon From Pistachio-Nut Shell", MSc. Thesis in Chemical Engineering, Middle East Technical University, Ankara, Turkey (2011)

- Pütün, A.E., Özbay, N., Önal, E.P., Pütün, E., "Fixed-bed pyrolysis of cotton stalk for liquid and solid products", Fuel Process Technology, 86, 1207-1219 (2005)

- Rafatullah, M., Ahmad, T., Ghazali, A., Sulaiman, O., Danish, M., Hashim, R., "Oil Palm Biomass as a Precursor of Activated Carbons: A Review", Critical Reviews in Enviromental Science and Technology, 43, 1117-1161 (2003)

- Savova, D., Apak, E., Ekinci, E., Yardim, F., Petrova, N., Budinova, T., Razvigorova, M., Minkova, V., "Biomass conversion to carbon adsorbents and gas", Biomass and Bioenergy, 21, 133-137 (2001)

- Shoaib, M., Al-Swaidan, H.M., "Optimization and characterization of sliced activated carbon prepared from date palm tree fronds by physical activation", Biomass and Bioenergy, 73, 124-134 (2015)

- Sing, K.S.W., Everett, D.H., Haul, R.A.W., Moscou, L., Pierotti, R.A., Rouquerol, J., Siemieniewska, T., "Reporting physisorption data for gas/solid systems with special reference to the determination of surface area and porosity", Pure and Applied Chemistry, 57(4), 603-619 (1985)

- Smisek, M., Cerny, S., "Active Carbon Manufacture, Properties and Aplications", Elsevier, New York (1970)

- Stenhouse, J., British Patent 1395 (1856), Chemical News, 3-78 (1861); 25-239 (1872)

- Şenel, G.İ., "Characterization of pore structure of Turkish coals and their chars obtained by carbonization and CO activation", PhD. Thesis in Chemical Engineering, Middle East Technical University, Ankara, Turkey (1994)

- Tan, I. A. W., and Hameed, B. H., Ahmad, A. L., "Equilibrium and kinetic studies on basic dye adsorption by oil palm fibre activated carbon.", Chemical Engineering Journal, 127, 111-119 (2007)

- Timur, S., Kantarlı, I.C., Onenc, S., Yanik, J., "Characterization and application of activated carbon produced from oak cups pulp", Journal of Analytical and Applied Pyrolysis, 89, 129-136 (2010)

- Tseng, R.L., "Physical and chemical properties and adsorption type of activated carbon prepared from plum kernels by NaOH activation", Journal of Hazardous Materials, 147(3), 1020-1027 (2007)

- Valente Nabais, J.M., Laginhas, C.E.C., Carrot, P.J.M., Ribeiro Carrot, M.M.L., "Production of activated carbons from almond shell", Fuel Processing Technology, 92, 234-240 (2011)

- Walker, P.L., "Chemistry and Physics of Carbon", Vol. 2, Marcel Dekker, New York, USA (1968)

- Xu, F., Yu, J., Tesso, T., Dowell, F., Wang, D., "Qualitative and quantitative analysis of lignocellulosic biomass using infrared techniques: A mini-review", Applied Energy, 104, 801-809 (2013)

- Xu, J., Chen, L., Qu, H., Jiao, Y., Xie, J., Xing, G., "Preparation and characterization of activated carbon from reedy grass leaves by chemical activation with H_3PO_4", Applied Surface Science, 320, 674-680 (2014)

- Yahşi, N.U., “Production and Characterization of Activated Carbon from Apricot Stones”, MSc. Thesis in Chemical Engineering, Middle East Technical University, Ankara, Turkey (2004)

APPENDIX A

THERMOGRAVIMETRIC ANALYSIS

Table A.1. Yield values of raw horse chestnut kernel

	Weight (mg)	**Temperature (°C)**	**Yield (%)**
Horse Chestnut Kernel	21.06 (Initial)	20.01	100.0
	19.83	100	94.2
	18.89	200	89.7
	11.95	300	56.7
	6.67	400	32.2
	4.73	500	22.5
	3.40	600	16.1
	2.61	700	12.4
	2.05	800	9.7
	1.56	900	7.4

Sample Calculation of Yield for raw material at 300°C,

$$Yield\,\% = \frac{W_f}{W_i} \times 100 = \frac{11.95}{21.06} \times 100 \tag{A.1}$$

$$Yield\,\% = 56.7\,\% \tag{A.2}$$

Table A.2. Yield values of phosphoric acid impregnated horse chestnut kernel

	Weight (mg)	**Temperature (°C)**	**Yield (%)**
Impregnation Ratio 1:1 (weight of H_3PO_4/weight of HCK)	24.85(Initial)	18.261	100.0
	22.83	100	91.8
	15.95	200	64.2
	13.12	300	52.8
	11.63	400	46.8
	10.46	500	42.1
	9.59	600	38.6
	9.00	700	36.2
	8.30	800	33.4
	6.87	900	27.6
Impregnation Ratio 2:1 (weight of H_3PO_4/weight of HCK)	26.86 (Initial)	16.86	100.0
	23.63	100	88.0
	16.41	200	61.1
	14.44	300	53.8
	13.12	400	48.8
	12.07	500	44.9
	9.25	600	34.4
	7.13	700	26.5
	5.83	800	21.7
	4.51	900	16.8

APPENDIX B

ANALYSIS OF N_2 SORPION DATA

B.1. Determination of BET Surface Area

BET surface areas of the products can be obtained by the physical adsorption data of nitrogen molecules on the surface (Brunauer et al., 1938).

Final form of BET equation can be expressed as;

$$\frac{P}{V(P_o - P)} = \frac{1}{V_m C} + \frac{C-1}{V_m C}\frac{P}{P_o} \tag{B.1}$$

According to the equation mentioned above, in a relative pressure range of 0.05-0.3 , a plot of $\frac{P}{V(P_o - P)}$ versus $\frac{P}{P_o}$ yields a line with a slope (S) and an intercept (I) which are given as;

$$S = \frac{C-1}{V_m C} \qquad and \quad I = \frac{1}{V_m C} \tag{B.2}$$

The graphical representation of BET equation is given in Figure B.1.

BET surface area can be determined using the following equation;

$$S_{BET} = \frac{V_m A_m N_A}{V_{mol}} \tag{B.3}$$

$$V_m = \frac{1}{(S+I)} \tag{B.4}$$

$$S_{BET} = \frac{CSA_{N_2} N_A}{V_{mol}\,(S+I)} \tag{B.5}$$

$$S_{BET} = \frac{\left[\left(CSA_{N_2}\, nm^2\right)\left(6.023 \times 10^{23}\ (1/mol)\right)\right]}{\left[(22414(cm^3/mol, STP))(10^{18}(nm^2/m^2)\ \ ((S+I)(g/cm^3, STP))\right]} \tag{B.6}$$

where CSA_{N2} denotes cross sectional area of a nitrogen molecule and has a numerical value of 0.162 nm^2 (Walker et al.,1968).

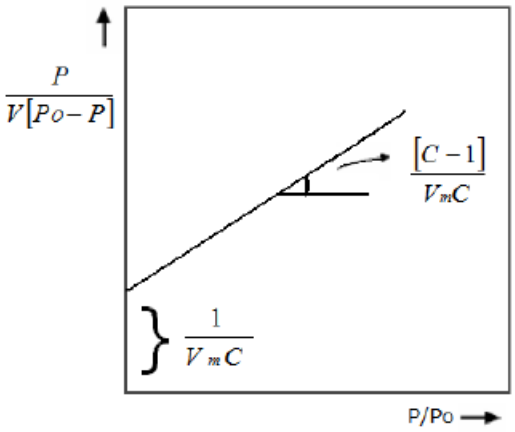

Figure B.1.Graphical representation of BET equation

APPENDIX C

REPRODUCIBILITY EXPERIMENTS

Reproducibility is considered as one of the fundamentals of the entire scientific method. Reproducing an experiment is key approach that researchers use to gain confidence in their conclusions. Reproducibility shows the variability of the experimental system caused by differences in operator behavior.

The basic principle of reproducibility research is that researcher should be able to reproduce the experiment, under the same conditions, and achieve the same results.

In this study, reproducibility of the experiments was done for by reproducing activated carbon at activation temperature of 500 and 700 ºC for impregnation ratio of 2:1 at the same process conditions.

Table C.1. BET surface area values and deviation values of reproducibility experiments

Impregnation Ratio (H_3PO_4/HCK)	Temperature ºC	BET Surface Area m^2/g		% Deviation
2:1	500	713.4	651.6	8.7
	700	814.8	830.4	1.9

Calculation for activated carbon produced at 500 ºC for 2:1 impregnation ratio;

$$\%\ Deviation = \frac{713.4 - 651.6}{713.4} x100 = 8.7\ \% \quad \text{(C.1)}$$

Calculation for activated carbon produced at 700 ºC for 2:1 impregnation ratio;

$$\%\ Deviation = \frac{830.4 - 814.8}{830.4} x100 = 1.9\ \% \quad \text{(C.2)}$$

APPENDIX D

EXPERIMENTAL DATA FOR METHYLENE BLUE NUMBER DETERMINATION

Methylene blue is a dark green powder with a characteristic dark blue color in aqueous solutions where it dissociates into an MB cation and a chloride anion. It is widely used in the evaluation of activated carbon in liquid phase adsorption. Methylene blue number (MBN) is a valuable indicator of adsorptive capacity of activated carbon.

A chemical compound absorbs the light at specific wavelengths and this is related with the electronic structure of the compound. Besides intensity of absorption of light depends on the quantity of the molecules between the light source and the detector. By using a UV spectrometer, quantitative and qualitative information of a given compound can be obtained by measuring the amount of ultraviolet and visible light absorbed by the sample placed in the device.

Firstly, a calibration curve was plotted with known concentrations of methylene blue solutions. Calibration curve data and calibration curve is given in Table D.1 and Figure D.1. After methylene blue adsorption experiments, samples were taken and diluted (if needed) before the measurement by UV spectrometer. Absorbance values of UV measurements and dilution ratios are shown in Table D.2.

Table D.1. Data for methylene blue concentration calibration curve

Concentration mg/L	Absorbance
0	0
1	0.202
2	0.384
4	0.823
6	1.161
8	1.587
10	1.857

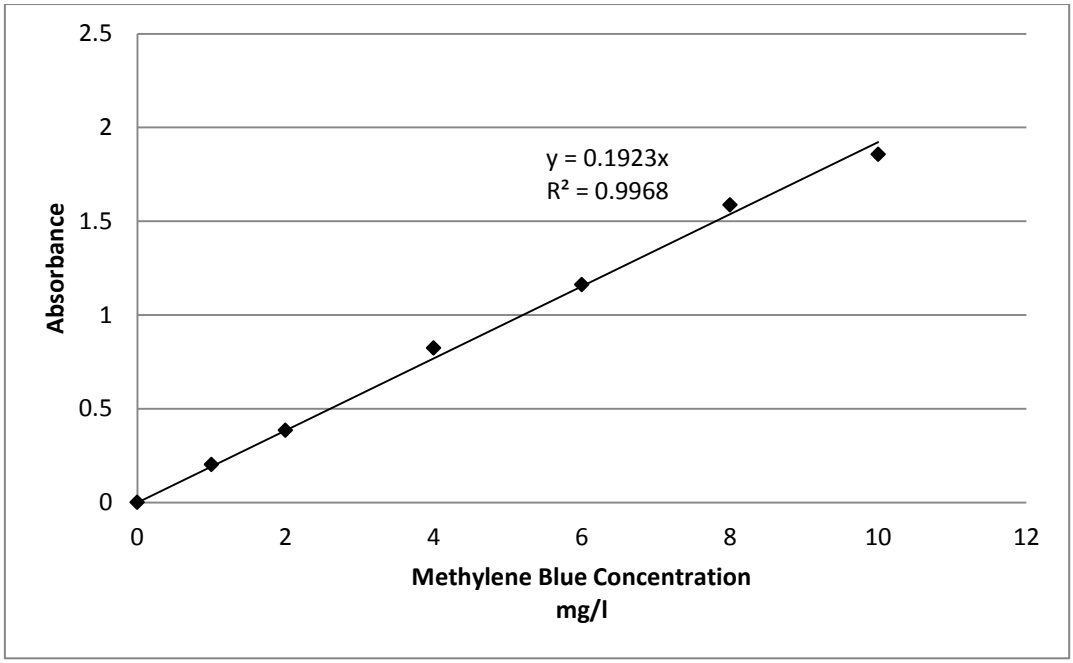

Figure D.1. Calibration curve for methylene blue experiments

Table D.2. Results of UV Spectrophotometer Measurements

Sample	Dilution	Absorbance
AC-1-300	1/200	0.091
AC-1-400	1/100	0.076
AC-1-500	1/100	0.035
AC-1-600	1/100	0.055
AC-1-700	1/100	0.016
AC-1-800	-	0.11
AC-2-300	1/100	0.15
AC-2-400	1/100	0.12
AC-2-500	-	0.475
AC-2-600	-	0.095
AC-2-700	-	0.073
AC-2-800	-	0.035

Sample Calculation for AC-2-800;

Concentration of blank experiment = 100 mg/L

Final concentration of solution;

$$\left(\frac{0.035}{0.1923}\right) \times 1 = 0.182\ mg/L \tag{D.1}$$

$$MBN = \frac{\left(C_{blank} - C_{final}\right)}{M_{AC}} \times V_{sol} \tag{D.2}$$

$$MBN = \frac{(100 - 0.182) mg/L}{0.1\ g} \times 0.05\ L = 49.9\ mg/g \tag{D.3}$$

$$S_{MB} = \frac{MBN \times MB\ Surface\ Area\ \times Avagadro\ Number}{MB\ Molecular\ Weight} \tag{D.4}$$

MB Surface Area= 1.62 x 10^{-18} m^2/molecule

MB Molecular Weight = 319.86 g/mol

Avagadro number= 6.02 x 10^{23}

S_{MB}= 152.2 m^2/g

$$\frac{S_{MB}}{S_{BET}} = \frac{152.2}{862.4} = 0.176 \qquad \text{(D.5)}$$